UNCLASSIFIED

AD NUMBER
AD393661
CLASSIFICATION CHANGES
TO: unclassified
FROM: confidential
LIMITATION CHANGES
TO: Approved for public release, distribution unlimited
FROM: Distribution authorized to U.S. Gov't. agencies and their contractors; Administrative/Operational Use; "Aug 1968. Other requests shall be referred to Air Force Aero Propulsion Lab., Wright-Patterson AFB, OH 45433. NOFORN.
AUTHORITY
31 Aug 1980, Group-4, per document marking; AFWAL ltr, 14 Dec 1983

THIS PAGE IS UNCLASSIFIED

THIS REPORT HAS BEEN DELIMITED
AND CLEARED FOR PUBLIC RELEASE
UNDER DOD DIRECTIVE 5200.20 AND
NO RESTRICTIONS ARE IMPOSED UPON
ITS USE AND DISCLOSURE.

DISTRIBUTION STATEMENT A

APPROVED FOR PUBLIC RELEASE;
DISTRIBUTION UNLIMITED.

CONFIDENTIAL

AFAPL-TR-68-8
Part I

(UNCLASSIFIED) EXPLORATORY DEVELOPMENT OF REDUCED LENGTH TURBO-PROPULSION COMBUSTION SYSTEMS

Part I. Preliminary Component Design and Development

J. J. Simon D. A. MacNaughton
R. J. Stettler J. T. Wyrobek
Allison Division • General Motors

TECHNICAL REPORT AFAPL-TR-68-8, PART I
August 1968

GROUP 4
Downgraded at 3 year intervals;
declassified after 12 years

SPECIAL HANDLING REQUIRED

NOT RELEASABLE TO FOREIGN NATIONALS

The information contained in this document will not be disclosed to foreign nationals or their representatives.

This material contains information affecting the national defense of the United States within the meaning of the espionage laws, Title 18, U.S.C., Sections 793 and 794, the transmission or revelation of which in any manner to an unauthorized person is prohibited by law.

Air Force Aero Propulsion Laboratory,
Air Force Systems Command
Wright-Patterson Air Force Base
Ohio 45433

CONFIDENTIAL

NOTICE

When Government drawings, specifications, or other data are used for any purpose other than in connection with a definitely related Government procurement operation, the United States Government thereby incurs no responsibility nor any obligation whatsoever; and the fact that the Government may have formulated, furnished, or in any way supplied the said drawings, specifications, or other data, is not to be regarded by implication or otherwise as in any manner licensing the holder or any other person or corporation, or conveying any rights or permission to manufacture, use, or sell any patented invention that may in any way be related thereto.

This is a reprint copy with Section IV, paragraph 6, pages 72 through 80 deleted for proprietary reasons.

Copies of this report should not be returned unless return is required by security considerations, contractual obligations, or notice on a specific document.

CONFIDENTIAL

AFAPL-TR-68-8
Part I

(UNCLASSIFIED)
EXPLORATORY DEVELOPMENT OF REDUCED LENGTH TURBO-PROPULSION COMBUSTION SYSTEMS

Part I. Preliminary Component Design and Development

J. J. Simon D. A. MacNaughton
R. J. Stettler J. T. Wyrobek

DOWNGRADED AT 3 YEAR INTERVALS;
DECLASSIFIED AFTER 12 YEARS
DOD DIR 5200.10

GROUP 4

Downgraded at 3 year intervals;
declassified after 12 years

SPECIAL HANDLING REQUIRED

NOT RELEASABLE TO FOREIGN NATIONALS

The information contained in this document will not be disclosed to foreign nationals or their representatives.

This material contains information affecting the national defense of the United States within the meaning of the espionage laws, Title 18, U.S.C., Sections 793 and 794, the transmission or revelation of which in any manner to an unauthorized person is prohibited by law.

STATEMENT #2 CLASSIFIED

In addition to security requirements which must be met, this document is subject to special export controls and each transmittal to foreign governments or foreign nationals may be made only with prior approval of AFAPL (APTC) WPAFB, OHIO. 45433

CONFIDENTIAL

FOREWORD

(U) Present combustion system technology using high pressure fuel nozzles in can-type combustors cannot cope with the advances in turbopropulsion engines. To maintain pace with engine advances, the combustion system (annular combustor) will require a low pressure fuel system unaffected by contaminated fuel and an integrated diffuser-combustor to reduce weight and size. The system will also require a high combustor dome air flow in conjunction with premix fuel modules to provide increased temperatures with uniform distribution, low pressure loss, and high combustor efficiency.

(U) Allison Division of General Motors Corporation undertook the exploratory development of reduced length turbopropulsion combustion systems for the United States Air Force, Air Force Systems Command, Aero Propulsion Laboratory (AFAPL), Wright-Patterson Air Force Base, Ohio. This work under Contract F33615-67-C-1939, Project No. 3066, Task No. 306603, was monitored for the Air Force by Mr. Robert E. Henderson/APTC and Mr. Morris D. Louick/SEKNB.

(U) The Phase I report draft was submitted on 15 January 1968 and covers the design, fabrication, and testing during the period from 1 July 1967 through 31 December 1967. The Allison number for this report is EDR 5610.

(U) This report contains no classified information extracted from other classified documents other than the periodic progress reports published in accordance with this contract.

(U) Publication of this report does not constitute Air Force approval of the report's findings or conclusions. It is published only for the exchange and stimulation of ideas.

Ernest C. Simpson
ERNEST C. SIMPSON
Chief, Turbine Engine Division
AF Aero Propulsion Laboratory

UNCLASSIFIED ABSTRACT

Advanced design turbo-propulsion engines for future aircraft require a compact, high performance combustion system for high thrust-to-weight ratios and an increased level of reliability. To attain this goal, two concepts based on maximum combustor dome airflow are being developed. The first is an integration of the diffuser and combustor to achieve minimum length and maximum efficiency with smoke free operation. The second is to achieve improved fuel injection using a high density premix fuel injection technique to obtain acceptable exit temperature patterns in a high temperature rise combustor. The fuel injection technique is the development of single modules for premixing of low pressure fuel and high velocity air ahead of the combustor dome. These modules are capable of accepting contaminated fuels and can be combined to permit testing as sectors of a full annular combustor.

Initial testing of the various fuel injection premix modules and different designs of the integrated diffuser-combustor under Phase I of this program has verified the soundness of the concepts being developed. Based upon these results, the most promising premix modules and the best diffuser-combustor design will be combined as sectors of a full annular combustor for further evaluation.

Distribution of this abstract is unlimited.

TABLE OF CONTENTS

LIST OF ILLUSTRATIONS

Preceding Page Blank

Preceding Page Blank

LIST OF TABLES

Preceding Page Blank

I INTRODUCTION

(C) The rapid advances in turbo-propulsion technology over the past several years have placed an ever-increasing demand upon combustion system performance. Future combustion systems will be required to support Air Force missions ranging from subsonic long endurance systems, advanced supersonic VTOL and strategic-tactical systems, to hypersonic systems for both accelerator and cruise vehicles. To meet effectively the requirements of these advanced mission types, combustors must have the operational flexibility to accept wide variations in compressor discharge pressure, temperature, and air flow while providing an acceptable exit temperature profile with minimum pressure loss and good combustion efficiency. Furthermore, advanced combustion systems must be lightweight and capable of accepting contaminated fuels while maintaining stable operation over the entire range of flight operating conditions. Exploratory investigations accomplished under Air Force Contract AF33(615)-1304 have indicated that high temperature rise combustion systems approaching stoichiometric exit conditions will require increased burner dome flow in conjunction with improved fuel injection techniques. Increased dome flow and high density fuel injection can provide as much as a 40 percent reduction in combustor length because of increased fuel-air mixing in the combustion zone. However, it is recognized that as the minimum combustor length is approached, combustion efficiency and exit temperature profile begin to deteriorate. Therefore, improved fuel injection techniques are desirable to maintain good fuel-air mixing thus insuring that combustion efficiency and exit temperature profile are maintained at acceptable performance levels. Any

further reduction in combustion system length must be accomplished through more effective utilization of the burner inlet diffuser which currently occupies a large percentage of the overall length of the combustion system. It is the purpose of this exploratory research and development program to investigate component techniques which will minimize the overall length of a combustion system from the compressor exit to the inlet of the turbine. Various integrated diffuser/combustor approaches will be investigated with emphasis on high dome flow, high temperature rise systems with exit temperatures approaching 3500°F using JP fuels. In addition, it is intended that low pressure differential fuel injection techniques be investigated to improve the contamination resistance of the fuel nozzles and enhance further reductions in the complexity and weight of the fuel system. Tradeoff investigations will be conducted to establish the optimum combustion system for various defined mission objectives. This program will provide the technology required to design efficient combustion systems with wide operating range and significantly reduced diffuser/combustor length. These systems will have predictable performance characteristics for advanced propulsion systems.

(C) The objectives of this exploratory research program are:

- To increase the level of operational reliability for turbo-propulsion systems
- To reduce combustion system weight and volume
- To provide the technology necessary to reduce the overall length of the combustion system by the application of advanced diffuser/combustor concepts and fuel injection techniques.

II FLOW PATH DESIGN FACTORS

(C) Phase I of this exploratory development program consisted of research investigations conducted to design and evaluate various combustion system configurations of reduced diffuser-combustor length. It also included investigations of fuel injection techniques of low pressure differential systems that would be capable of accepting contaminated fuels.

(C) This initial phase is the first of a comprehensive three phase program. The comprehensive program spans an exploratory pressure range of 0.3 to 20 atmospheres and inlet temperatures to 1200°F, with the following design point performance goals:

- A combustion efficiency, $\eta_b \geq 98\%$
- A pressure loss, $\Delta P/P \leqslant 5\%$
- An average exit temperature, T = 3500°F
- A maximum temperature rise, T = 2300°F
- An exit temperature profile, $\dfrac{T_{Max} - T_{Avg}}{T_{Avg} - T_{In}} = .15 \text{ to } .20$
- To demonstrate a performance and sizing computer program, sensitive to mission and engine operating conditions, for the combustion system that can be substantiated by test.

(C) The hardware required to conduct the initial phase of this program was sized to reflect a continuity of results with Phase II and Phase III. The initial designs; therefore, are based on facility capabilities to enable the complete air flow, temperature, and pressure demonstration of a 120° sector of an annular combustion system. This sizing was also

influenced by inlet and exit conditions of specific Air Force missions used as guide lines. These missions are:

- Subsonic long endurance
- Advanced supersonic VTOL
- Advanced supersonic strategic/tactical
- Hypersonic accelerator and cruise

(C) The four missions were examined and an inlet velocity of 548 ft/sec and exit velocity of 700 ft/sec were selected as a representative condition. The initial design features are listed in Table I and a complete flow path of the initial design components is shown in Figure 1.

(C) TABLE I DESIGN FEATURES

Feature	Value
Diffuser inlet velocity	548 ft/sec
Diffuser outlet velocity	304 ft/sec
Diffuser length	4.5 in.
Diffuser area ratio, outlet to inlet	1.78
Diffuser pressure drop	$<$ 1.5%
Premix module length	1.8 in.
Premix module heat load	40 $X10^6$ BTU/atm-cu.ft-hr.
Combustor volume heat load	16.4 $X10^6$ BTU/atm-cu. ft-hr
Pitch line diameter	14.45 in.
Combustor height	2.94 in.
Combustor length	7.35 in.
Combustor volume	.568 cu. ft.

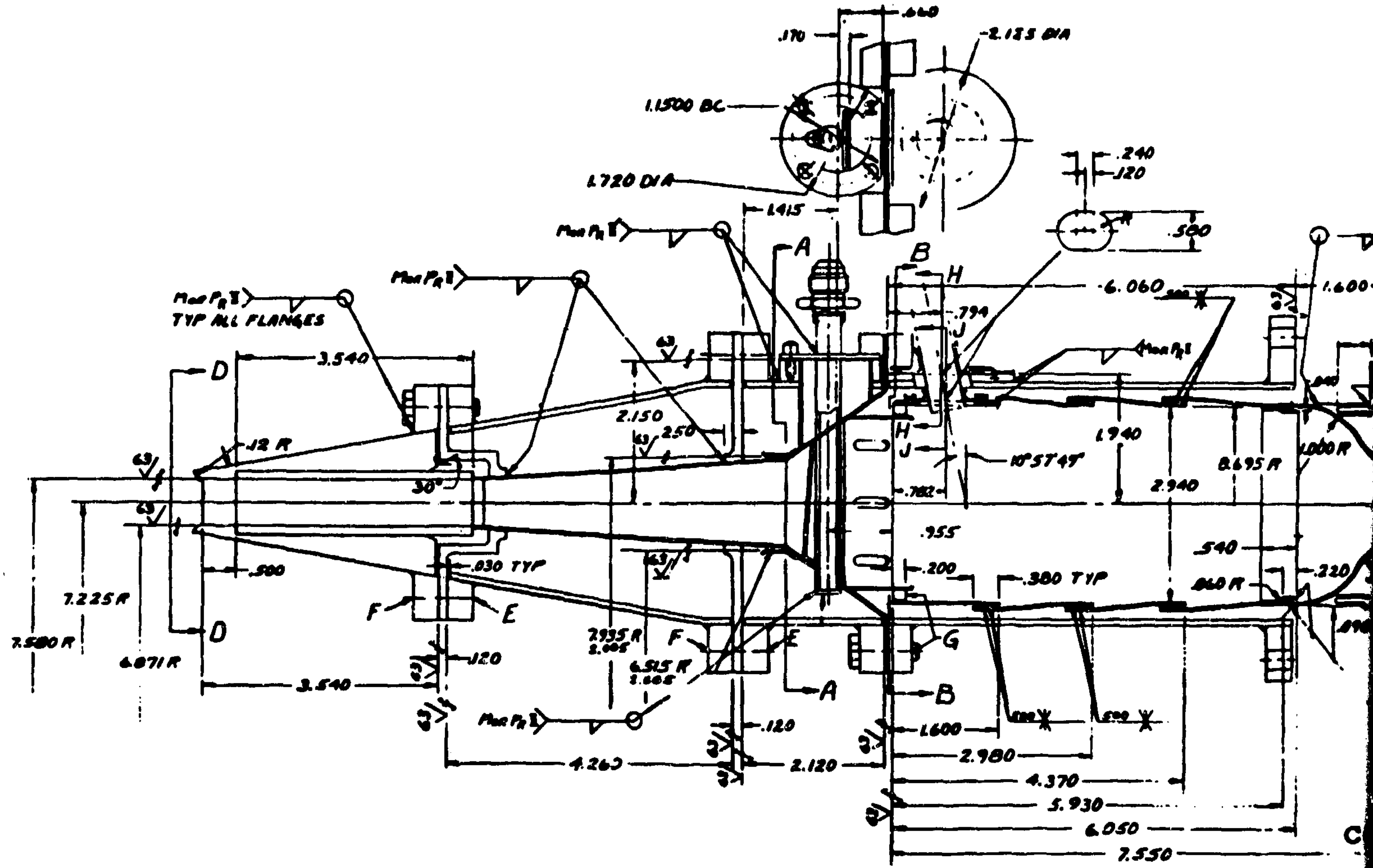

Figure 1. Complete flow path of the initial design components.

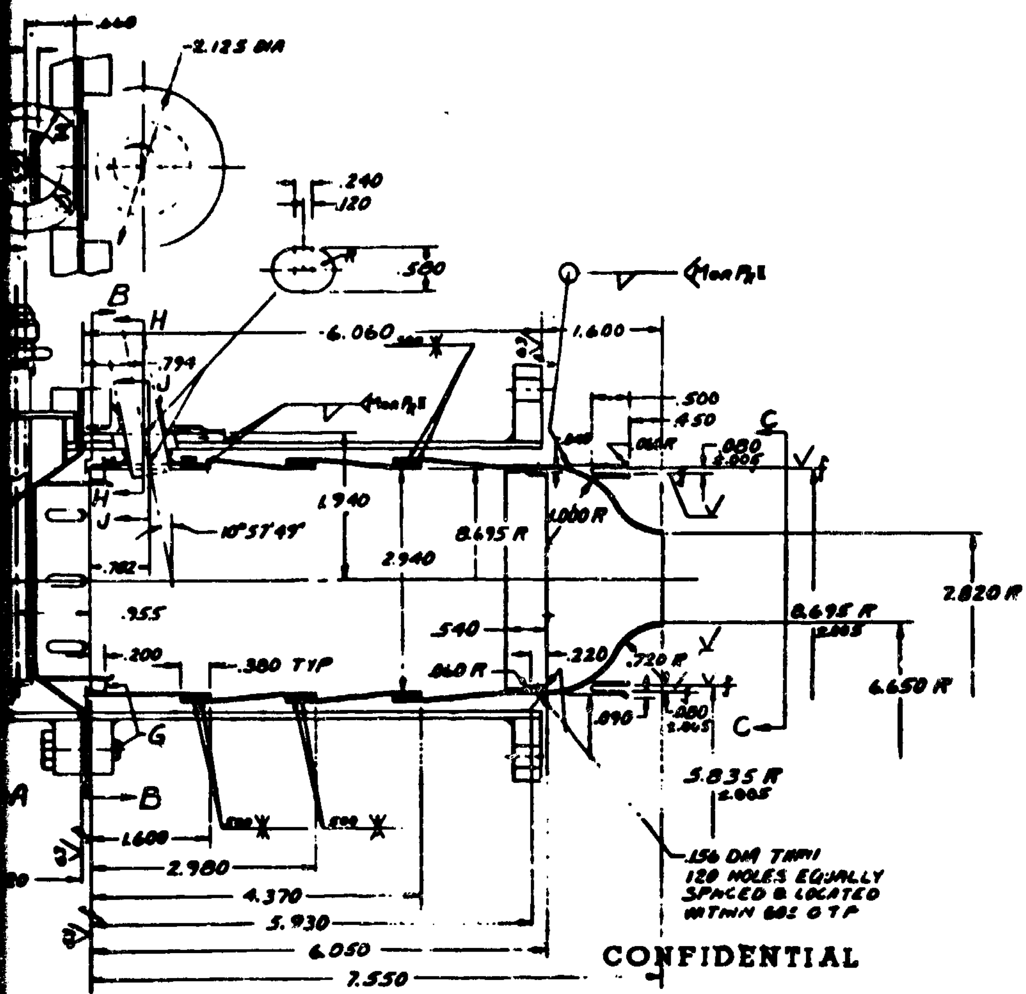

of the initial design components.

Combustor dome area	134.5 sq. in.
Combustor reference area	158 sq. in.
Combustor length/ height ratio	2.5
Combustor exit velocity-hot maximum	700 ft/sec
Combustor and module pressure drop	3.5%

(C) The use of premix fuel modules makes the combustion system conducive to scaling for other sizes. From the initial design a 4X size scaled sector version will be fabricated. This will be used to determine the effects of scaling on the diffuser, the premix modules, and the combustor. Figure 2 shows a comparison of the initial and scaled versions. This evaluation is a part of the Phase II portion of this program.

(C) The air velocity at the premix inlet was established at 304 ft/sec based on two considerations. These considerations were the pressure loss dumping into the combustor as described in Figure 3 and the small advantage which could be incurred by utilizing additional air energy for atomization as shown in Figure 4. The areas through the premix module, primary zone, and dilution air passages were designed to maintain the velocity of 304 ft/sec.

(C) The air flow to the combustor is a straight flow through the combustor head plate or dome. This flow path, in several annular combustors, has demonstrated an advantage in establishing a balanced primary zone and in reducing the diffuser length. The combustor was designed to reflect present technology as used with high pressure fuel atomizers. The combustor volume reflects a heat loading of 16.4 X 10^6 Btu/atm-cu.ft-hr. at a

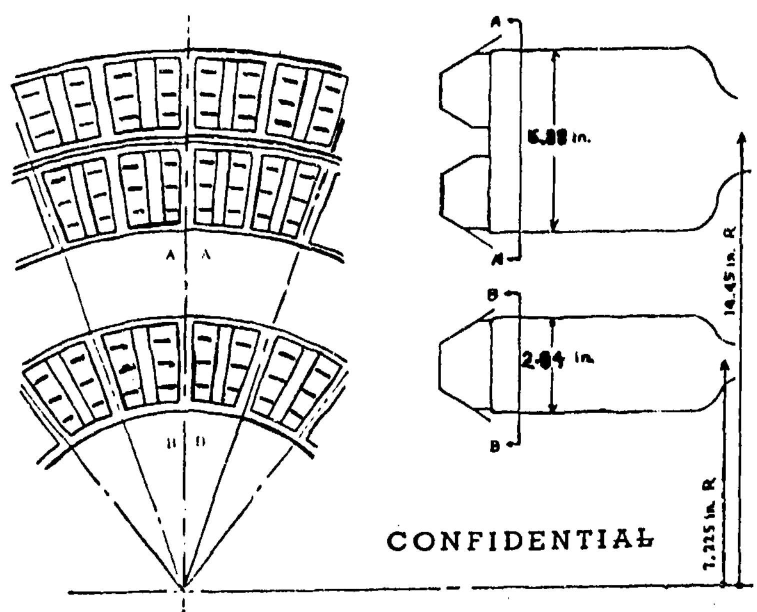

Figure 2. Scaling to 4X size using modular concept.

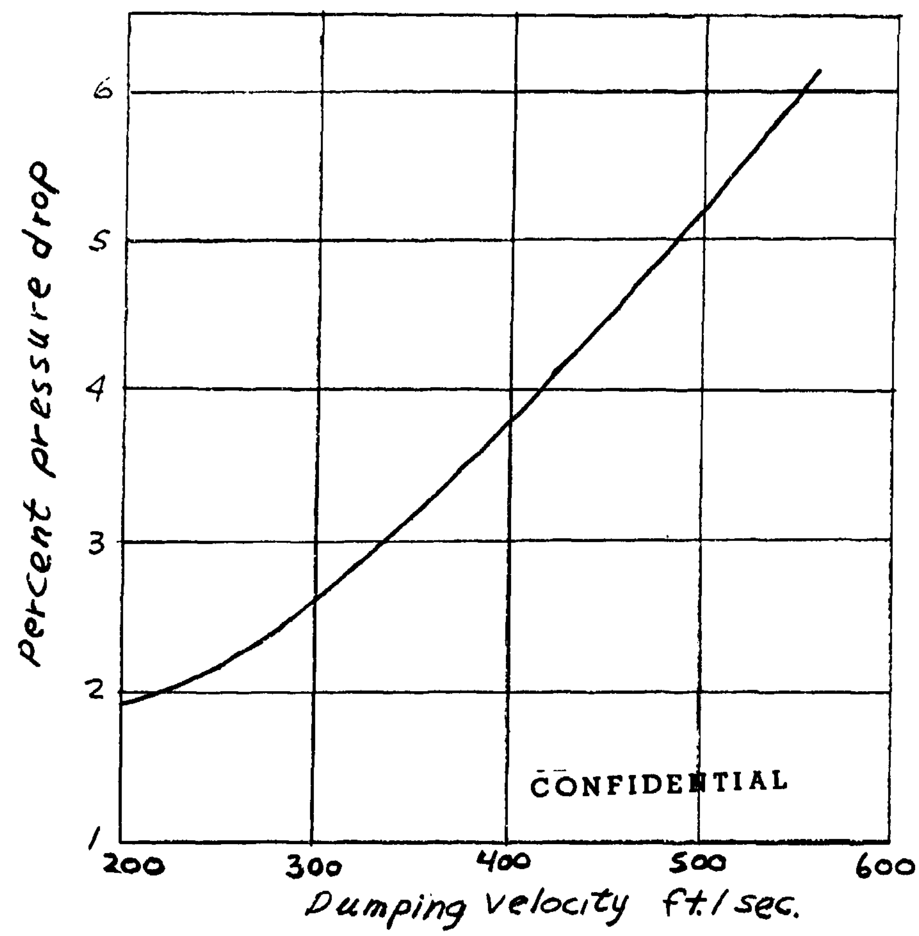

Figure 3. Estimated loss incurred in dumping diffuser discharge velocity.

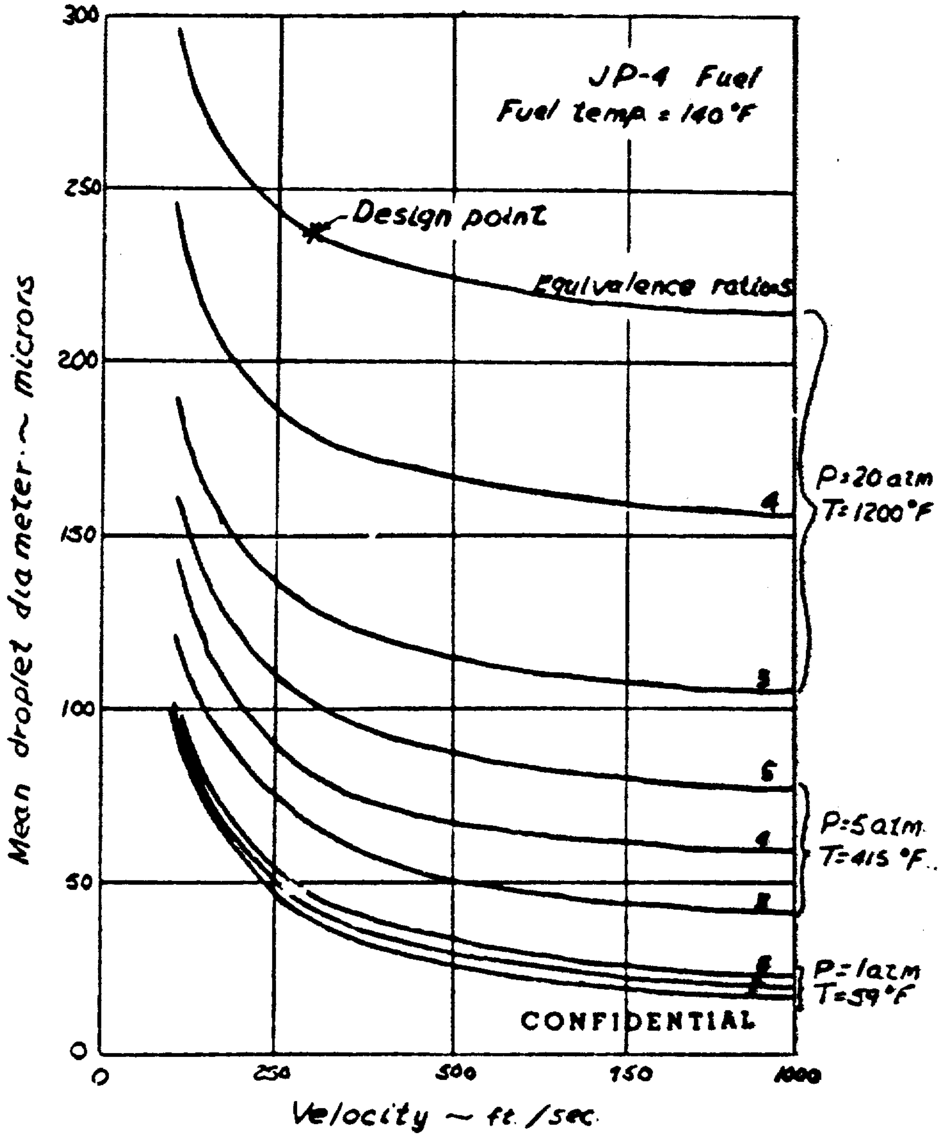

Figure 4. Mean droplet diameter versus atomization velocity for various equivalence ratios.

pressure of twenty atmospheres.

(C) The initial system was designed to permit replacement of each component for close evaluation of modifications and design limitations. Rig and component hardware for cold flow testing were designed to enable the comparative evaluation of changes leading to reduced diffuser length. The cold flow test rig was also designed to establish the variations in fuel atomization described by air velocity, air direction, and type of atomization surface. Hot or burning test equipment was designed to evaluate the reaction zone length, the mixing of the dilution air for temperature traverse quality, and the heat rejection to the side walls that accompanies the high dome flow premix reaction.

III INTEGRATED DIFFUSER-COMBUSTOR

1. Requirements

(C) The integration of the diffuser and combustor is to achieve minimum length and maximum aerodynamic efficiency. Selection of the integrated diffuser-combustor configurations was based on aerodynamic design studies. The evaluation of these configurations was based on diffuser performance characteristics as effected by variations in:

- Shape factor
- Mach number
- Flow factor
- Diffuser width to length ratio
- Axial area progression
- Inlet to exit area ratio

(C) This section describes the analytical design study of an integrated annular diffuser-combustor capable of recovering pressure with a mass flow of 64 lb/sec at a discharge pressure of 294 psia and a Mach number of 0.296. The major portion of the air flow (84%) is directed through the dome. The remaining portion (16%) is split in the upper passage (9%) and the lower passage (7%) and is used for combustor cooling.

2. Aerodynamic Design Studies

(C) A feasibility study was made with the following requirements as related to optimum engine and combustor performance:

- Shortest possible length
- Integration of air diffusing path within the fuel atomization module
- Low pressure loss
- Uniform velocity profile at the diffuser exit

(C) A parametric study was made of pressure recovery (C_p) versus width to length ratio ($N/\Delta R$) and inlet to exit area ratio. This was based on performance data collected from actual tests of many diffusers. This experience on performance of engine diffusers operating behind axial flow compressors was correlated with the work in References (1, 2, 3 and 4). This correlation includes the use of a radial velocity profile ratio ($V_{max}/V_{avg} = 1.15$) at the diffuser inlet. See Figure 5 for the typical engine diffuser radial velocity profile. The variations in performance resulting from an undesirable velocity profile at the inlet to the diffuser are shown in Figure 6. These curves were established as a result of correlated test data with theoretical research performance based on many different diffusers.

(C) The aerodynamic design studies led to the selection of four different diffuser designs. These diffusers must perform at a wide range of Mach numbers and provide a uniform circumferential exit velocity profile. The optima of diffuser geometry and peak pressure recovery correlations were established by taking the momentum losses and reaction rates, which affect the combustors, into consideration. The aerodynamic analysis includes the

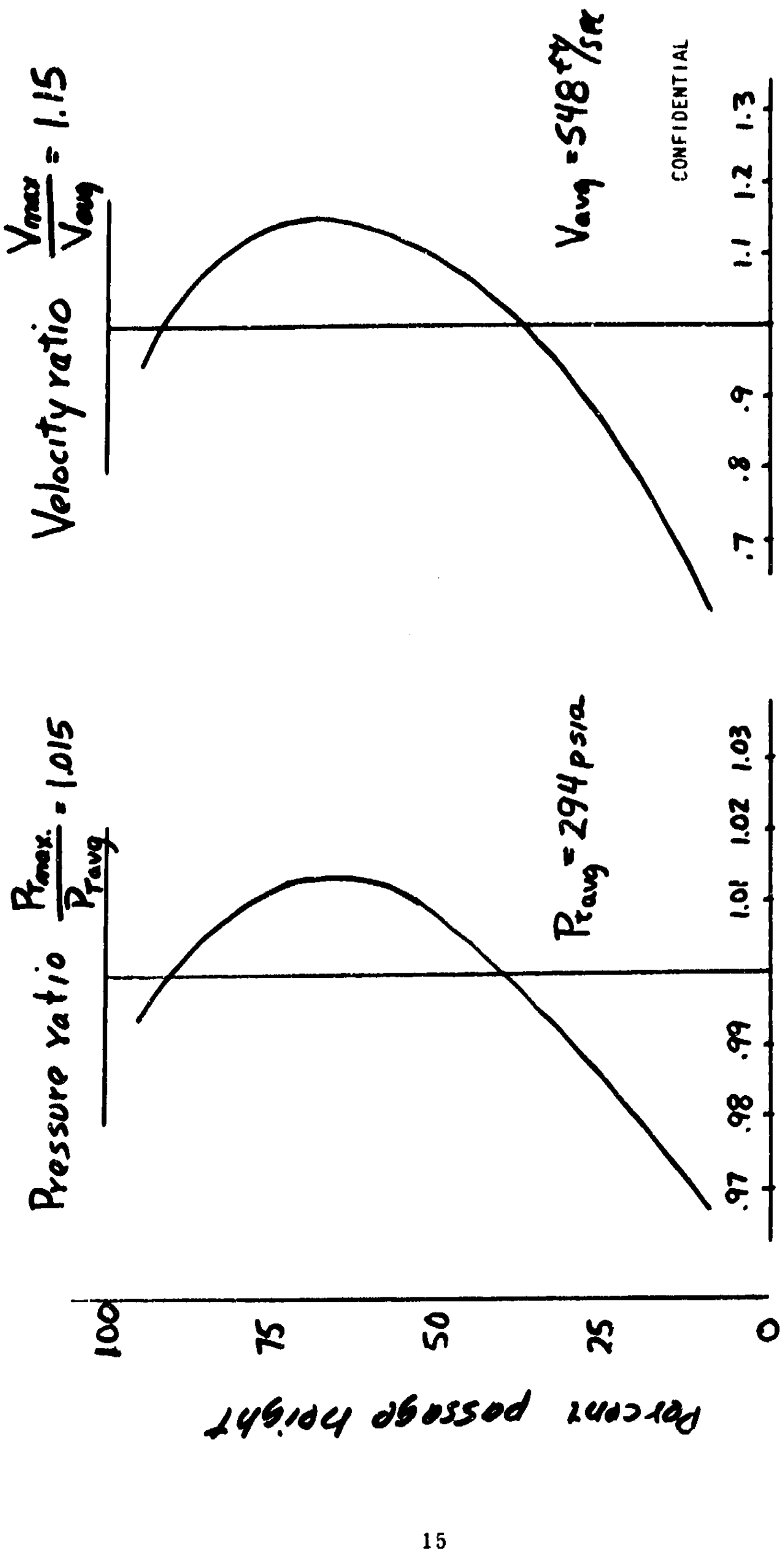

Figure 5. Predicted compressor discharge pressure and velocity profiles.

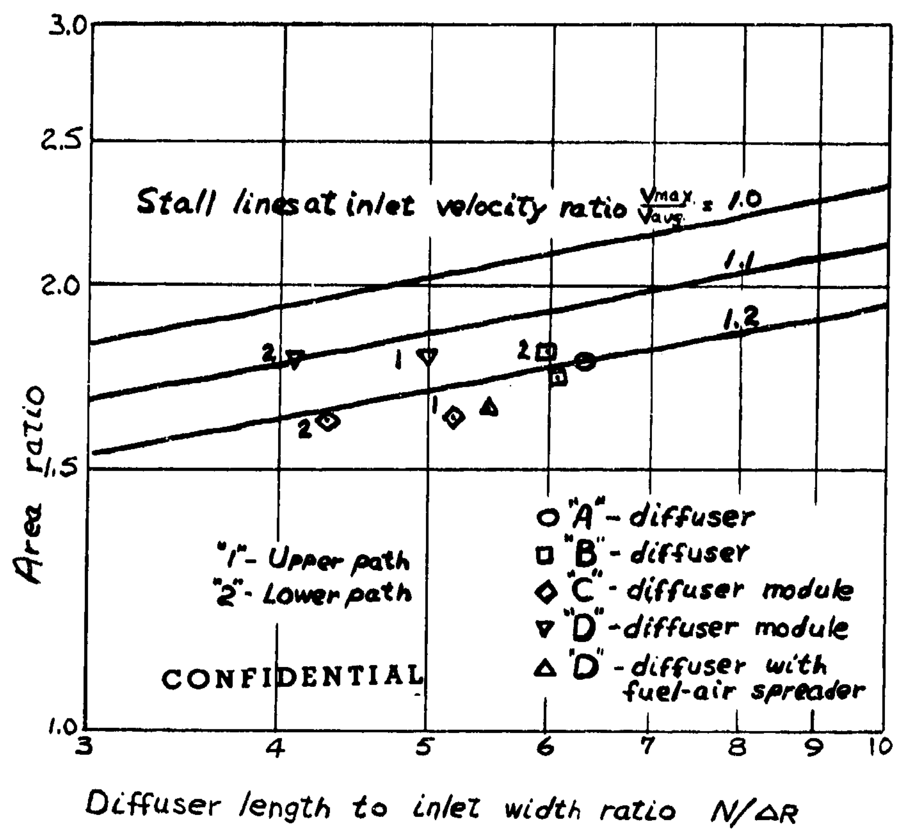

Figure 6. Diffuser performance data for "A", "B", "C", and "D" diffusers.

computed performances of the four diffuser designs.

3. Mechanical Design

(C) Four diffusers were designed. The first, an "A" diffuser is a single passage, straight dump, annular diffuser which is bounded on the inner and outer sides by a conical surface and has a cross-sectional form of a ring. This design is shown in Figure 7. The design parameters for optimum size and predicted performance are shown in Table II and Figures 8 and 9.

(C) The flow visualization rig with the "A" diffuser is shown in Figure 10. A straight section preceding the diffuser inlet provides a smooth inlet flow with symmetric boundary layers. Pressure distribution measurements are taken at the diffuser inlet and outlet. A five element pressure rake and two static pressure taps at each location give the pressure distribution for comparison with predicted analytical values. The installation of plastic models of the other diffuser designs provide similar data.

(C) The combustion rig with the "A" diffuser is also shown in Figure 7. The straight section and the diffuser section of this rig can be varied in length by the use of interchangeable sections. This will allow the diffuser angle to vary. This design allows a maximum number of test configurations with a minimum of hardware fabrication. All four diffusers will be tested on this rig. This

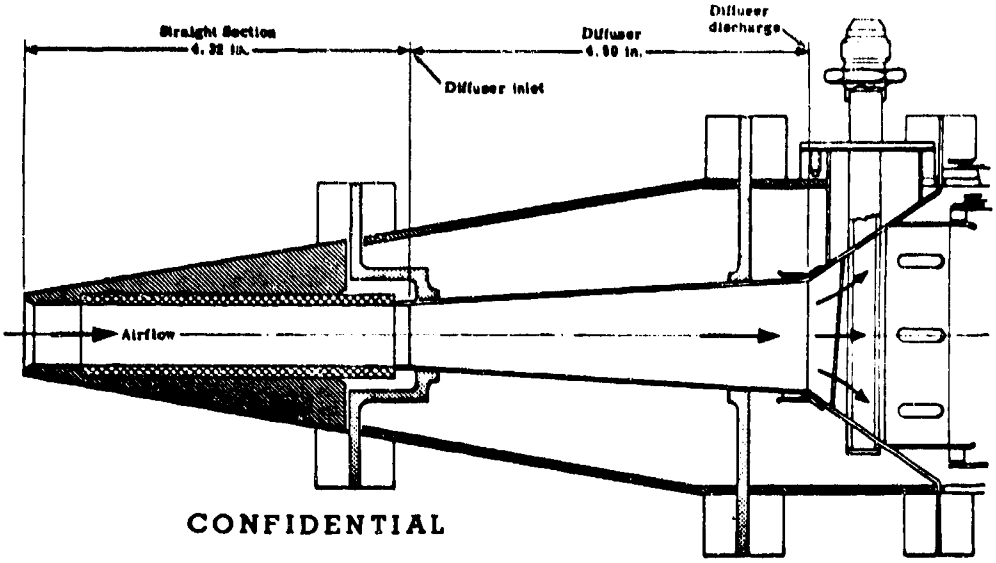

Figure 7. Combustion rig diffuser flow path.

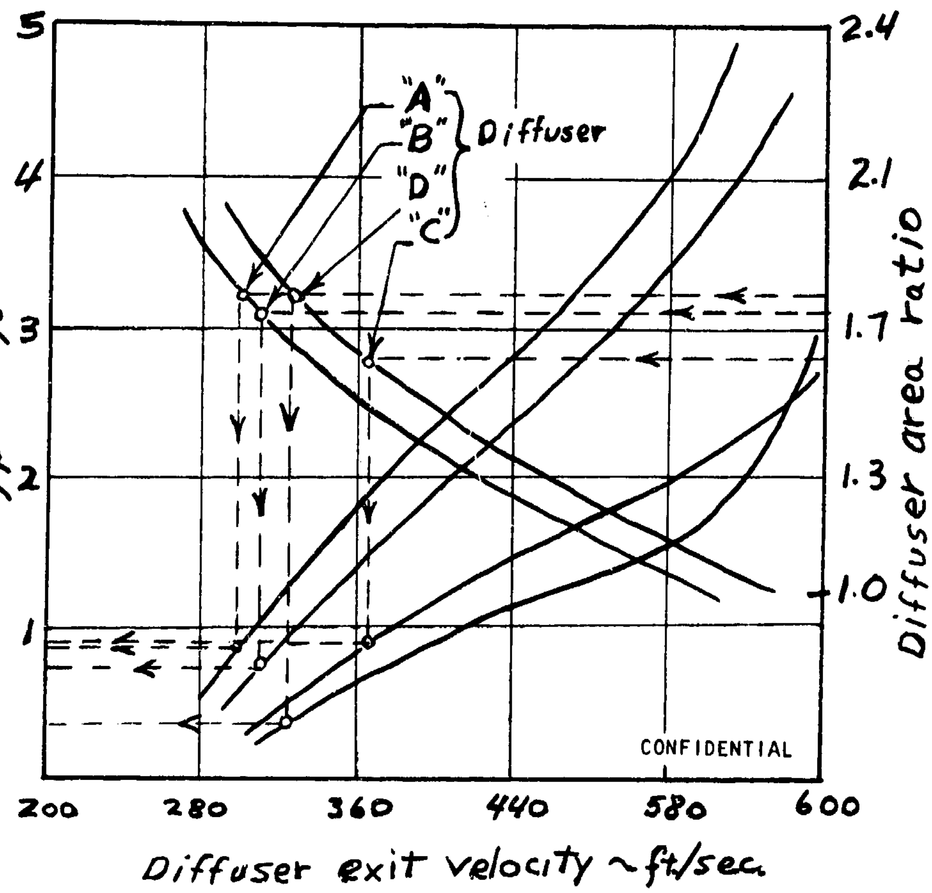

Figure 8. Estimated diffuser losses.

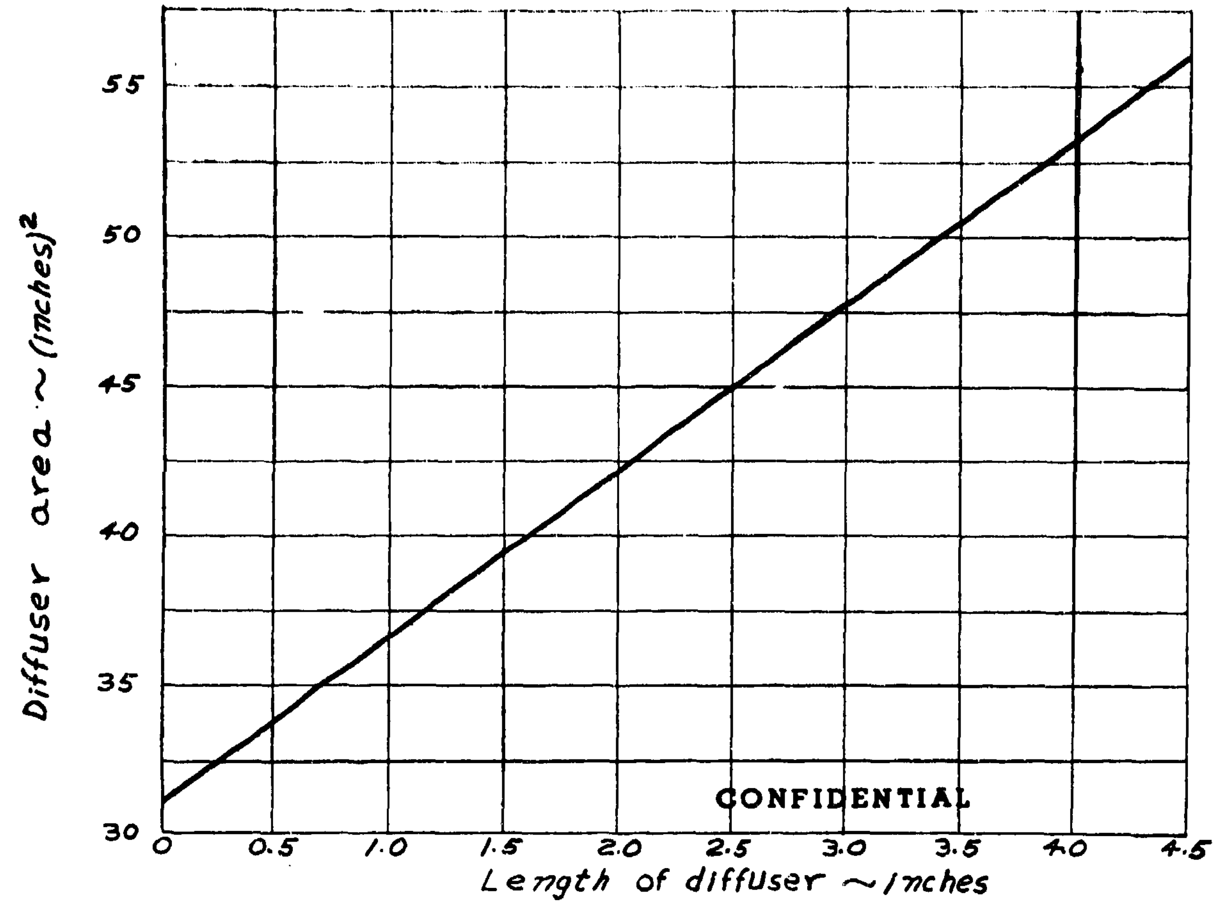

Figure 9. Diffuser area versus length of diffuser, "A"-diffuser.

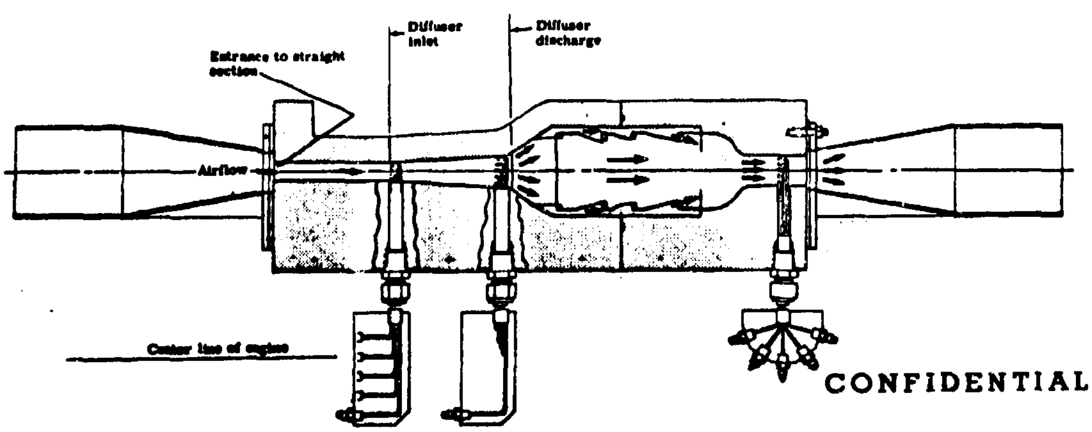

Figure 10. Flow visualization rig.

(C) Table I

"A": Annular single path dump diffuser with inlet vanes

Airflow	Wa lb/sec	64
Compressor discharge pressure	Pto psia	302.8
Diffuser inlet total pressure	Pt_1 psia	294.0
Diffuser inlet static pressure	P_{s1} psia	276.7
Diffuser inlet temperature	T_1 °R	1460
Diffuser inlet velocity avg.	V_1 Ft/sec	548
Diffuser inlet Mach number	M_{n1}	0.296
Diffuser inlet width	ΔR_1 in	.709
Diffuser inlet area	A_1 in^2	32.19
Diffuser length	N in	4.5
Diffuser length to inlet width ratio	$N/\Delta R$	6.35
Diffuser exit to inlet area ratio	AR	1.78
Diffuser inlet velocity ratio	Vmax/Vavg	1.15
Pressure recovery	C_p	40.5%
Diffuser discharge pressure	P_{t2} psia	288.9
Diffuser discharge pressure	P_{s2} psia	283.7
Diffuser outlet velocity	V_2 ft/sec	304
Diffuser outlet Mach number	M_{n2}	.163
Diffuser outlet area	A_2 in^2	57.29
Compressor exit vanes losses	$\frac{\Delta Pt}{Pto}$	3%
Total diffuser losses(including dumping loss)	$\frac{\Delta Pt}{Pt_1}$	2.63%

portion of the program is part of Phase II.

(C) The "B" diffuser as shown in Figure 11 is a two passage annular dump diffuser which has been shortened by the addition of circumferential splitters to accomodate scaling to 4X size These splitters are located through the compressor exit guide vanes to provide a mass air flow division at the plane where the compressor discharge profile is most uniform. The optimum size and predicted performance are based upon the specified design parameters in Table III and Figures 8 and 12.

(C) The "C" diffuser is a two passage, channeled diffuser and is shown in Figure 13. This design incorporates compressor exit vanes, diffuser, and fuel atomization modules in the shortest possible axial length. The splitter was added for performance improvement. This design also permits scaling to 4X size. The diffusion system consists of four major components. These are 120 compressor exit vanes, 1 circumferential splitter, 20 diffuser modules, and 20 fuel injection modules. As shown in Figure 13, the inlet consists of bellmouth double row vanes to ensure a smooth flow of air. The circumferential splitter divides the air passage into an upper and lower flow path. The side walls of the fuel injection modules serve as walls for the diffuser The airflow is allowed to diffuse in a mushroom type diffuser and is dumped into a quasi-plenum with a velocity of 365 ft/sec. Both upper and lower diffuser passages are designed to have the desired rate of diffusion based upon the analytical studies. The diffuser characteristics are shown in

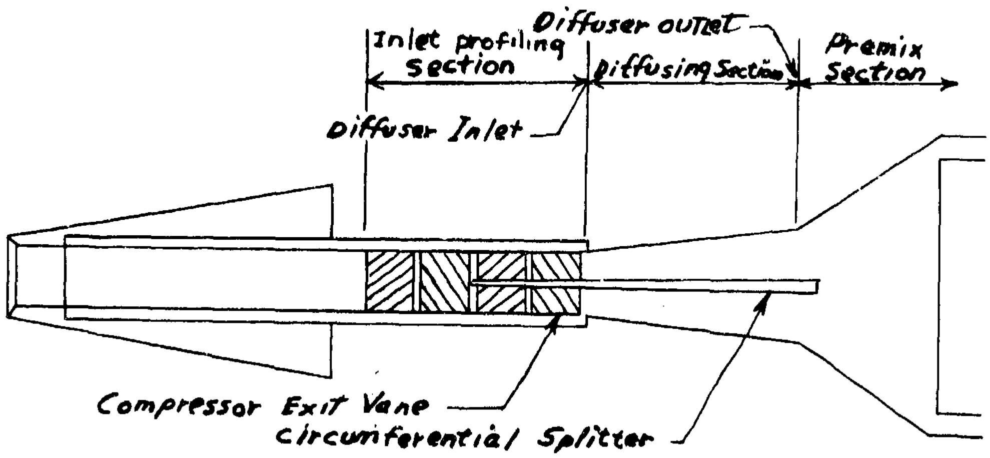

Figure 11. Combustion rig "B" diffuser flow path.

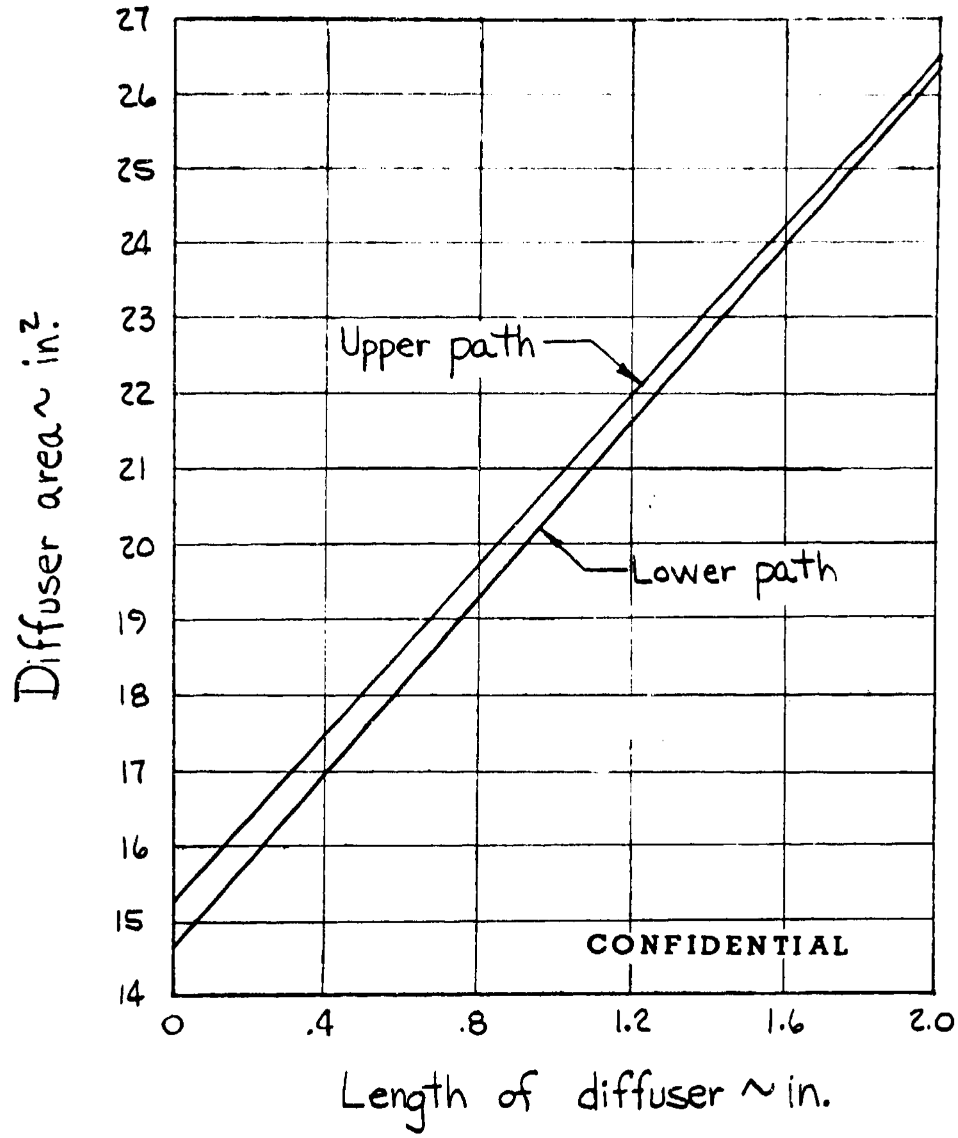

Figure 12. Diffuser area versus length of "B"-diffuser.

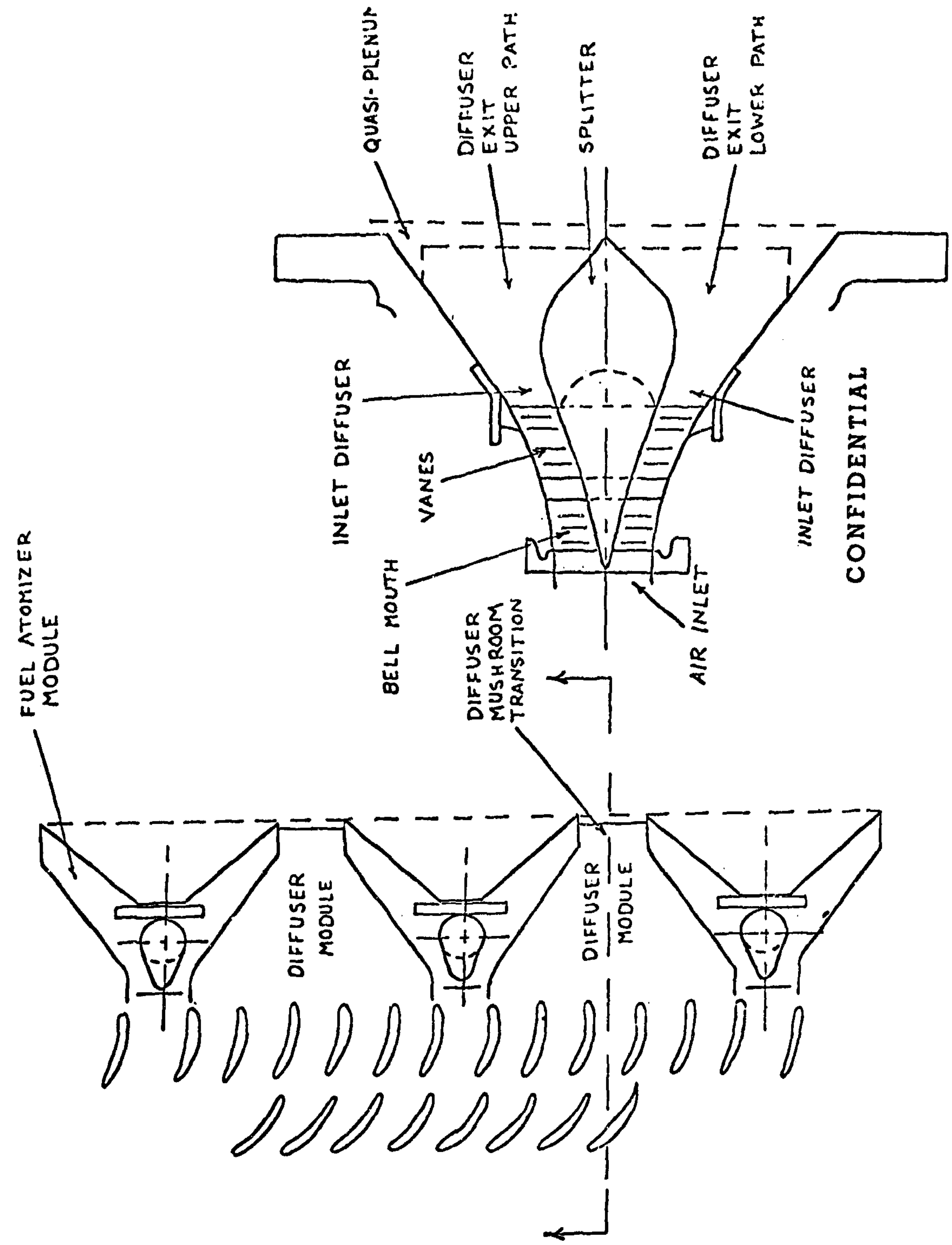

Figure 13. Combustor rig diffuser "C" flow path.

(C) Table III

"B": Annular two path dump diffuser with circumferential splitter and inlet vanes

	Path	Upper	Lower
Airflow	Wa lb/sec	33.3	30.7
Compressor discharge pressure	P_{t_0} psia	302.8	302.8
Diffuser inlet pressure	P_{t_1} psia	295	293
Diffuser inlet pressure	P_{s_1} psia	273.9	273.5
Diffuser inlet temperature	T_1 °R	1460	1460
Diffuser inlet velocity avg.	V_1 ft/sec	607	584
Diffuser inlet Mach number	M_{n_1}	.328	.315
Diffuser inlet width	ΔR_1 in	.3275	.3315
Diffuser inlet area	A_1 in^2	15.26	14.66
Diffuser length	N in	2.0	2.0
Diffuser length to inlet width ratio	$N/\Delta R$	6.1	6.0
Diffuser exit to inlet area ratio	AR	1.73	1.8
Diffuser inlet velocity ratio	Vmax/Vavg	1.1	1.1
Pressure recovery	C_p %	43.6	43.5
Diffuser discharge pressure	P_{t_2} psia	291.3	290.1
Diffuser discharge pressure	P_{s_2} Psia	283.1	282.0
Diffuser outlet velocity	V_2 ft/sec	375	375
Diffuser outlet Mach number	M_{n_2}	.202	.202
Diffuser outlet area	A_2 in^2	26.43	26.37
Compressor exit vanes losses	$\Delta Pt/P_{t_0}$ %	2.65	3.35
Total diffuser losses (including dump loss)	$\Delta Pt/P_{t_1}$ %	2.64	2.40

Table IV and Figures 8, 14, and 15.

(C) The "D" diffuser is also a two passage channeled diffuser and is similar in design principles to "C". The number of fuel injection modules was increased from 20 to 30 thereby changing the flow path distribution. The four major components of this diffuser version are 90 compressor exit vanes, 1 circumferential splitter, 30 diffuser modules, and 30 fuel injection modules. These fuel injection modules have upper and lower diffusing paths as shown in Figures 16 and 17. The "D" diffuser characteristics are shown in Table V and Figures 8, 18, and 19.

(C) Diffuser "A" was shown in Figure 7 with no compressor exit guide vanes in front. Figure 20 shows the "A" diffuser preceded by guide vanes. The compressor exit guide vanes are shown with "B" and "C" diffusers in Figures 11 and 13. Diffuser "D" is shown with compressor exit guide vanes in Figure 21. These guide vanes have proven in various combustion rigs to simulate closely the compressor exit velocity profile found in engines.

(C) The inlet tip and hub diameters remained the same for the four diffusers. The "A", "B", and "C" diffusers are preceded by 120 compressor exit guide vanes. For the "C" diffuser, the 120 vanes match with the use of the 20 fuel injection modules. For all diffusers, approximately 1/6 of the air passes through the fuel injector modules. For the "A" and "B" diffusers, the remaining 5/6 of the air is dumped into the plenums between each of the fuel modules and is directed into the main combustion chamber.

(C) Table IV

"C": Channeled two path diffuser with circumferential splitter and integrated bell-shaped inlet vanes passages

			Diffuser module		Fuel inj.module	
		Path	Upper	Lower	Upper	Lower
Airflow total	Watot	#/sec	27.75	25.58	5.55	5.12
Airflow per module	Wa	#/sec	1.388	1.279	.2775	.2560
Compressor discharge press	Pto	psia	302.8	302.8	302.8	302.8
Diffuser inlet pressure	Ptl	psia	295	293	295	293
Diffuser inlet pressure	Psl	psia	272.8	274.3	282	280
Diffuser inlet temperature	Ttl	°R	1460	1460	1460	1460
Diffuser inlet velocity	V1	ft/sec	623	570	486	485
Diffuser inlet Mach number	M_{n1}		.336	.308	.262	.261
No. Diffuser modules			20	20		
No.Fuel atomiz.modules					20	20
Diffuser inlet width	ΔR_1	in	.291	.354		
Diffuser length	N	in	1.5	1.5		
Diffuser length to width ratio	$N/\Delta R_1$		5.2	4.3		
Diffuser inlet area	A_1	in^2	.622	.624	.155	.145
Diffuser inlet velocity ratio	Vmax/Vavg		1.1	1.1	1.1	1.1
Diffuser discharge press.	Pt_2	psia	292.3	290.8		
Diffuser discharge press.	P_{s2}	psia	284.4	284.2		
Diffuser outlet velocity	V2	ft/sec	370.	350.		
Diffuser out Mach number	M_{n2}		.199	.184		
Diffuser outlet area	A_2	in^2	1.01	1.01		

(U) TABLE IV (con't)

		Path	Diffuser module Upper	Diffuser module Lower	Fuel inj. module Upper	Fuel inj. module Lower
Diffuser outlet to inlet area ratio	AR		1.63	1.62		
Pressure recovery	C_p	%	52.4	52.5		
Losses through compressor exit vanes	$\Delta P/Pt_1$	%	2.65	3.35	2.65	3.35
Total losses including dumping per (1) module	$\Delta P/Pt_1$	%	2.25	1.87	2.20	2.22
Total annular diff. losses	$\Delta P/Pt_1$		1.7			
Total annular premix entrance losses	$\Delta P/Pt_1$				.4	

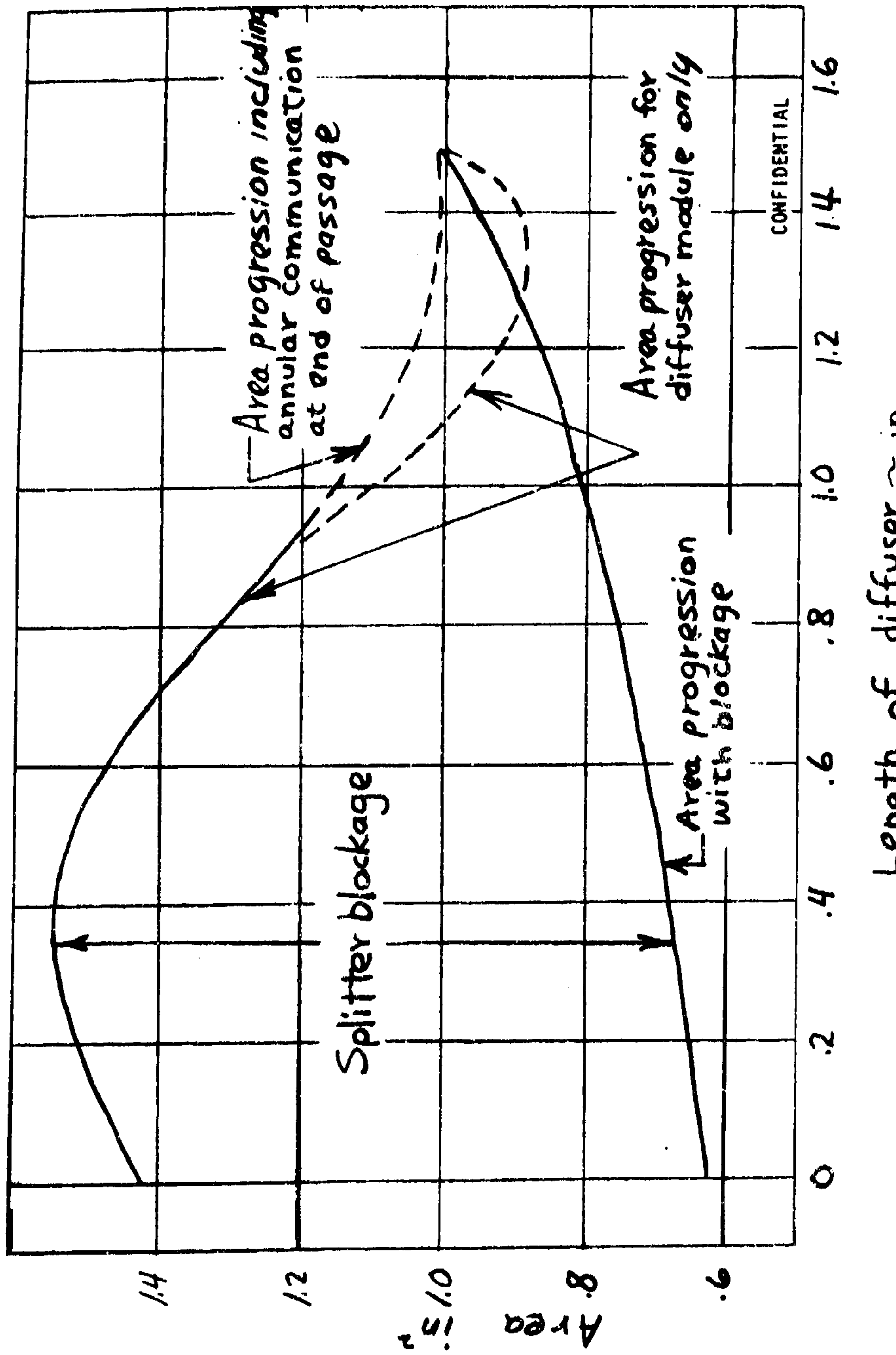

Figure 14. Area progression versus diffuser length "C"-diffuser, upper path.

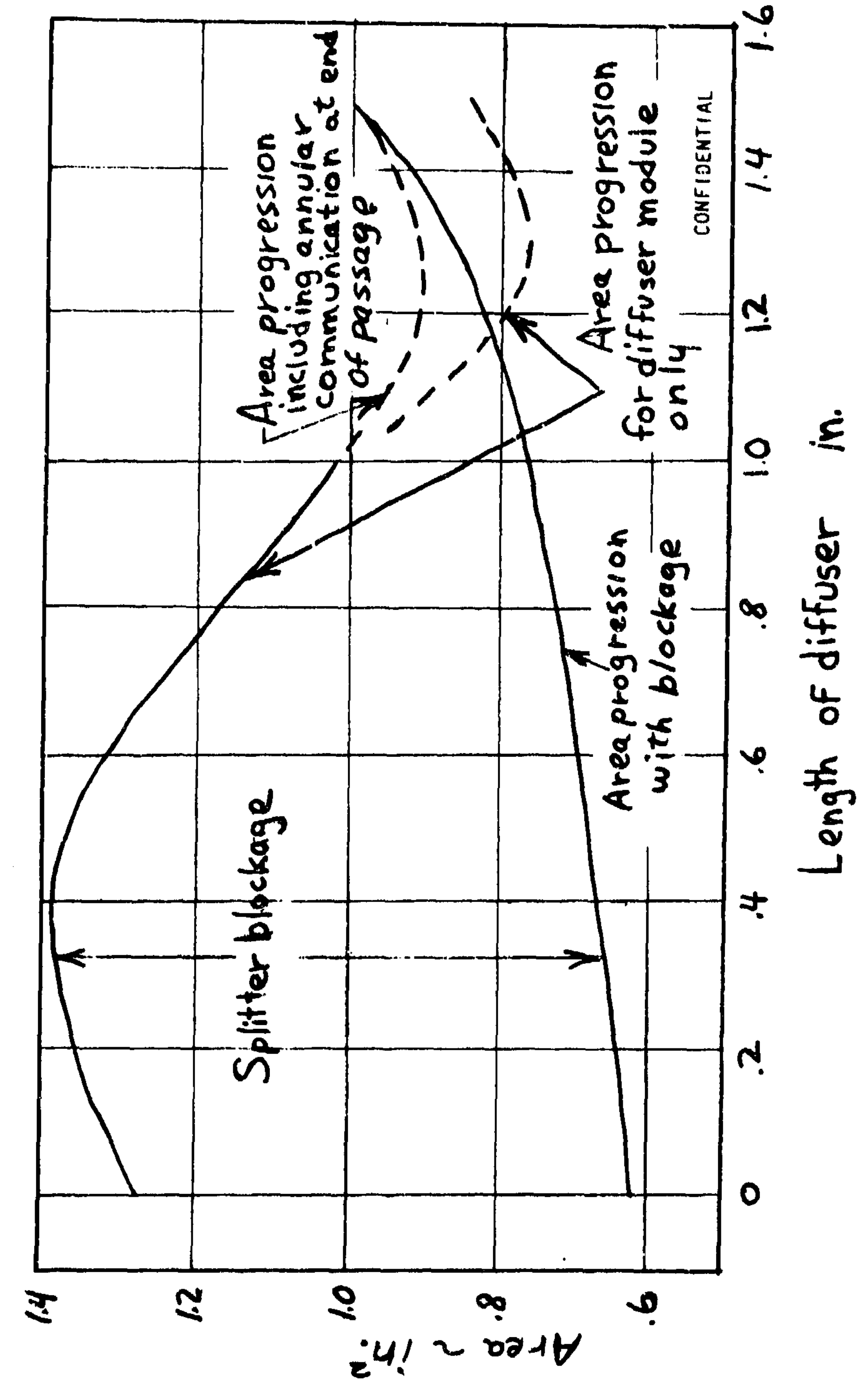

Figure 15. Area progression versus diffuser length "C"-diffuser, lower path.

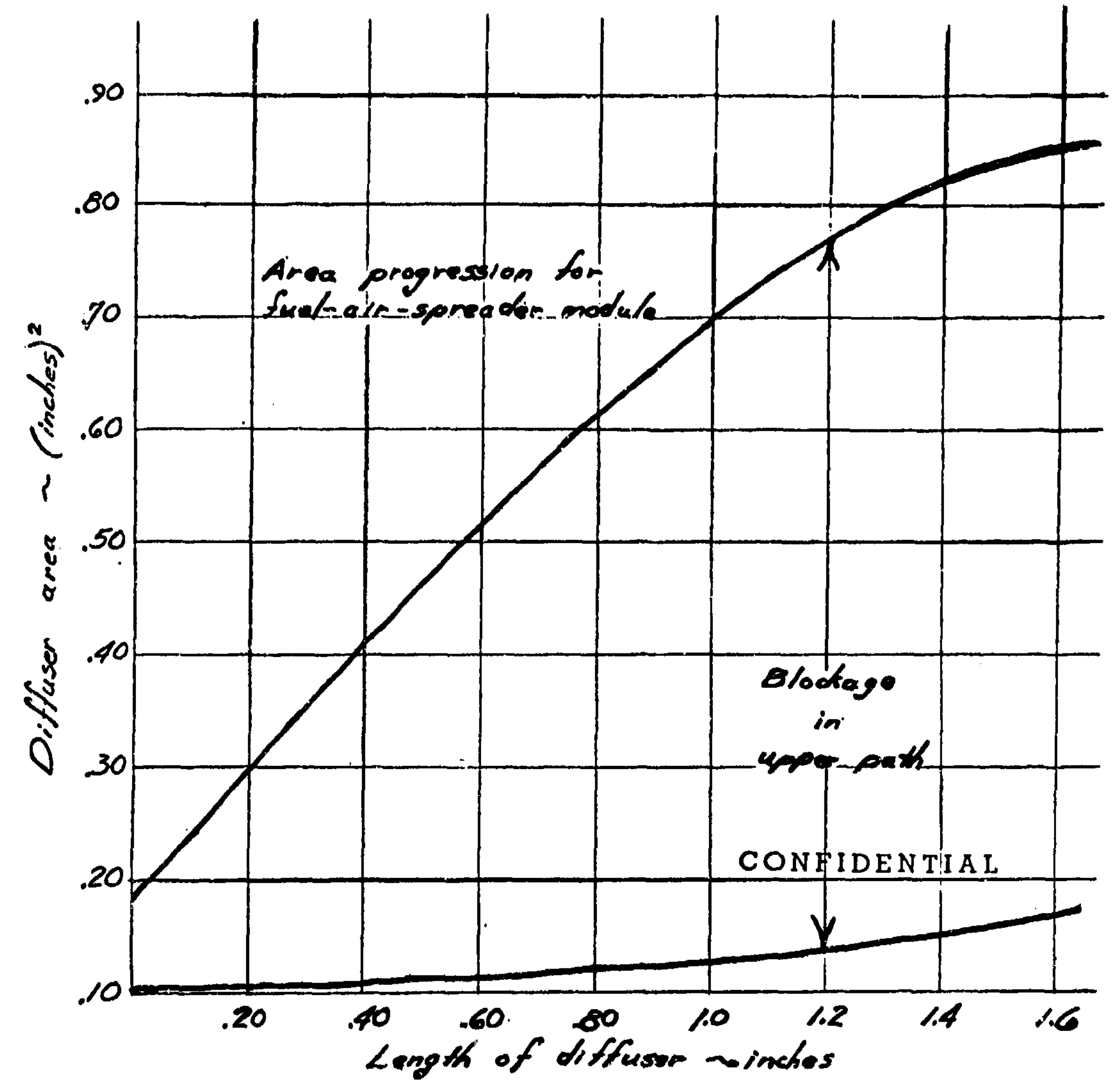

Figure 16. Diffuser area versus length of diffuser "D"-diffuser, fuel-air spreader module, upper path.

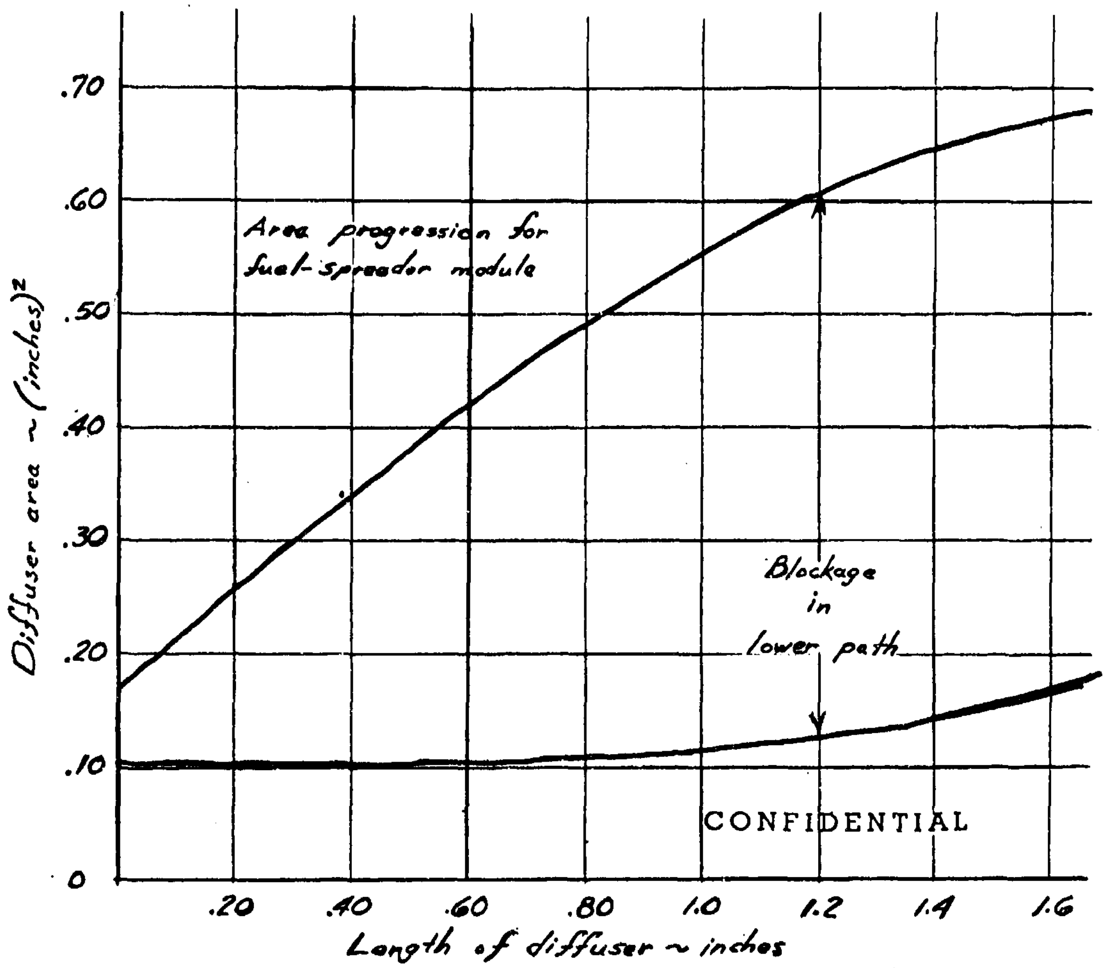

Figure 17. Diffuser area versus length of diffuser "D"-diffuser, fuel-air spreader module, lower path.

(C) Table V

"D": Channeled two path diffuser

		Path	Diffuser Diff. Module Upper	Diffuser Diff. Module Lower	Diff Channel Upper	Diff Channel Lower	Fuel vapor Module Upper	Fuel vapor Module Lower
Airflow total	W_{atot}	#/sec	22.2	20.46	5.55	5.12	5.55	5.12
Airflow per module	W_a^x	#/sec	.740	.681	.185	.170	.185	.170
Compressor discharge press	P_{to}	psia	302.8	302.8	302.8	302.8	302.8	302.8
Diffuser inlet pressure	P_{T_I}	psia	295.	293	295	293	295	293
Diffuser inlet pressure	$\dot{P}_{S_I}$	psia	272.5	274.5	276.1	277.5	281	279.5
Diffuser inlet temperature	T_I	°R	1460	1460	1460	1460	1460	1460
Diffuser inlet velocity	V_I	ft/sec	622	570	570	520	490	485
Diffuser inlet Mach number	M_{n1}		.338	.307	.307	.280	.269	.261
No. Diffuser modules			30	30				
No. Fuel atomiz. modules					30	30	30	30
Diffuser inlet width	R_1	in	.291	.354	.30	.30		
Diffuser length	N	in	1.45	1.45	1.65	1.65		
Diff. length to inlet width ratio	$N/\Delta R_1$		5.0	4.1	5.5	5.5		
Diffuser inlet area	A_1	in^2	.3319	.333	.1030	.1032		
Diffuser inlet veloc. ratio	$\frac{V_{max}}{V_{avg}}$		1.1	1.1	1.1	1.1	1.1	1.1

(C) Table V (con't)

		Path	Diffuser: Diff. Module Upper	Diffuser: Diff. Module Lower	Diffuser: Diff. Channel Upper	Diffuser: Diff. Channel Lower	Fuel vapor Module Upper	Fuel vapor Module Lower
Diffuser Discharge Press	P_{T_2}	psia	292.8	291.3	291.5	290.5		
Diffuser Discharge Press	P_{S_2}	psia	286.1	285.6	286.3	285.1		
Diffuser outlet velocity	V_2	ft/sec	338	316	300	307		
Diffuser outlet Mach number	M_{n_2}		.182	.169	.161	.164		
Diffuser outlet area	A_2	in^2	.590	.595	.167	.151		
Diff. Outlet to inlet area ratio	AR		1.78	1.78	1.65	1.65		
Pressure recovery	C_p	%	60.5	60.4	54	49		
Losses through compr. exit vanes	$\Delta P/P_{T_1}$	%	2.65	3.35	2.65	3.35	2.65	3.35
Total losses including dumping per one (1) module	$\Delta P/P_{T_1}$	%	1.50	1.23	1.77	1.46	2.37	2.30
Total annular diffuser losses	$\Delta P/P_T$	%	.91		.54			
Total annular premix entrance losses	$\Delta P/P_{T_1}$	%					.4	

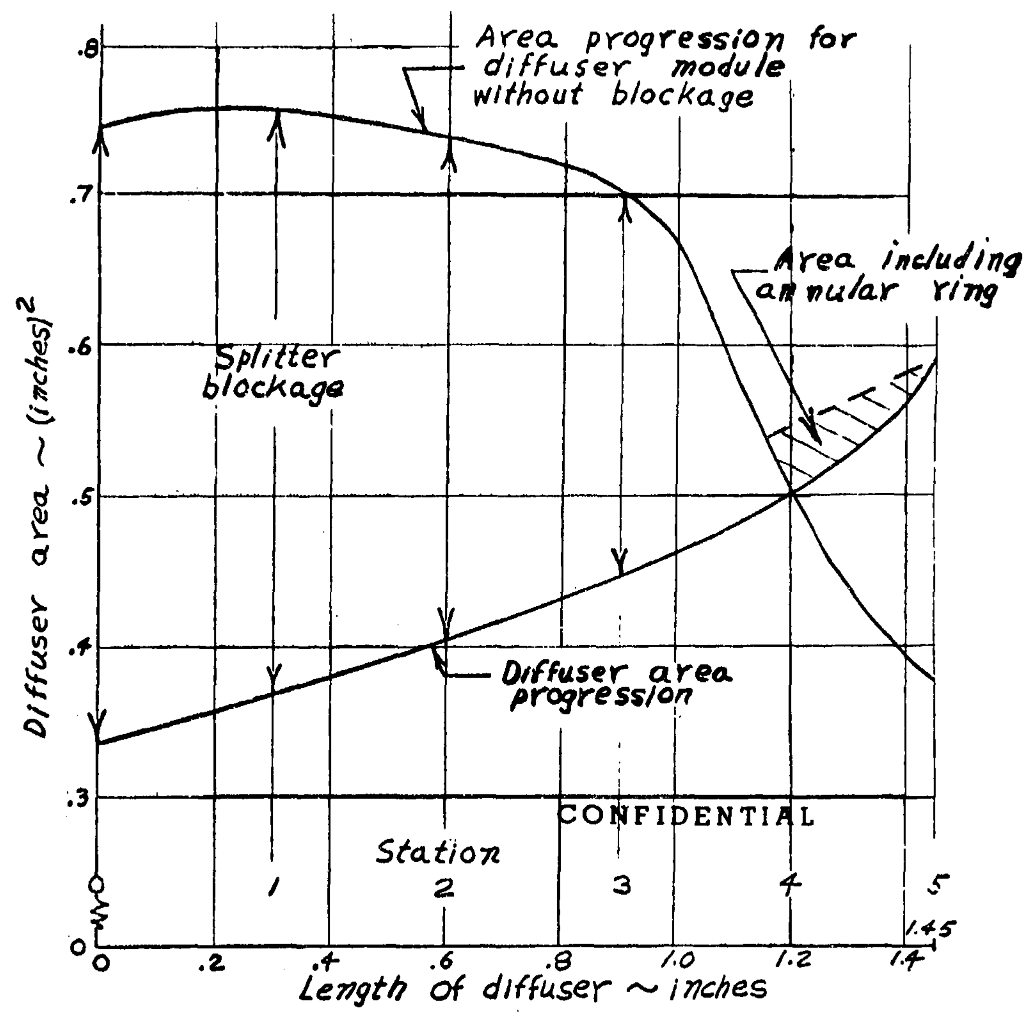

Figure 18. Upper path of "D"-diffuser area versus length of diffuser.

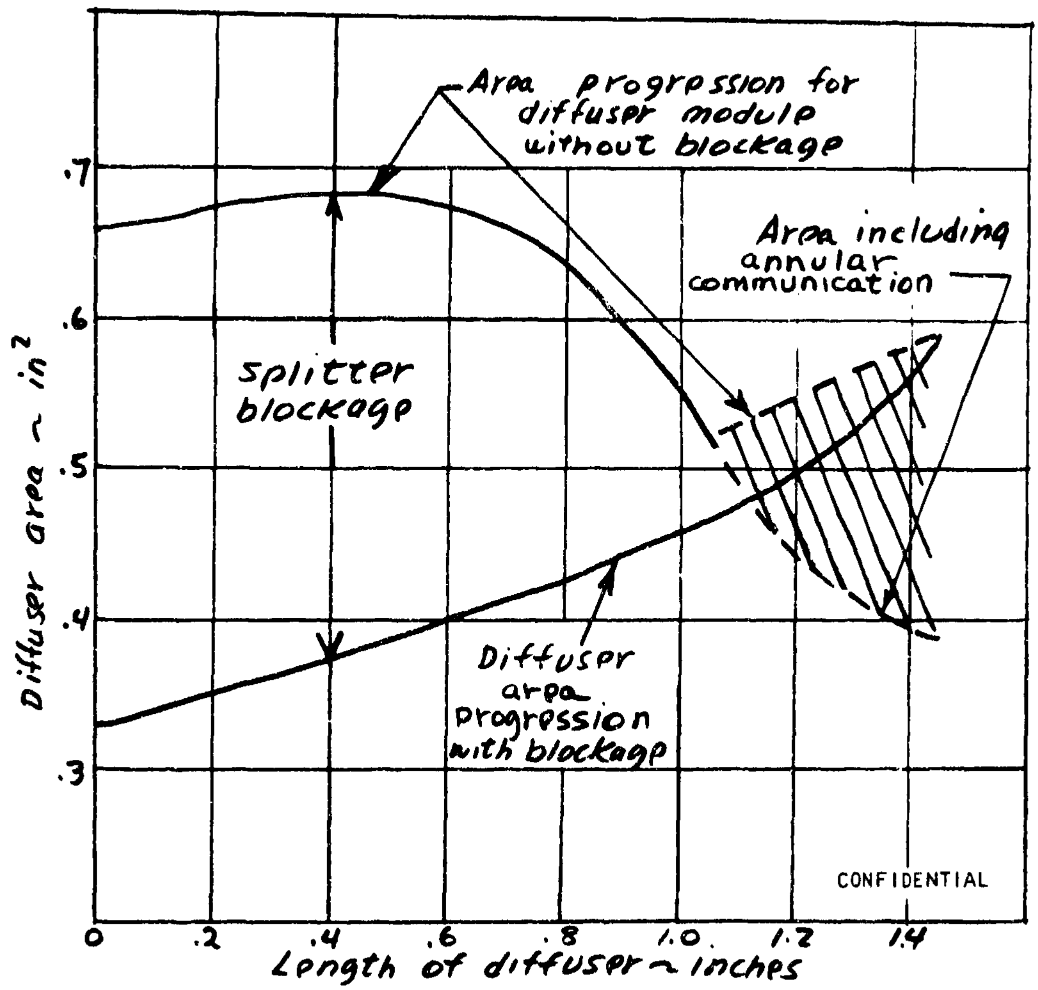

Figure 19. Lower path of "D"-diffuser area versus length of diffuser.

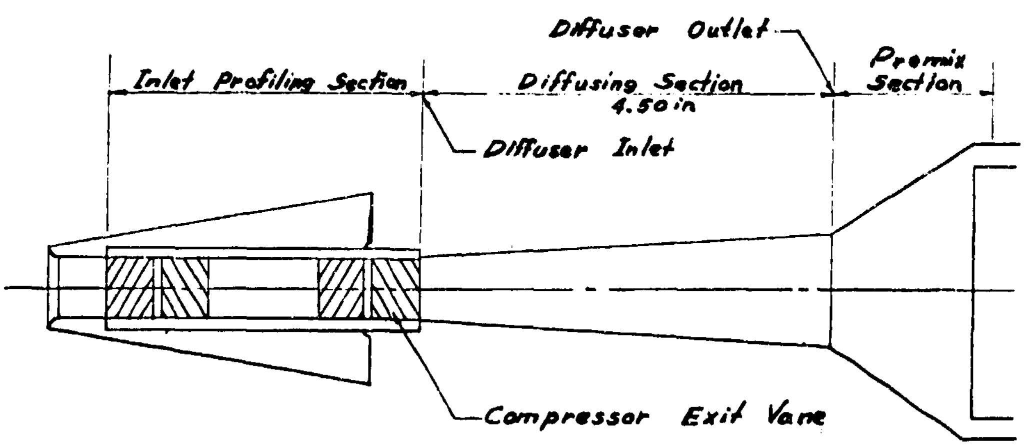

Figure 20. Combustion rig "A" diffuser flow path.

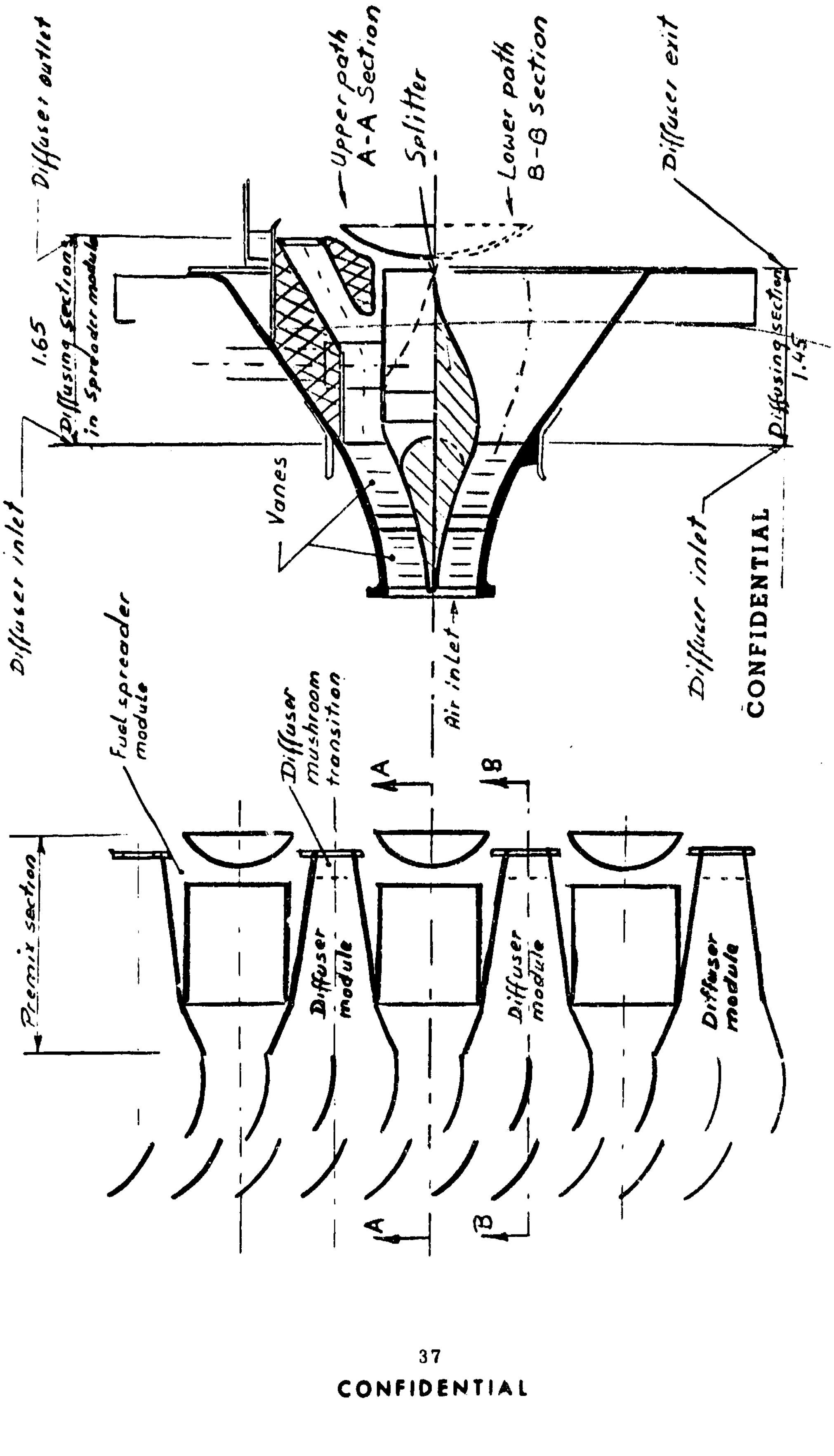

Figure 21. Combustion rig "D" diffuser flow path.

In the "C" diffusers these plenums have the shape of small channeled diffusers. This can be seen in Figure 13. In order to accommodate the 30 fuel injection modules used with diffuser "D", it was necessary to reduce the number of compressor exit vanes to 90 to maintain a match between vanes and modules. The use of 90 vanes results in a better pressure and velocity distribution entering the passage, in a reduction of frontal area blockage, and in an improvement of flow.

4. Design Criteria and Predicted Performance

(C) The design of the integrated diffuser-combustor was to have minimum axial length, which was not to be changed during size scaling. The circumferential splitter was incorporated into three of the four designs to provide a more uniform velocity profile and a better diffuser efficiency, and to permit scaling up to 4X size with no increase in axial length. Peak diffuser performance is vital in connection with the fuel injection module concept because a higher kinetic energy must be converted into pressure in this portion of the system. To assure maximum performance, the following factors must be incorporated:

- Minimum friction (short length and rapid deceleration)
- Minimum boundary layer thickness (short length and slow deceleration)
- Retarded separation (slow deceleration)
- Maximum diffusing (rapid deceleration and long length)

(C) These factors are contradictory. Therefore the determination of an optimum combination is necessary. The optimum recovery of these diffusers was investigated and the influence of the velocity inlet profile on the pressure recovery was considered in this investigation. The correlated design curves shown in Figure 6 were chosen to calculate the overall efficiency of these four diffuser systems. The results are given in the tabulated characteristics for each diffuser. From Figure 6, the predicted performance points of the four diffuser designs are obtained. The best performance is the "D" diffuser with an inlet to exit area ratio (AR) of 1.78 and a width to length ratio ($N/\Delta R$) of 5.0 for the upper passage and an AR of 1.78 and $N/\Delta R$ of 4.1 lower passage.

5. Analysis

(C) One of the important factors in the determining of any diffuser is the variation of the cross-sectional area with the path length. This variation in the passage width progresses along a mean line which is a curved arc lying in an axial plane. See Figures 13 and 21. To gain some insight into the manner in which the pressure and velocity might be expected to change along the length of such a diffuser, calculations were made for two-dimensional flow. In Figure 22 the ratio of static-to-total-pressure and the Mach number are plotted against path length for the case where the inlet Mach number is 0.3. This is for the "A" diffuser. The same calculations are repeated for the other three diffuser versions, "B", "C", and "D" and are shown in Figures 23 through 28.

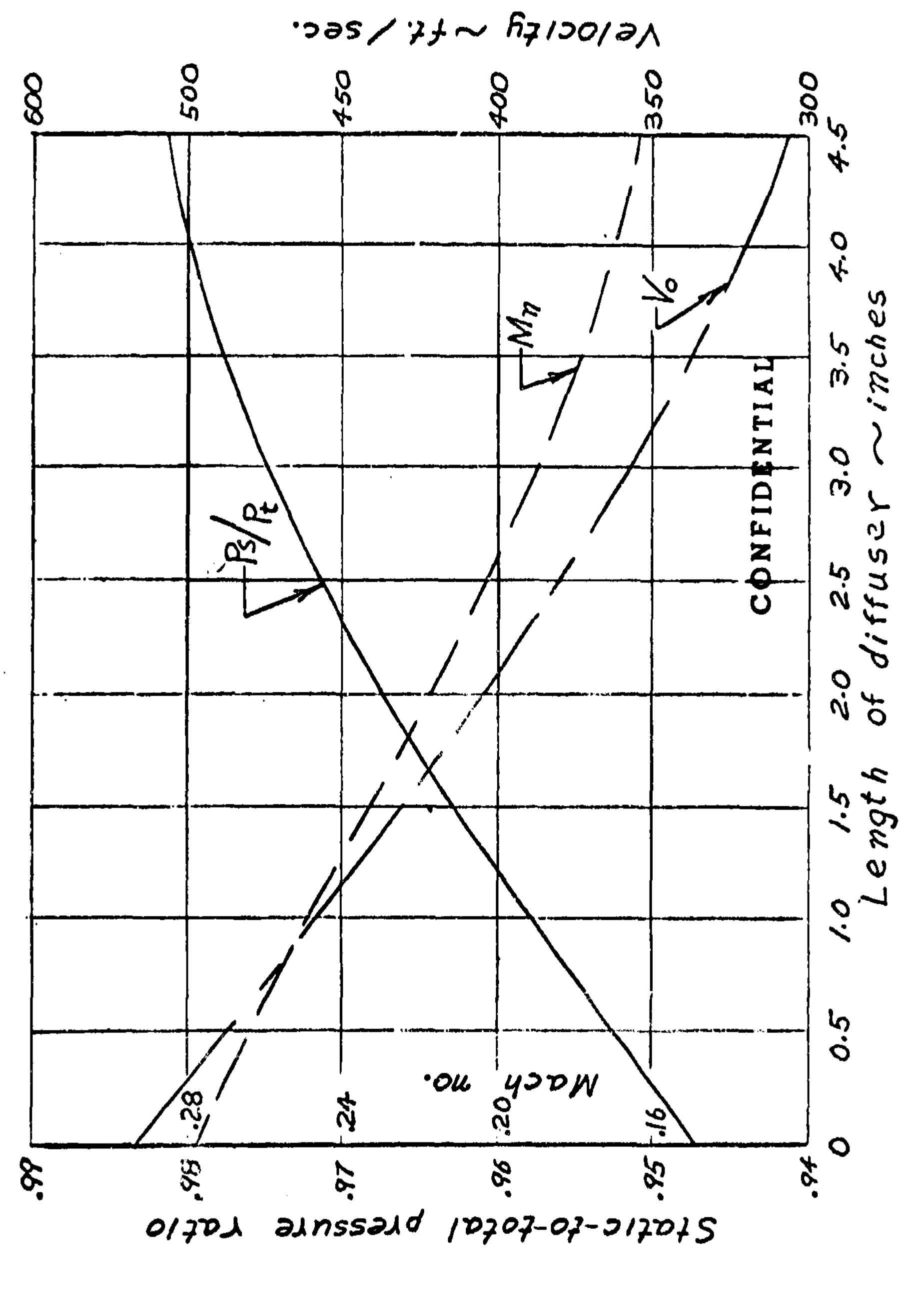

Figure 22. Diffuser parameters versus length of diffuser, "A"-diffuser.

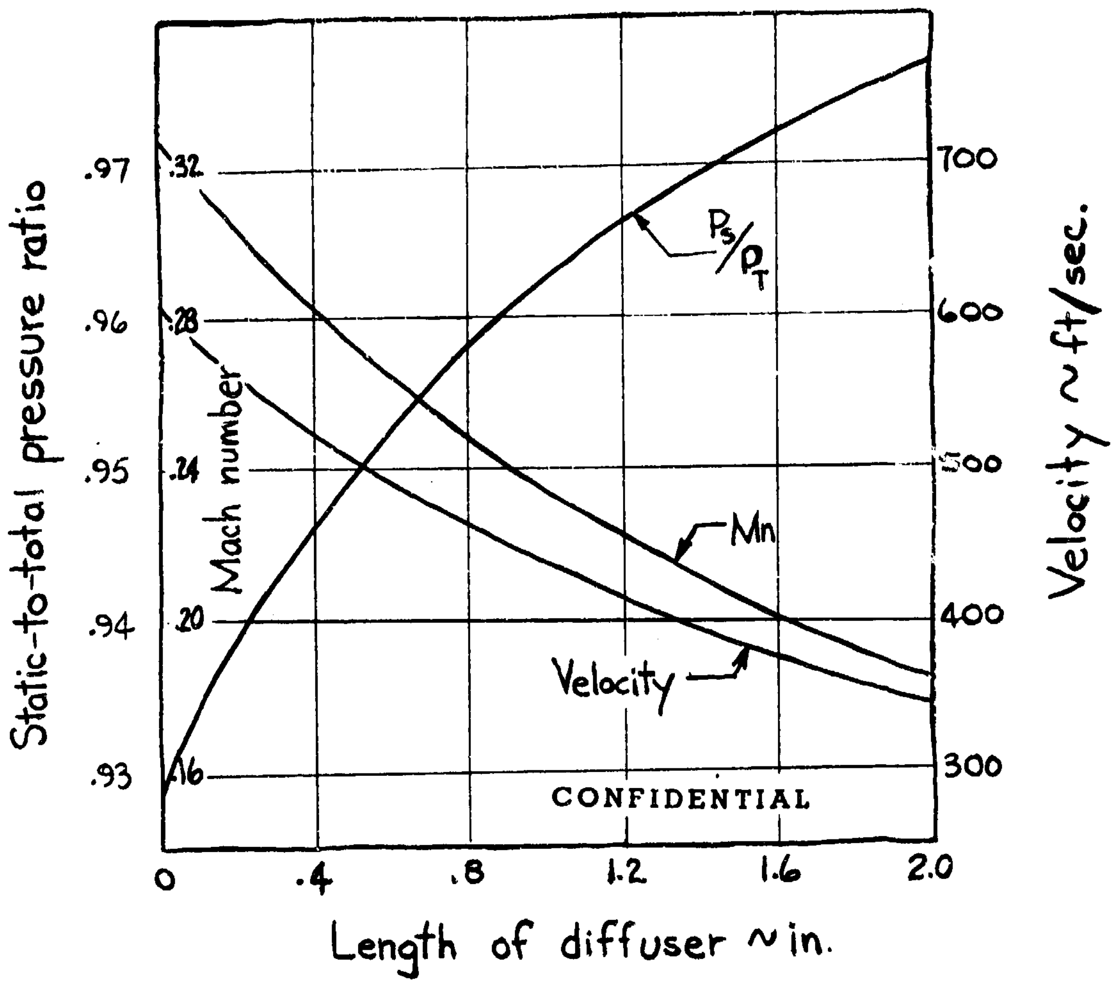

Figure 23. Diffuser parameters versus length of diffuser, "B"-diffuser, upper path.

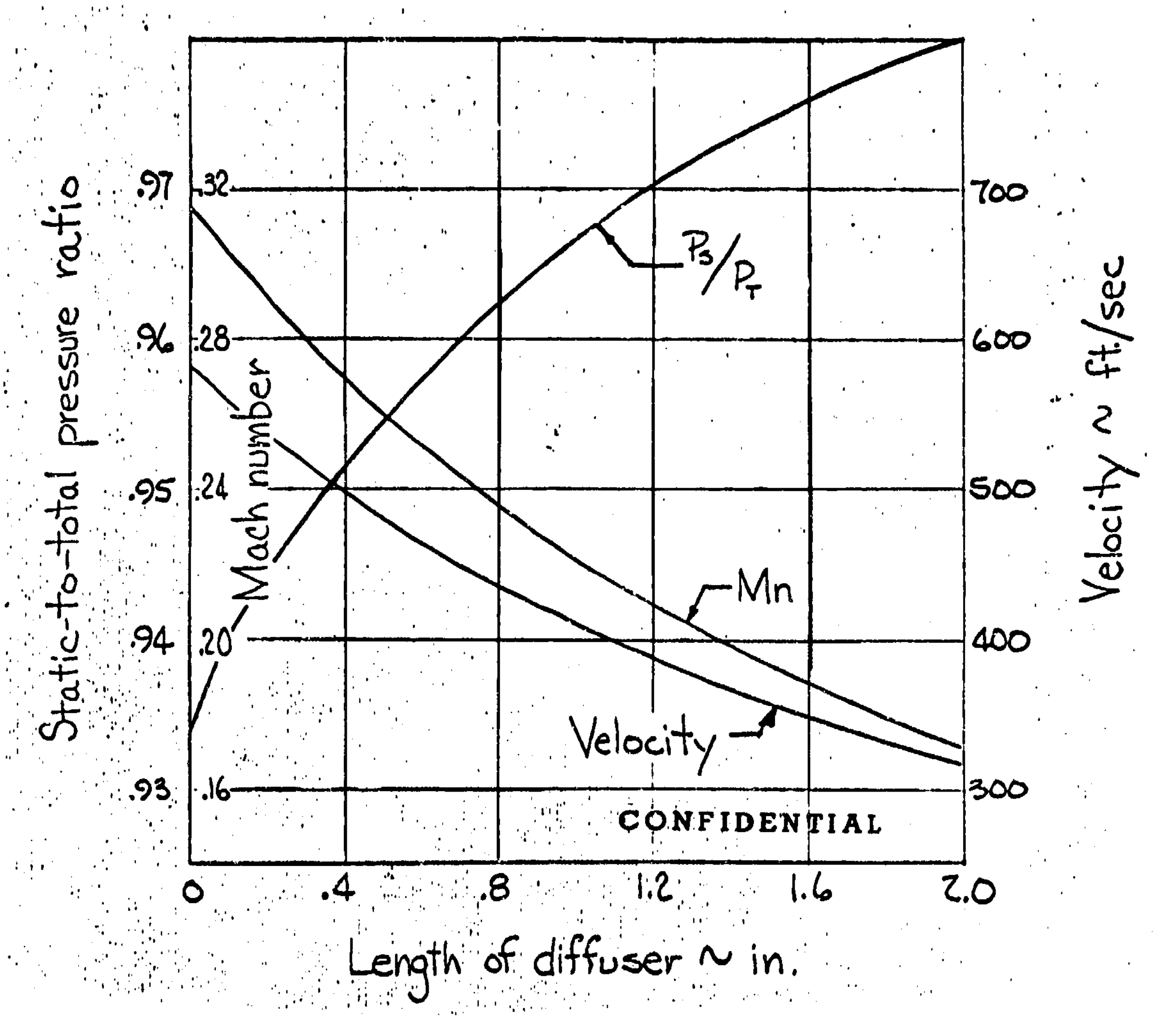

Figure 24. Diffuser parameters versus length of diffuser, "B"-diffuser, lower path.

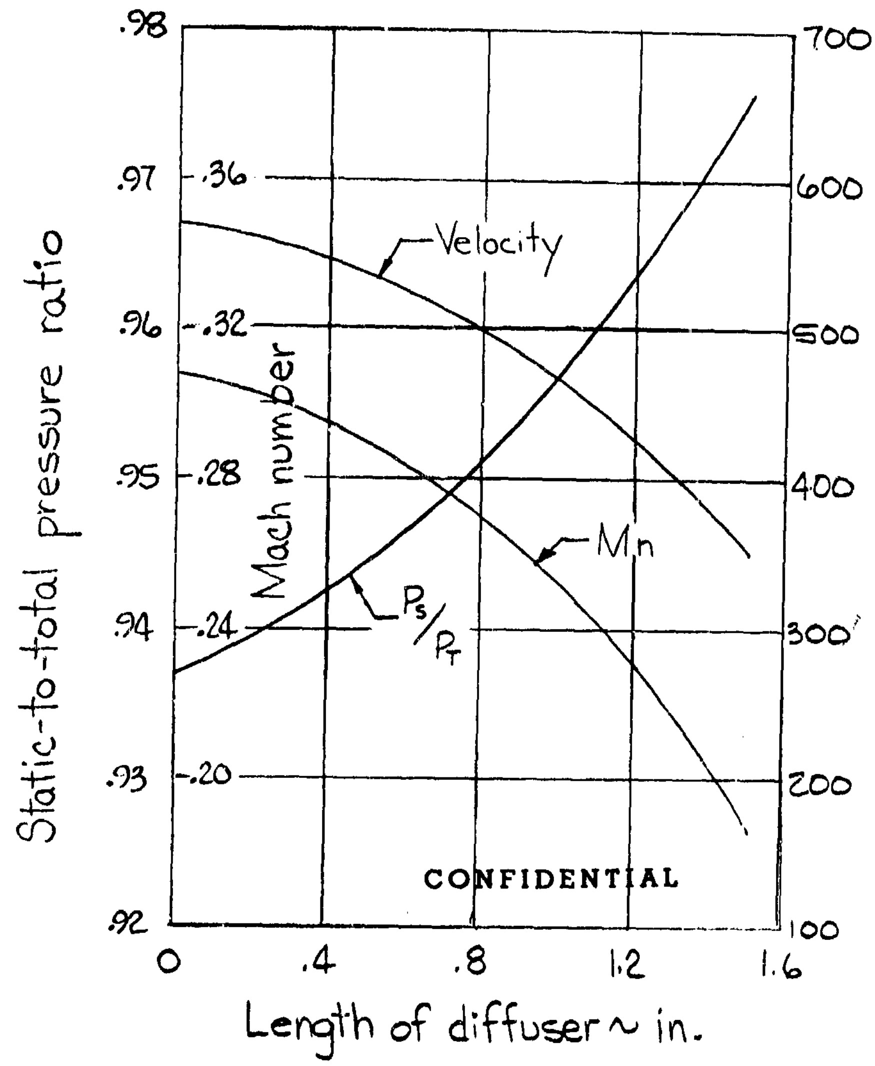

Figure 25. Diffuser parameters versus length of diffuser, "C"-diffuser, lower path.

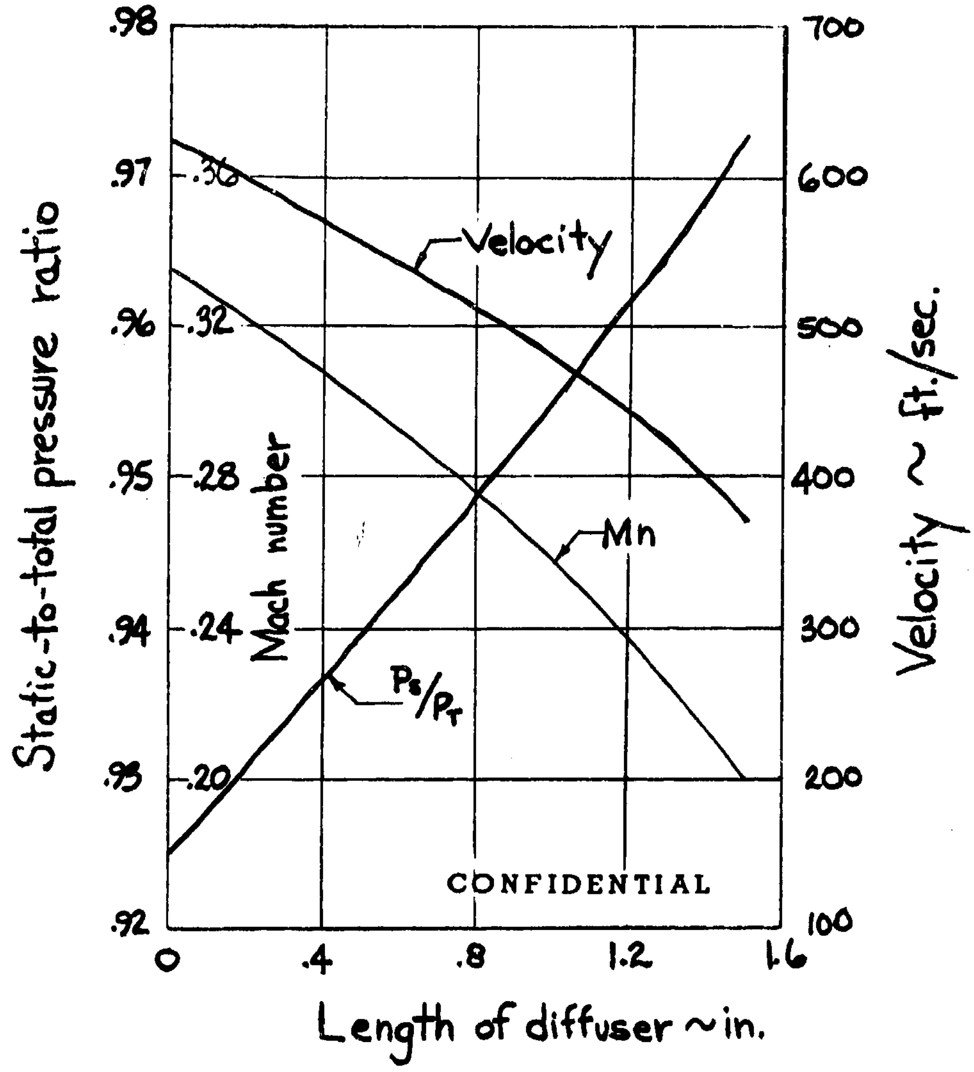

Figure 26. Diffuser parameters versus length of diffuser, "C"-diffuser, upper path.

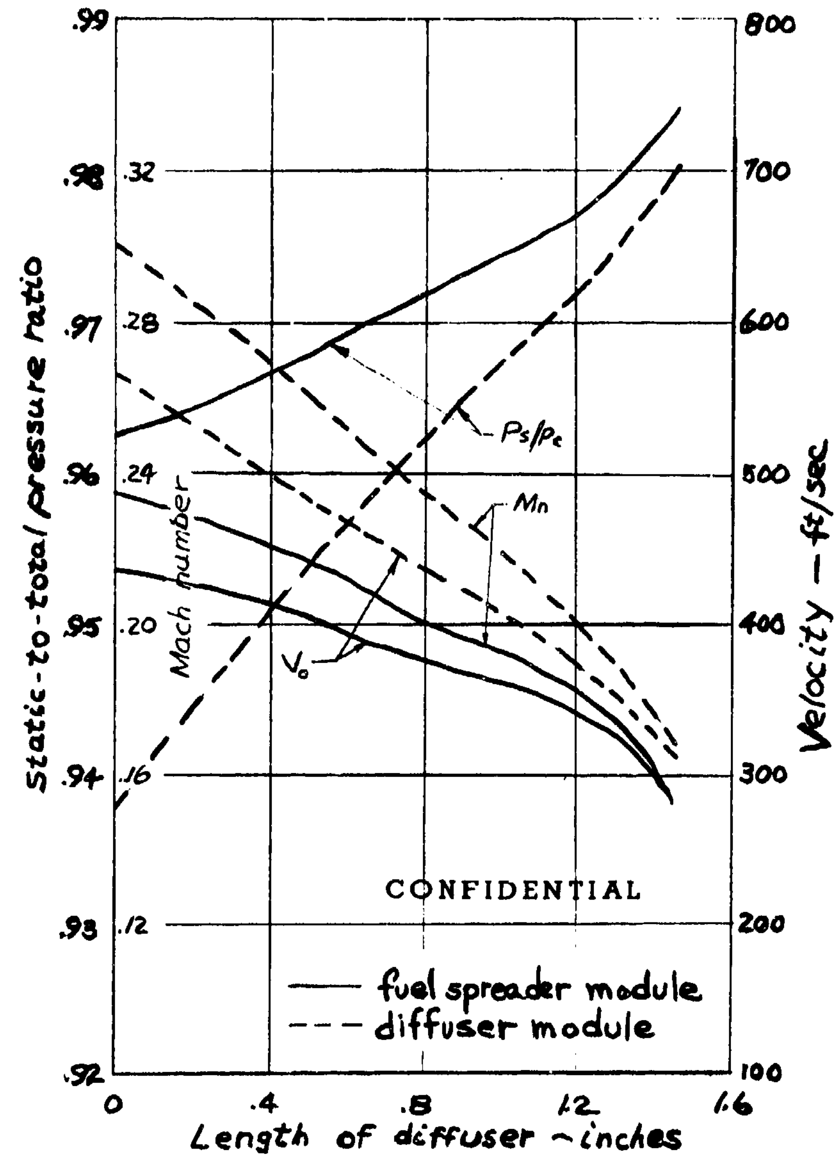

Figure 27. Diffuser parameters versus length of diffuser, "D"-diffuser, lower path.

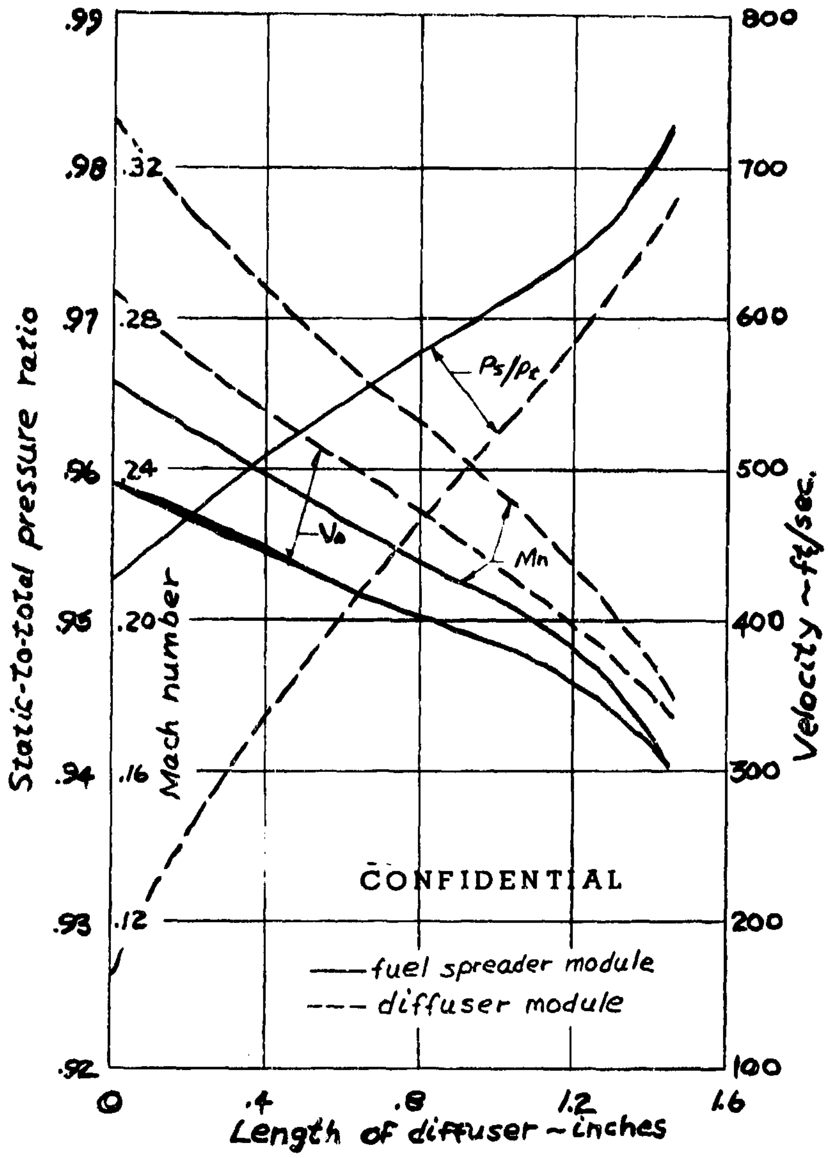

Figure 28. Diffuser parameters versus length of diffuser, "D"-diffuser, upper path.

(C) It is evident from Figure 21 that static pressure rise and Mach number change the fastest, with respect to distance traveled by the air, at the entrance to the diffuser. This is typical of diffusers with linear area distribution ("A" and "B") as shown in Figures 22, 23, and 24. It might be stated (Reference 5) that the pressure rises most rapidly where the air has the greatest kinetic energy. On the other hand, it might be explained (Reference 6) that the high velocity and steep gradient just past the inlet are unfavorable for stable flow conditions and tend to generate a separation. Accepting the latter hypothesis, it would be preferable to increase the cross-sectional area more slowly at the front of the diffuser and more rapidly at the rear of the diffuser. Applying this philosophy to an axially symmetric diffuser converts a straight wall conical diffuser into a bell shape. In the three dimensional diffuser the bell shape area progression is incorporated into the cross-sectional area at an increasing rate with distance. Diffusers "C" and "D" are this type.

(C) In the cases of "B", "C", and "D", the diffuser inlet geometry, mean path, and area ratio remain essentially the same. From Figures 22, 23 and 24 and Figures 25, 26, 27 and 28, it is seen that for the first two-thirds of the path length the cross-sectional area of "C" and "D" is below that of the "A" and "B" design. Then to

achieve the same overall area ratio, the cross-sectional area of "C" and "D" increases rapidly in the last quarter of the diffuser.

(C) In looking for a means to reduce significantly the length of the diffuser and to facilitate scaling without going beyond the shortest length, it was decided a three dimensional channel (two of whose opposing faces diverge while the other opposing converge) would have the greatest potential. To get an indication of the baseline from which the axial length reduction could be made, Figure 13 presents a sketch of a top developed view in the meridional plane of the three dimensional channeled diffuser. This geometry characterizes the diffuser which is the basis for the "C" and "D" configurations.

(C) Although the conical is undoubtedly the ideal diffuser configuration, it was realized that no completely conical diffuser channels were possible within the given geometric limitations of the "C" and "D" diffusers. Therefore, a rectangular inlet cross-section could not be avoided. On this basis, a channel with a constantly changing cross-sectional shape was designed. This begins with a rectangular throat wider in the horizontal direction, then through a gradual transition, downstream of the throat, takes on the shape of a square, and finally returns to a rectangular shape wider in the vertical direction at the exit location.

(C) This cross-sectional variation providing a smooth change in area is based on the following considerations:

- The rate of area change just downstream of the rectangular diffuser inlet was made to follow more closely the optimum of two-dimensional criteria since its correction was two-dimensional in this region.
- The rate of area change near the exit was selected not to exceed that indicated for optimum of the annular diffuser (Figure 6).

(C) The resulting exit-to-inlet area ratio remained at the optimum for the two-dimensional configurations. A sector of this diffuser rig is shown in Figure 21.

(C) The design parameters of the engine diffusers presented in Tables II through V are compared to the work in References (1, 2, 3, and 4) in Figure 6. The line for velocity ratio equal to 1.0 is taken from Reference (5) and is the line of first appreciable stall determined with no inlet velocity profile. The line for velocity ratio equal to 1.2 is taken from Reference (4) and Reference (1) and is the line of first appreciable stall with a jet-type inlet profile and velocity ratio equal to 1.2.

IV PREMIX FUEL INJECTION

1. General Considerations

(C) Development of gas turbine combustion systems with exit temperatures approaching stoichiometric levels require efficient operation with a high temperature rise and a high heat load. The limited test data available in combustion literature indicates a declining burner efficiency with increasing temperature rise. This development effort is based primarily on the premise that insufficient mixing of the air and fuel ahead of the reaction zone accounts for the efficiency decline. The solution of this problem constitutes a major portion of this Phase I effort.

(C) Five fuel injection modules were designed and developed. Each module consists of an air blast system for fuel atomization and a combustor dome air inlet system to introduce and mix the remaining combustor air with the atomized fuel. The design of these modules was based on the following operational requirements:

- Low pressure fuel system
- Increased number of fuel injection points
- Ability to operate on contaminated fuels
- Premixing of the air and fuel ahead of the combustor dome.
- High dome air flow
- Smoke free operation

(C) The burner gas path is designed for 84% of the air flow injected through the combustor dome. The other 16% is used to cool the combustor walls through conventional film cooling louvres. The combustion air flow distribution is:

- Primary air 50%
- Dilution air 22%
- Premix air 12%
- Combustor cooling air 16%

(C) The purpose of the Phase I single module testing was to develop and compare the atomization qualities of the various module designs. The single module test rig is shown on Figure 29 for cold flow testing and Figure 30 for hot flow testing. The gas path simulates the design gas path shown in Figure 1 with the omission of combustor wall cooling air passages. The rig walls are externally air cooled to eliminate the effects of cooling film on performance data. The heat loss through the walls was measured and taken into account during efficiency calculations. The detailed air flow distribution for the premix combustion systems is shown in Figure 31. The development testing was divided into cold flow visualization and burning performance evaluation.

(C) The fuel injection modules were designed to the following Phase II burner sector operating conditions:

- Burner inlet temperature 1200°F
- Burner inlet pressure 20 atm

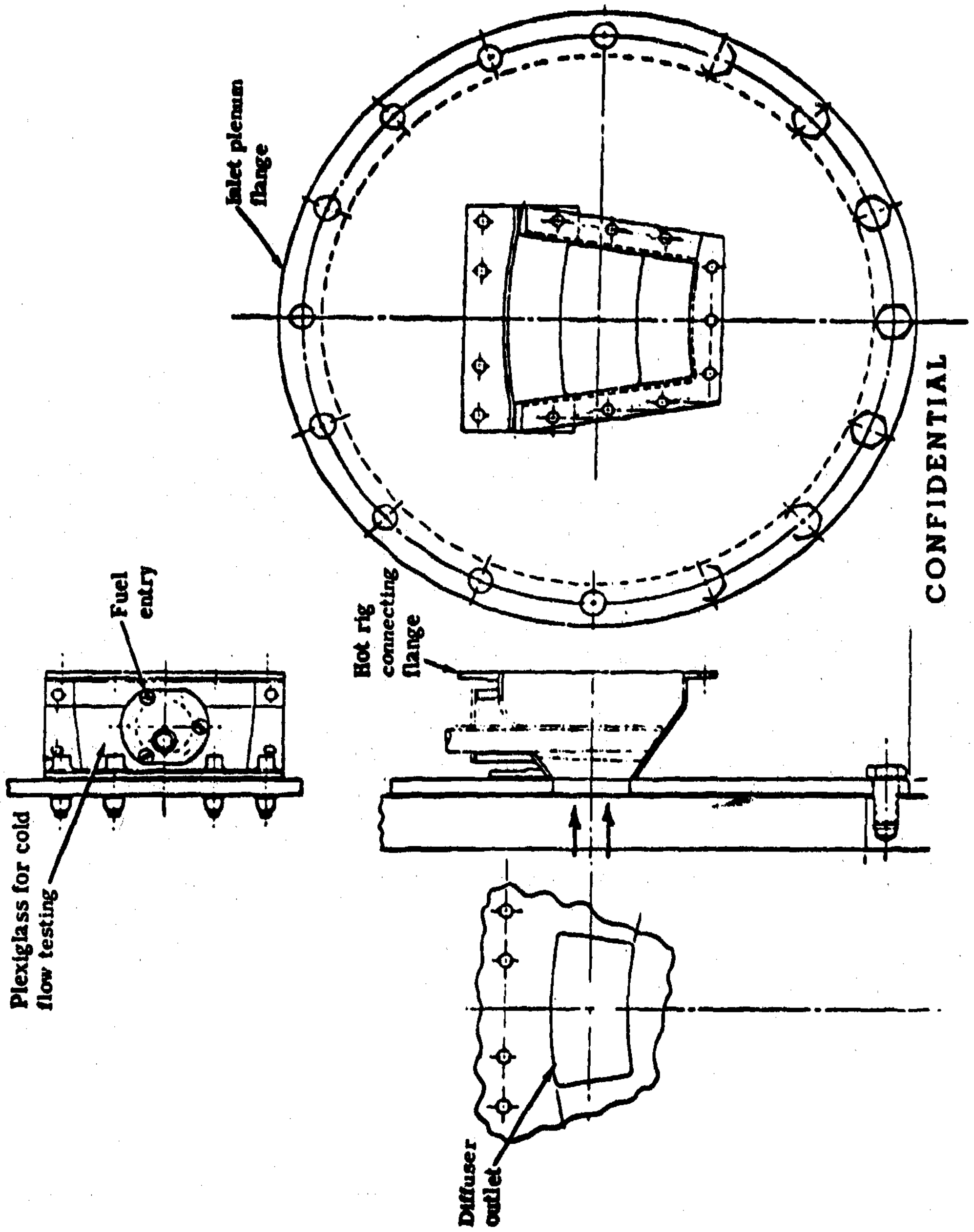

CONFIDENTIAL

Figure 29. Single-module rig-cold flow configuration.

- Burner mass flow 60 lb/sec
- Burner temperature rise 2300°F

(C) The equivalence ratio ϕ, actual fuel-air ratio divided by the stoichiometric fuel-air ratio, was set at five. This was a compromise between sufficient turndown ratio and a realistic atomization at twenty atmospheres pressure. Figure 4 shows the effects of operating variables (burner inlet pressure and temperature) and design variables (air injection velocity and equivalence ratio) on mean droplet diameter of the atomized fuel.

(C) The fuel modules were fabricated of plexiglass for visual observation of the mechanisms that effect atomization and droplet distribution. Water was substituted for fuel as a safety measure. Figure 32 shows the physical properties of kerosene fuels and water that effect droplet breakup yield comparable results under the prevailing test conditions. Strobe lighting techniques were used to study droplet distribution and estimation of droplet size. Collimated lighting techniques were used to study droplet distribution and effects of downstream mixing on droplet coalescence. A flow tuft probe was used to map the air flow characteristics of the dome air entry slots and the recirculation patterns developed by the modules. A photographic record of the droplet field for each module was taken for a comparative evaluation. Figure 33 shows the photographic arrangement. The droplet field was back lighted with a spark gap strobe light.

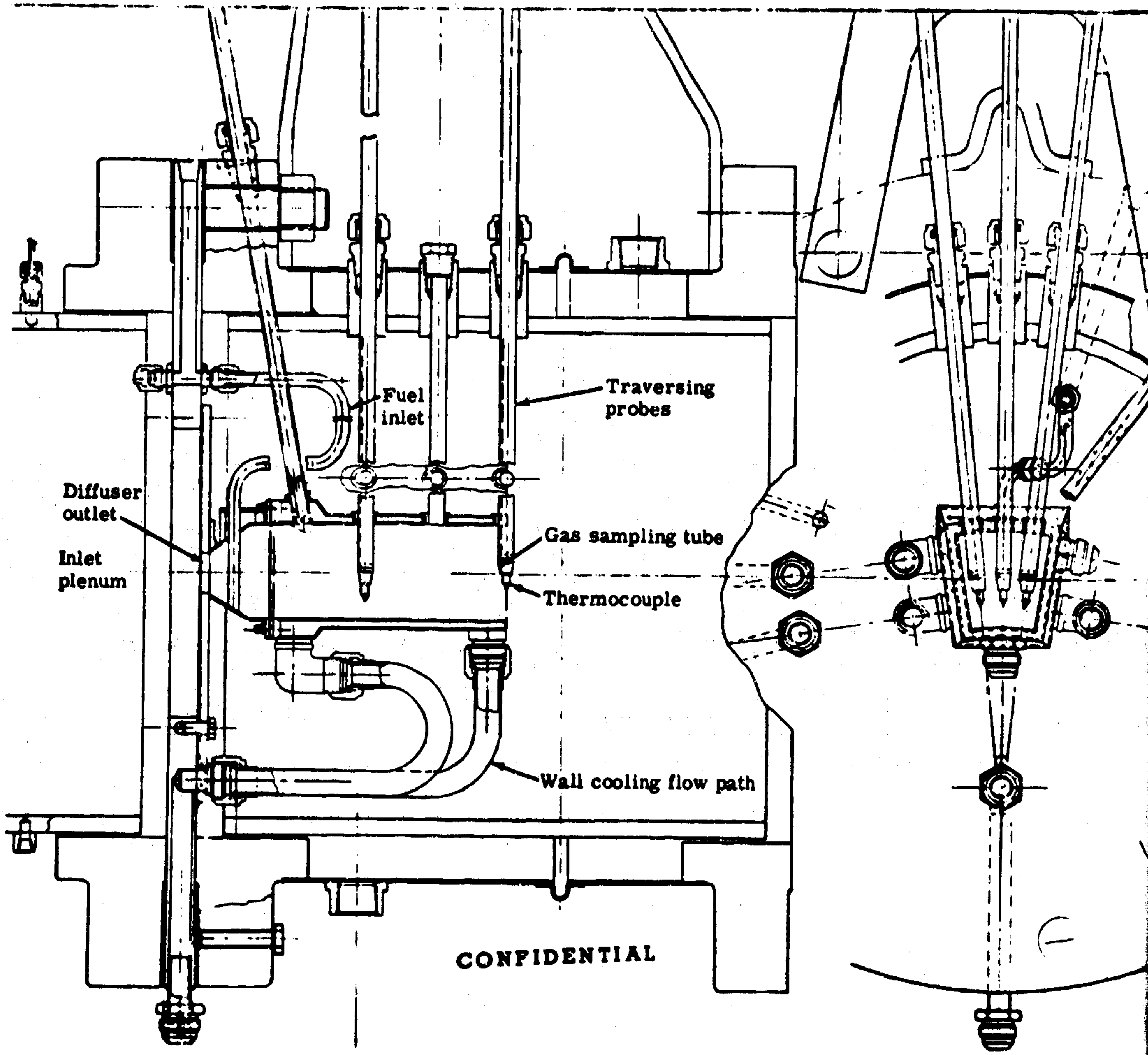

Figure 30. Single-module rig-hot flow configuration.

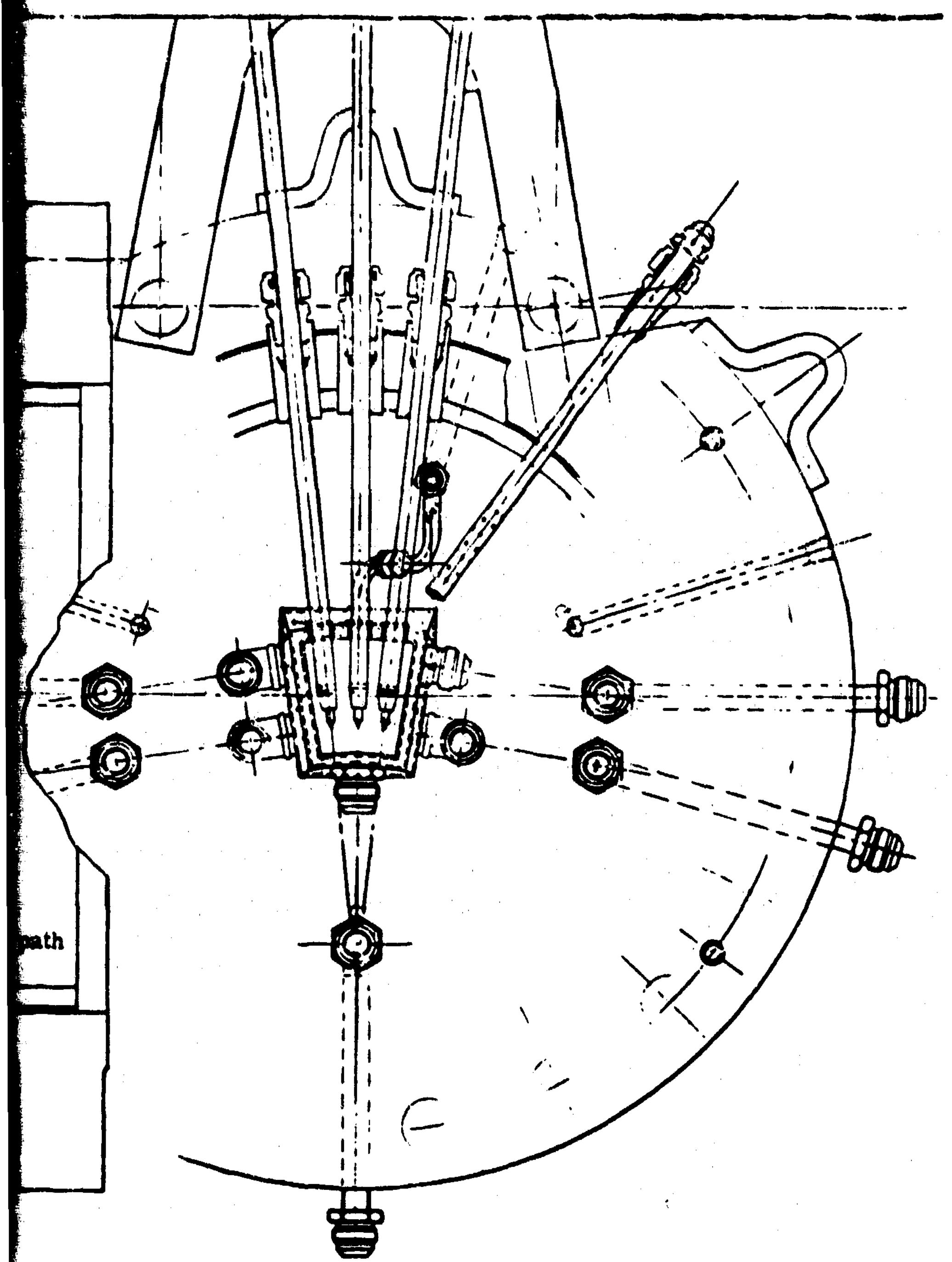

hot flow configuration.

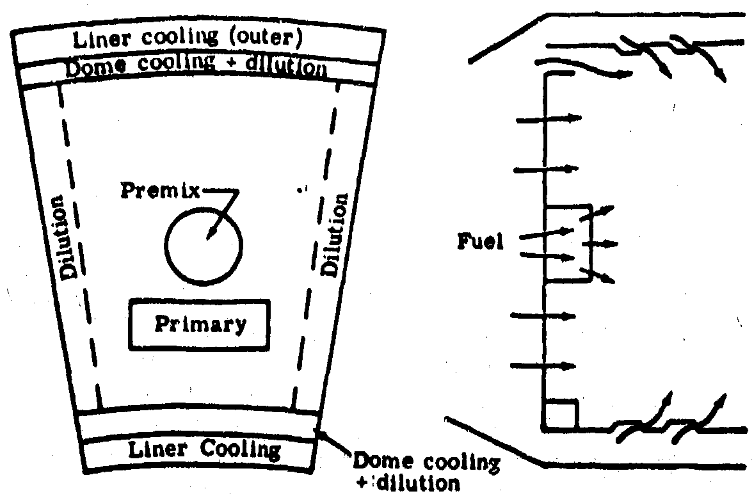

Description	Flow split
Liner cooling	
Outer wall	0.09
Inner wall	0.07
Dome cooling + dilution	
Outer	0.13
Inner	0.09
Premix	0.12
Primary + dilution	0.50
Total	1.00

CONFIDENTIAL

Figure 31. Airflow split in premix combustion systems.

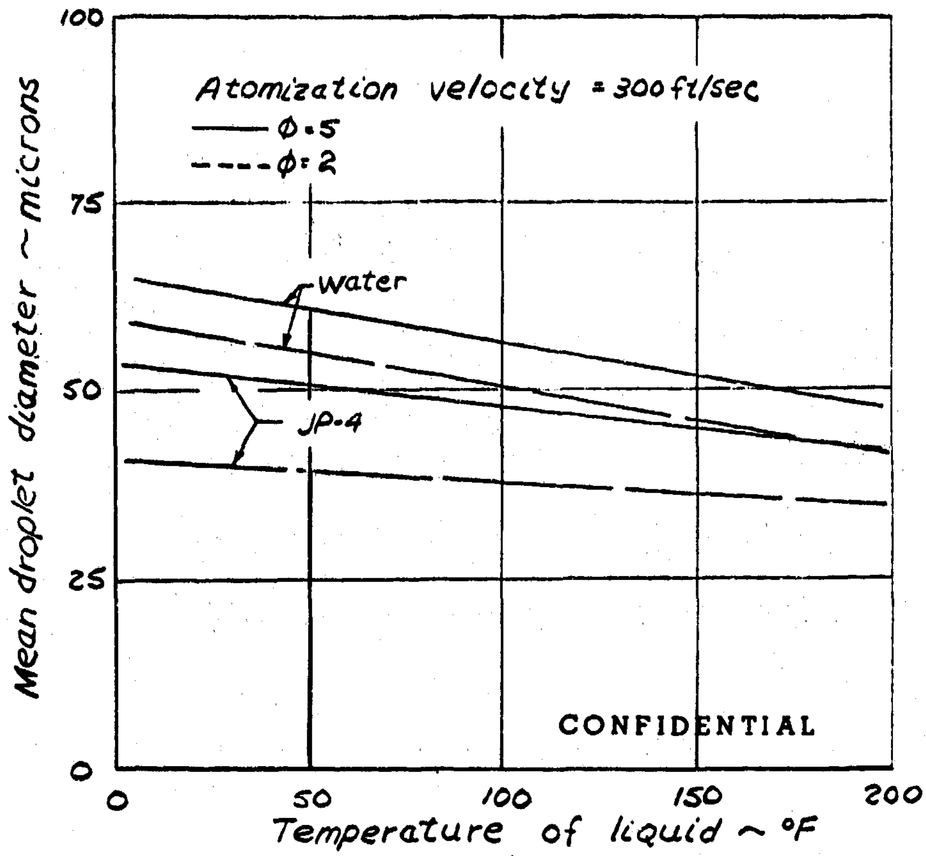

Figure 32. Mean droplet diameter versus temperature for fuel and water.

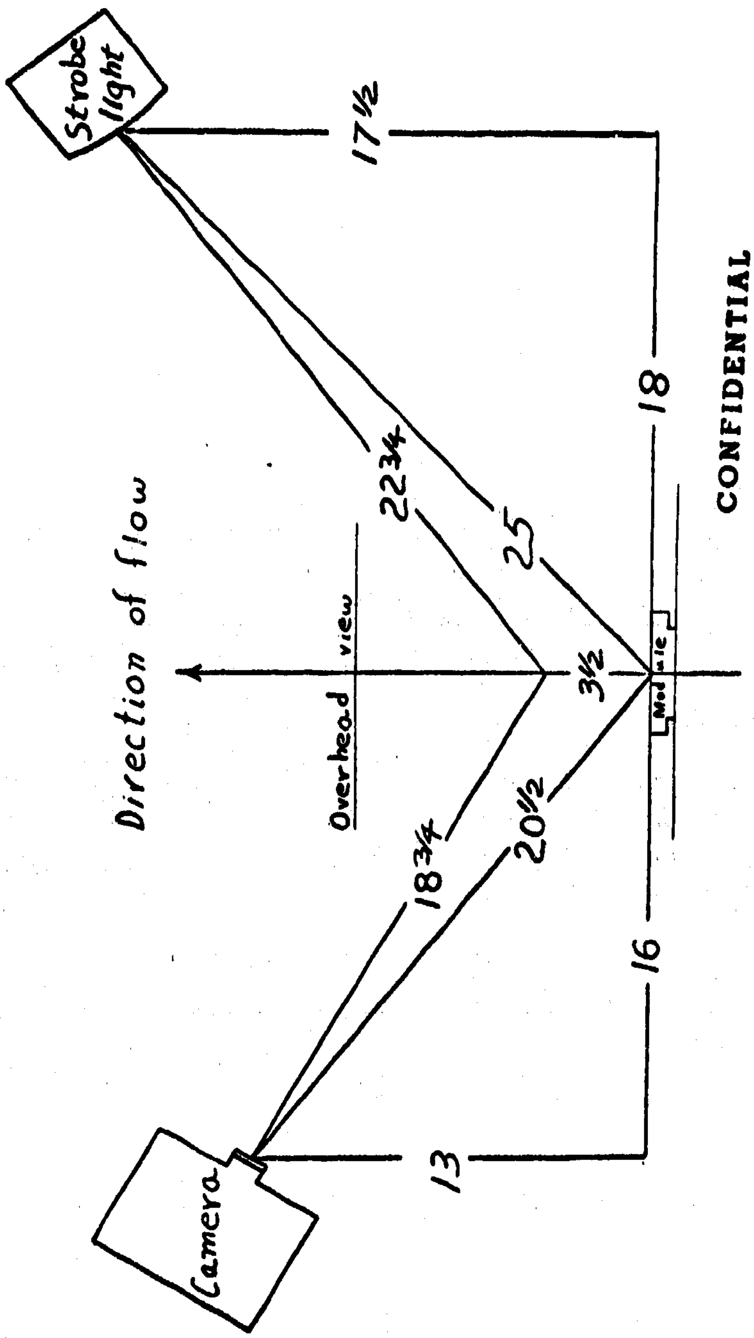

CONFIDENTIAL

Figure 33. Camera and lighting for droplet photography.

(C) The plexiglass configurations were phased into metal modules for evaluation of the atomization, vaporization, and mixing potential of the injector designs under burning conditions. Three dimensional temperature traverses were recorded with radial traversing probes. A sample isotherm temperature plot is shown in Figure 34. The temperature traverses were checked with chromatograph samples taken through the same radial traversing probes. Smoke samples were taken at the exit plane through the same probes and recorded using Bacharach spot sampling techniques. The overall pressure drop was recorded as module inlet total pressure minus the burner outlet total pressure.

2. Vee Gutter Module

(C) The vee gutter module shown in Figure 35 is sized to have 20 modules per annular combustion liner. This module design combines fuel-air premix and high dome air flow with the vee gutter recirculation developed for afterburner systems. The vee gutter concept was not used in the circumferential plane of the afterburner but was developed in the radial plane to:

- Optimize the recirculation pattern of the high aspect ratio slot to mix the primary-dilution air with the fuel-air premix flow
- Achieve modular linearity for development changes in liner height
- Allow independent removal of the components of the fuel distribution system

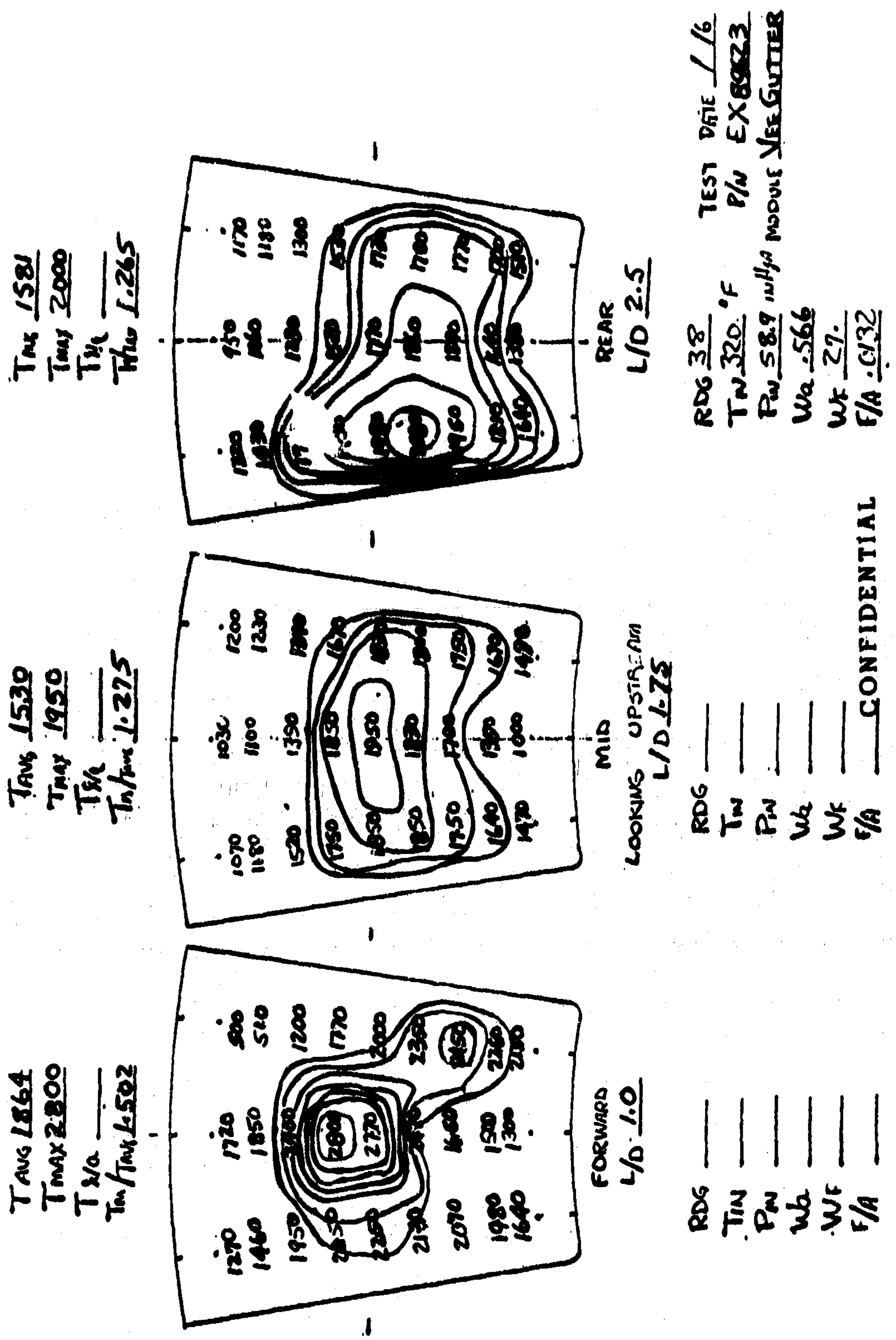

Figure 34. Three dimensional isotherm plot.

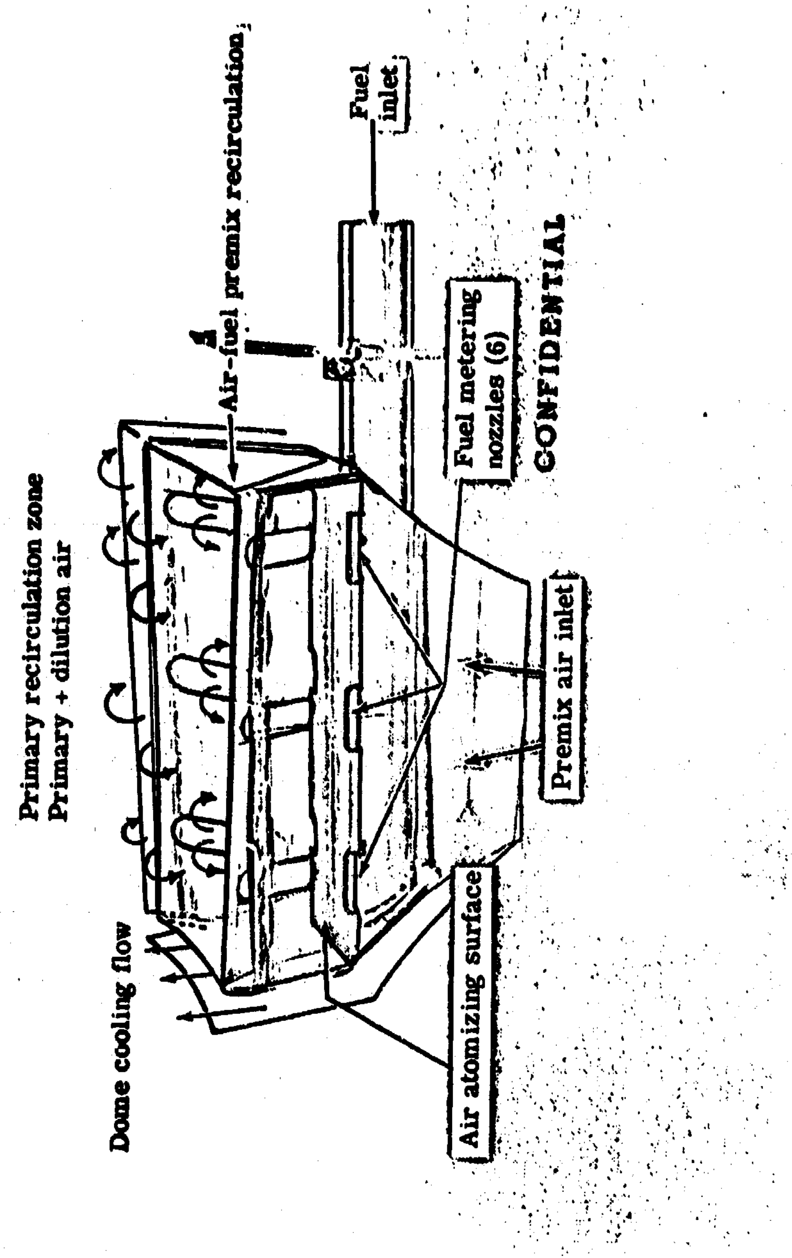

Figure 35. Vee gutter module.

(C) In the vee gutter module the fuel is atomized by air at a velocity of 304 ft/sec flowing across the atomizing surface. The mixture, designed for an equivalence ratio of five, flows through the six slots into the recirculation zone. The remaining air flow is injected through the high aspect ratio radial slots between modules. The vee gutter fuel distribution tube was designed to match a fuel injection jet to each injection slot. There are 6 injection points for each module and 120 for a full annular combustor.

(C) The atomization of the fuel from this module is of a nature to create the existence of a wide distribution of fuel droplet sizes. The distribution is made mechanically using a large number of injection points. The flow quality at the design point premix equivalence ratio of five and the premix velocity of 304 ft/sec is shown in Figure 36. Supports have been added to this pictured model for rigidity to enable the flow study of the air both inside and outside of the vee.

3. Swirl Chamber Module

(C) The swirl chamber module shown in Figure 37 is used to provide 30 modules per annular liner. Each module consists of one vertex chamber and one fuel injection point. Visual studies, Reference (8), indicates a boundary layer exists on the end wall of the conventional vortex chamber which does not become part of the vortex flow. To recover this lost volume, the swirl chamber module has the vortex energized by air emission through two swirl vanes located through the vortex

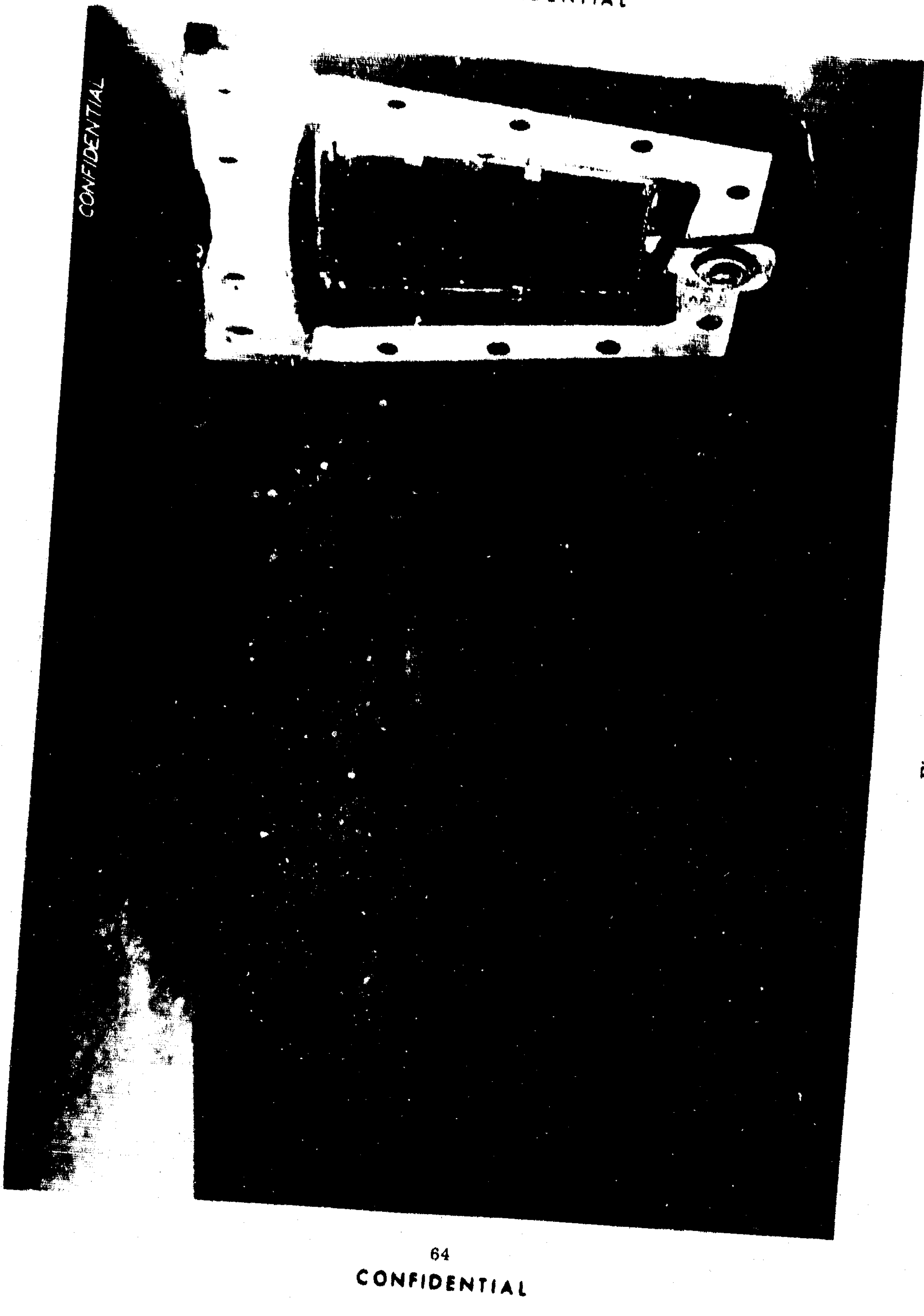

Figure 36. Vee gutter droplet field.

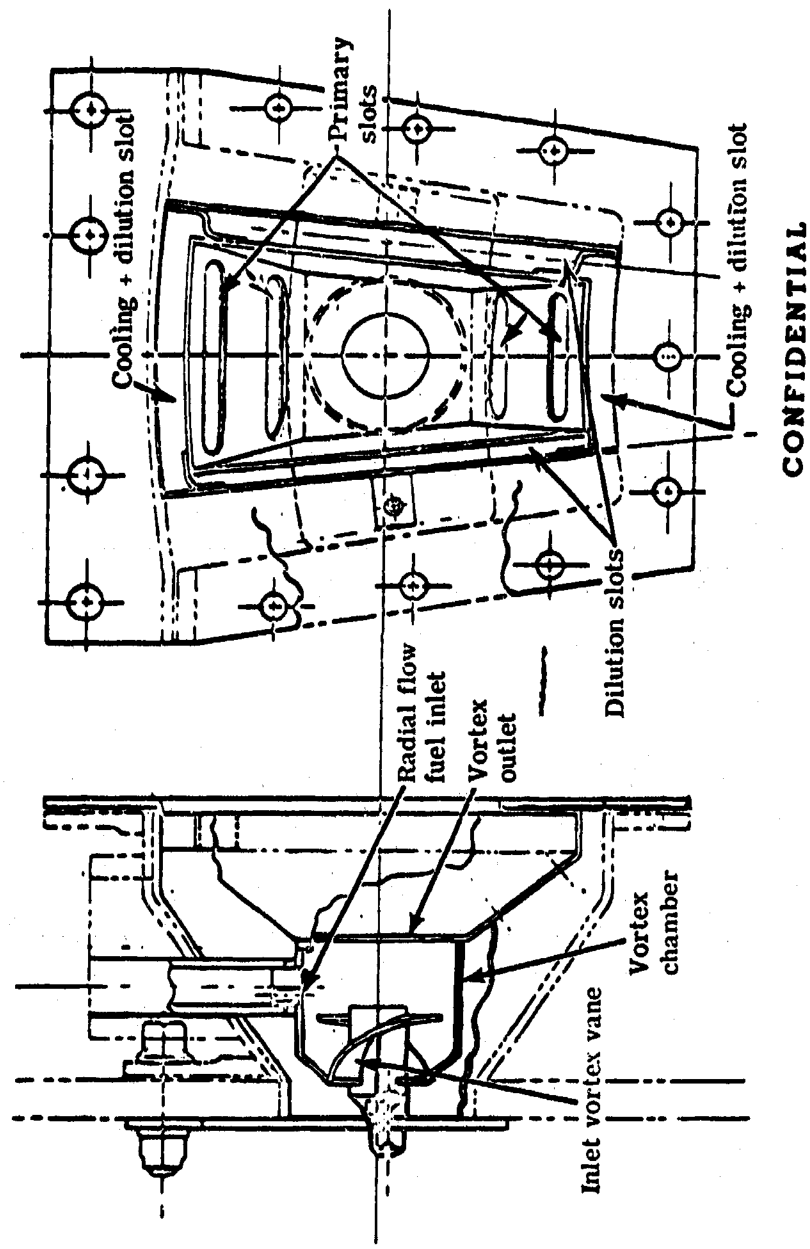

Figure 37. Swirl chamber module.

chamber end wall. The use of the boundary layer area to drive the vortex results in a more efficient use of the chamber axial length. The same flow visualization studies, Reference (8), also predict optimum mixing occurs with the fuel injection in a radial plane. This module has fuel injection in a radial plane. Primary air is introduced through high aspect ratio slots located in the module cone. The dilution air entry is through radial slots between fuel modules.

(C) Flow conditions inside the swirl chamber and in the module cone were evaluated using water in air. The spray quality at maximum water flow conditions and 304 ft/sec ambient air flow is shown in Figure 38. Spray quality was not affected by a change in simulated equivalence ratio and was changed very slightly by a change in velocity above 304 ft/sec. The circulation from the cone slots surrounding the swirl chamber was altered during the water and air flow testing. The testing of the altered module confirmed both the high degree of mixing within the module cone and a well established circulation for primary zone reaction. This single point injection module was designed to demonstrate a higher degree of primary atomization than in the vee gutter without the coverage by numerous jets.

4. Conical Fuel-Air Spreader Module

(C) The conical fuel-air spreader module, Figure 39, is sized for a

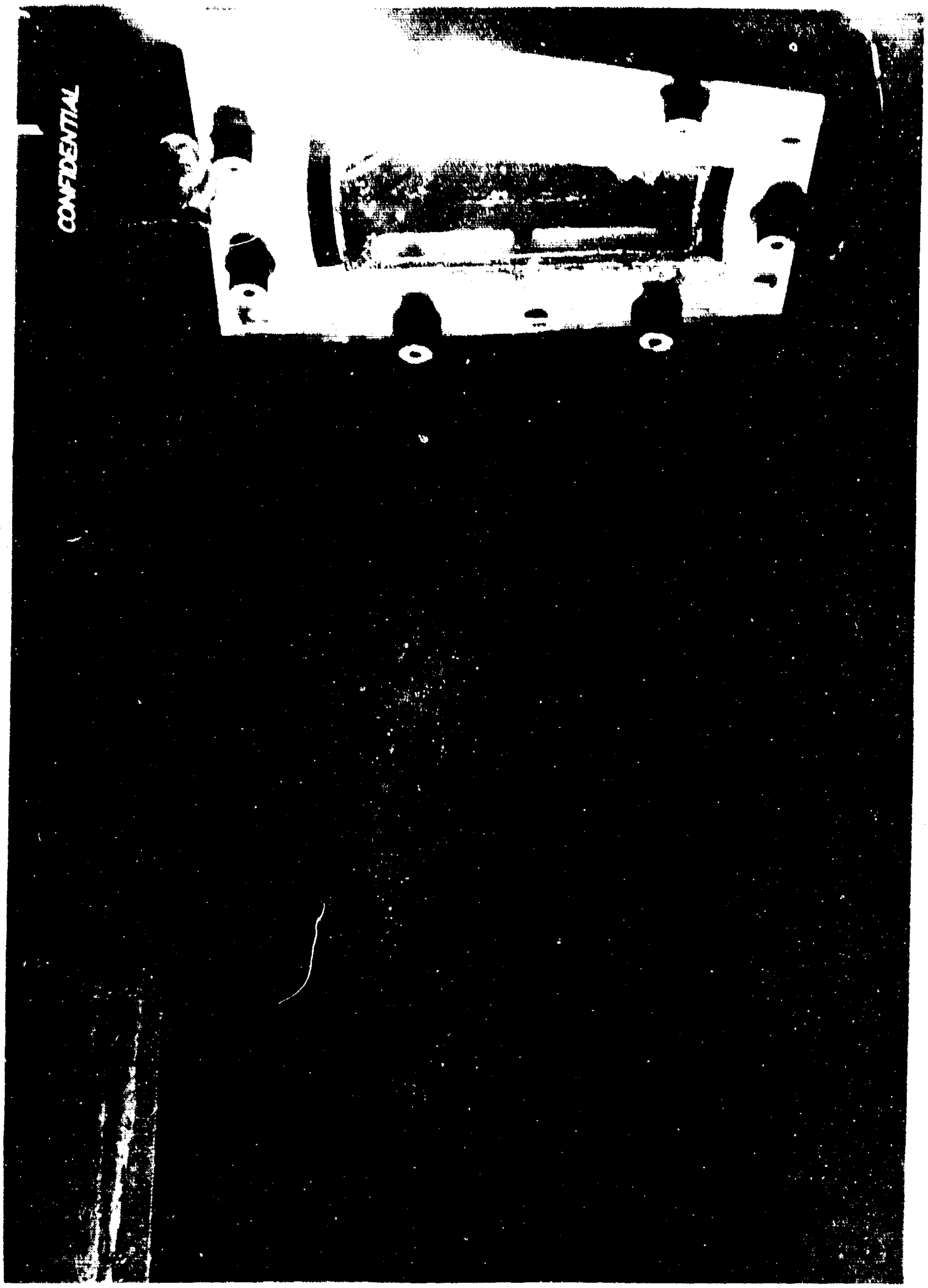

Figure 38. Swirl chamber module droplet field.

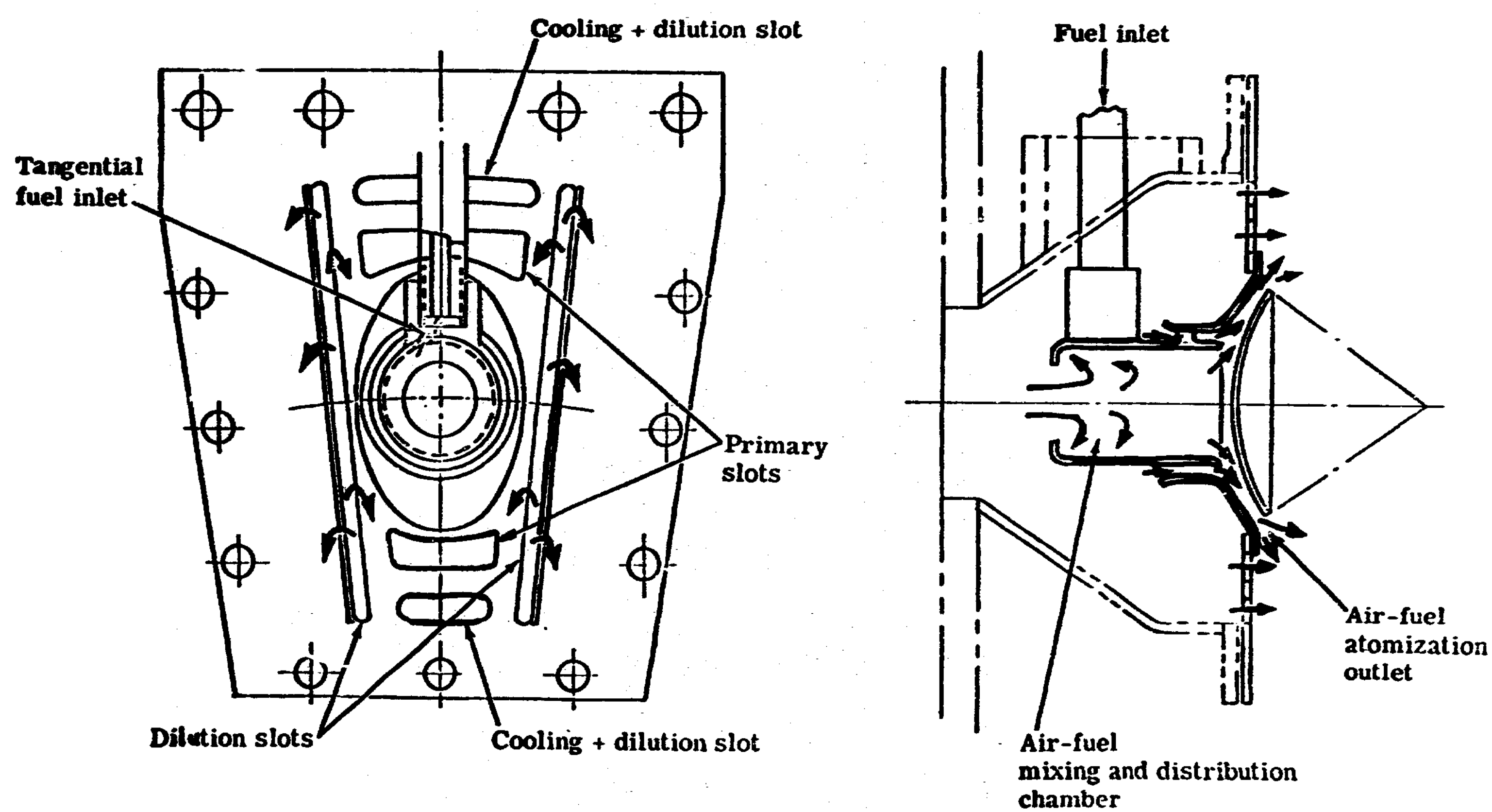

CONFIDENTIAL

Figure 39. Conical fuel-air spreader module.

single row fuel distribution of 30 modules per annular combustor. This module has a radial fuel entry to the inner air mixing chamber. This chamber performs the dual function of providing fuel-air mixing and even distribution around the exit cone. Atomization occurs at the exit of the inner mixing chamber. The atomized fuel is surrounded and carried to the reaction zone by primary air through the inner and outer chamber passages. This is shown in Figure 40 where mixing air is on both sides of the atomized fuel. This type of fuel addition should give the finest fuel spray since coalescence is prevented and the droplets held in suspension by surrounding the atomized fuel with air. The distribution from this model shows a wide dispersion of drops resulting from the smaller droplet size.

5. Double Reversal Chute Module

(C) The double reversal chute module shown in Figure 41 is sized for 20 modules per liner. Each module has four fuel distribution points. The fuel-air premix chute encloses the fuel metering nozzles and the fuel atomizing surface. From this chute, the atomized mixture enters an enclosed primary mixing zone for mixing and dilution with the primary airflow. This mixture enters the combustion zone for burning. The remaining dilution air is ducted in four chutes adjacent to the premix chutes. The flow channel for air to each area of the dome has been constructed as a separate duct. This was accomplished in an effort to get the effect of direct placement of primary air and dilution air.

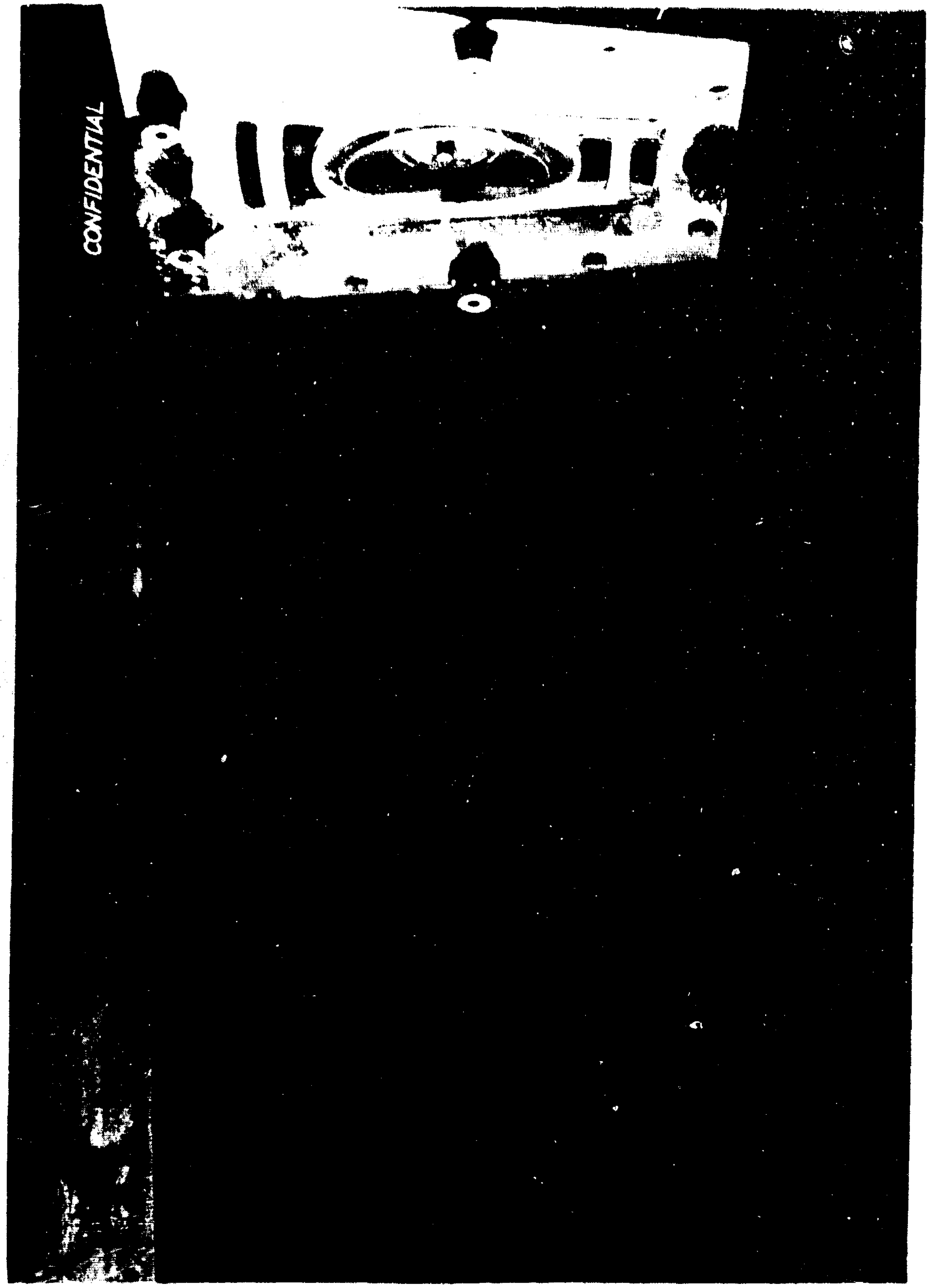

Figure 40. Conical fuel-air spreader module droplet field.

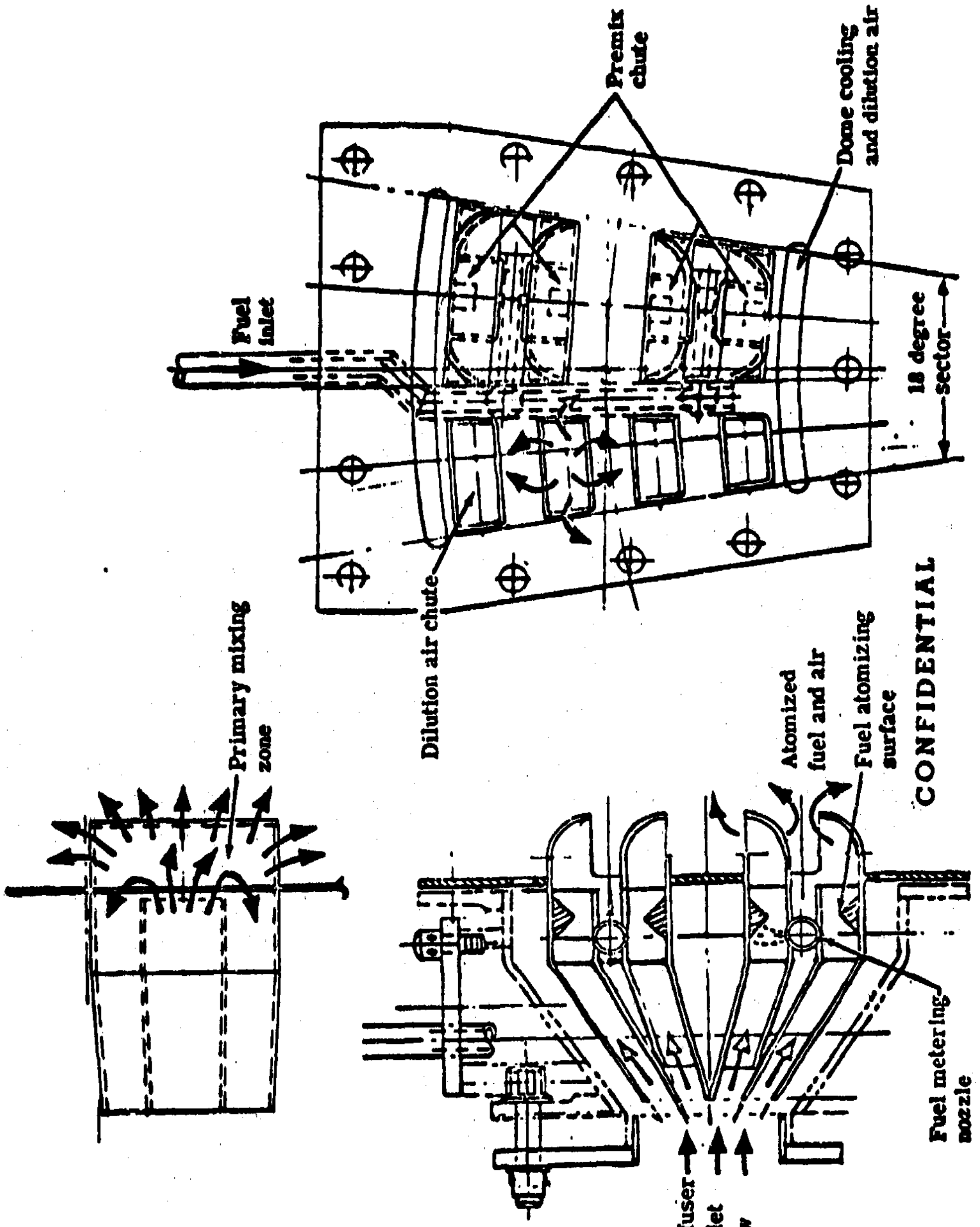

Figure 41. Dougle reversal chute module.

V CONTAMINATED FUELS TEST

(C) The basic test system for testing contaminated fuels with premix modules is shown on Figure 51. This system comprises three elements. A motor driven belt driven at a regulated speed carries regulated quantities of contaminant for dumping into the fuel supply. A dual piping system has been sized to retain the contaminants in suspension. A vane type pump and the necessary regulating valves are used to control the fuel flow.

(C) The fuel used was Mil-G-313[illegible] Ty[illegible] [illegible] contaminated per Mil-E-5007B. Each module was tested for [illegible] the following cycle:

- Minimum fuel flow [illegible]
- Maximum fuel flow [illegible]
- Zero fuel flow 5 sec

(C) Fuel flow versus pressure drop were recorded before and after the test using clean fuel. During the running with contaminated fuel, a flow check was made at one-half hour intervals.

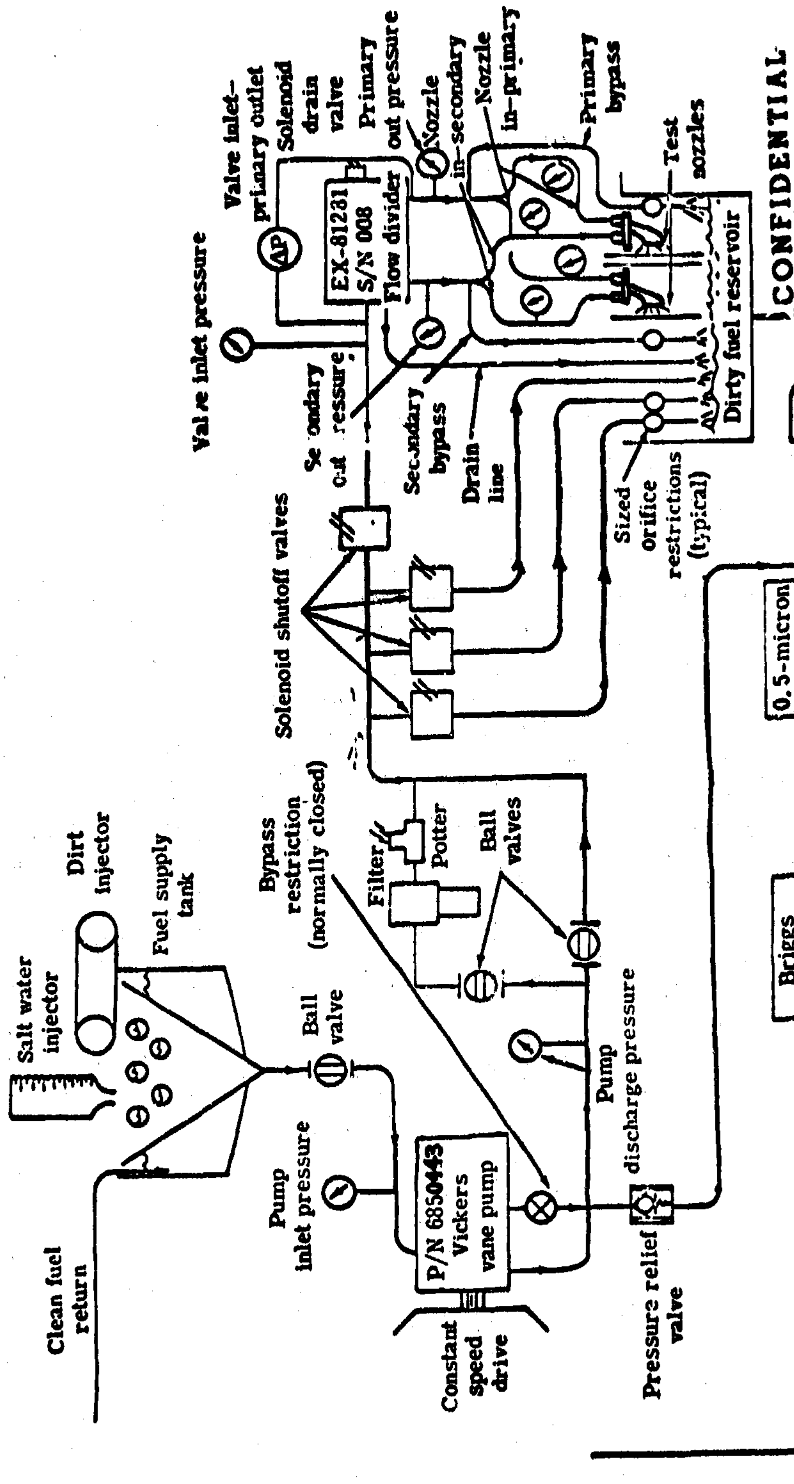

Figure 51. Test equipment configuration and contaminant for fuels contaminated per MIL-E-5007B.

VI FUEL INJECTION COMPUTER PROGRAM

(C) The fuel injection computer program is modeled on a fuel injection system which depends upon fuel atomization, vaporization, and the mixing of fuel and primary air as functions of:

- Premix air injection velocity, pressure and temperature
- Fuel velocity and temperature
- Physical properties of the fuel
- Injector orientation relative to the air stream
- Combustor physical dimensions

(C) The formulation of the preliminary equations for atomization and vaporization was based on the work in Reference (7). The theoretical model will be correlated with the data from Phase I single module testing. The three dimensional arrays of temperature and chromatograph surveys will be correlated with the reaction rate parameter. The reaction rate parameter correlated the burner efficiency with the burner operating variables. The level of burner efficiency will then be related to the overall effects of atomization, vaporization, and mixing as a function of the operating variables.

(C) The correlation of the predicted model performance to actual test performance will continue through Phase II and Phase III testing. The fuel injector portion of the computer program is a part of a more extensive computer program which will result in computerized predictions. These predictions will be the fuel droplet size, evaporation rate, and mixing potential of air atomized fuel systems over the operating ranges described by the four Air Force mission requirements.

(C) The preliminary computer program dealing with fuel properties and mixing was used to generate the data shown in Figure 4.

VII TEST RESULTS

1. Single Module Burning Tests

(C) The purposes of the burning section of Phase I testing on the single module rig were:

- Develop the particular premix system of each module
- Compare the effectiveness of the various premix designs
- Obtain correlation data for the computer prediction program that models the atomization, vaporization and mixing regime of the high dome flow combustor.

Data Acquisition

(C) The modules were tested at three fuel-air ratios over two operating conditions.

Parameter \ Condition	#1	#2
Inlet Total Pressure in.HgA	60	150
Inlet Total Temperature °F	300	500
Dome Velocity ft/sec	300	300

The maximum burner exit temperature was limited to 3200°F to maintain a reasonable life on the thermocouples and chromatograph sampling probes. The three operating fuel-air ratios were selected to give the widest range and still have stable rig conditions. This range is desirable for the method used to calculate module design fuel-air ratios*.

*Module design fuel-air ratio is the ratio at which the burner efficiency derived from gas chromatograph analysis was a maximum.

Observations and Comparisons of Modules

(C) Table VIII is a summary of the observations and comparisons of the five modules. The double reversal chute module has been eliminated from further consideration. This module is too limited on flame holding stability and, consequently, would not sustain below a fuel-air (F/A) of 0.018. The dilution chutes gave good dilution mixing. However, the design of the premix chutes did not provide enough recirculation to promote a back mix combustion zone.

Premix Equivalence Ratio

(C) A premix equivalence ratio of five was the initial design point for the modules. At the design point the overall F/A ratio is 0.0418 and 12.5% of the air flow is required for proper fuel-air premix. During initial hardware development a range of equivalence ratios were tested. This testing was done prior to flow coefficient definition for the various air flow passages. The Vee gutter module stability was increased with increasing equivalence ratio. Increasing the equivalence ratio above five results in a lower fuel air design; thus, a lower lean blowout F/A ratio. Although the lean blowout characteristics were desirable, development will be directed toward increasing the design F/A ratio to maintain combustion efficiency during high temperature rise operations.

Pressure Drop

(C) The single module rig simulates the inlet flow to the module from a dump diffuser at an exit velocity of 300 feet per second. The total pressure drop across the module, between module inlet and burner exit, is shown in Figure 52.

Burner Efficiency

(C) The burner efficiency was calculated from gas chromatograph sampling at three axial stations. Figure 53 shows chromatograph efficiency as a function of overall fuel-air ratio (FAO). The efficiency of the Vee gutter falls off

(C) TABLE VIII

Observations and Comparisons of Modules

	Vee Gutter	Swirl Chamber	Fuel-Air Spreader	Venturi Vortex	Double Reversal Chute
Design Fuel-Air	.017	.021	.031	.015	—
Lean Blowout F/A	.0075	.014	.015	.012	.018
Fuel Droplet Distribution	Good Homogeneous Field	Good Homogeneous Field	Heavy Concentration at Root and Tip	Conical Distribution Similar to Fuel Nozzle	Non-Homogeneous
Droplet Size	Uniform Coarse	Uniform Coarse	Fine	Fog	Wide Variation
Burner Recirculation	Strong-Well Defined in Radial Plane	Strong-Concentrated Around Swirl Chamber Exit	Weak-Small Zone Behind Spoon Shape Fuel Spreader	Undesirable Recirculation into Vortex Chamber	Good Dilution Mixing Zone
Flame Holding Stability	Well Seated at Low Fuel-Air Ratios	Well Seated	Well Seated	Not Seated Completely	Not Seated (Curtailing further Development).
Temperature Profiles Hub-Tip	Even	Cool Tip	Cool Tip	Hot Core	Hot Core

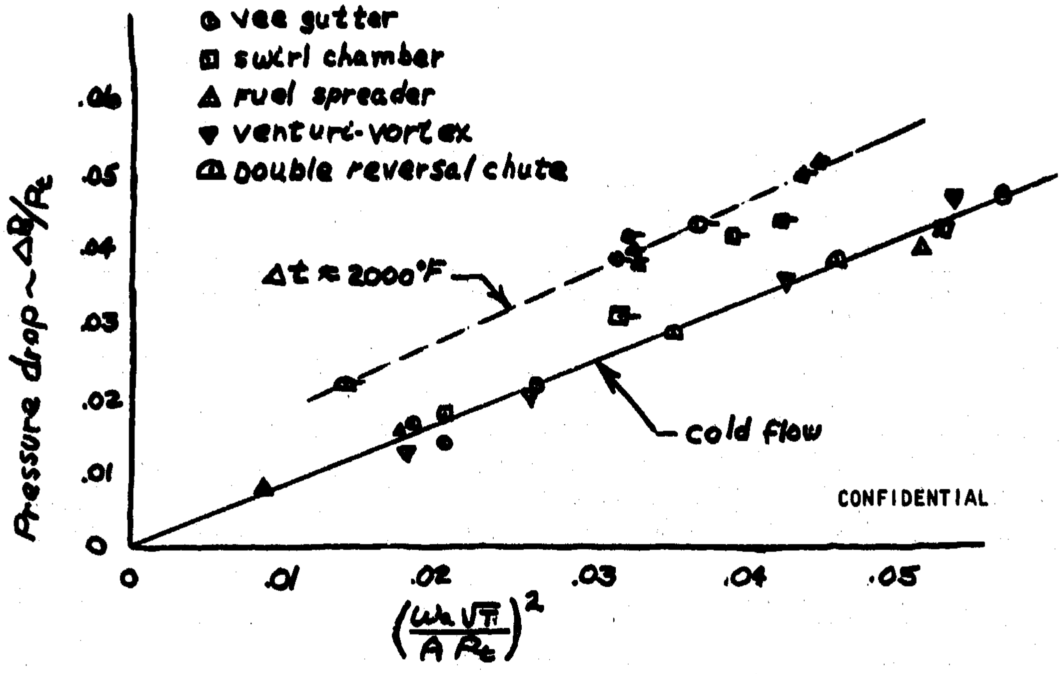

Figure 52. Pressure drop versus Mach number under cold and burning conditions.

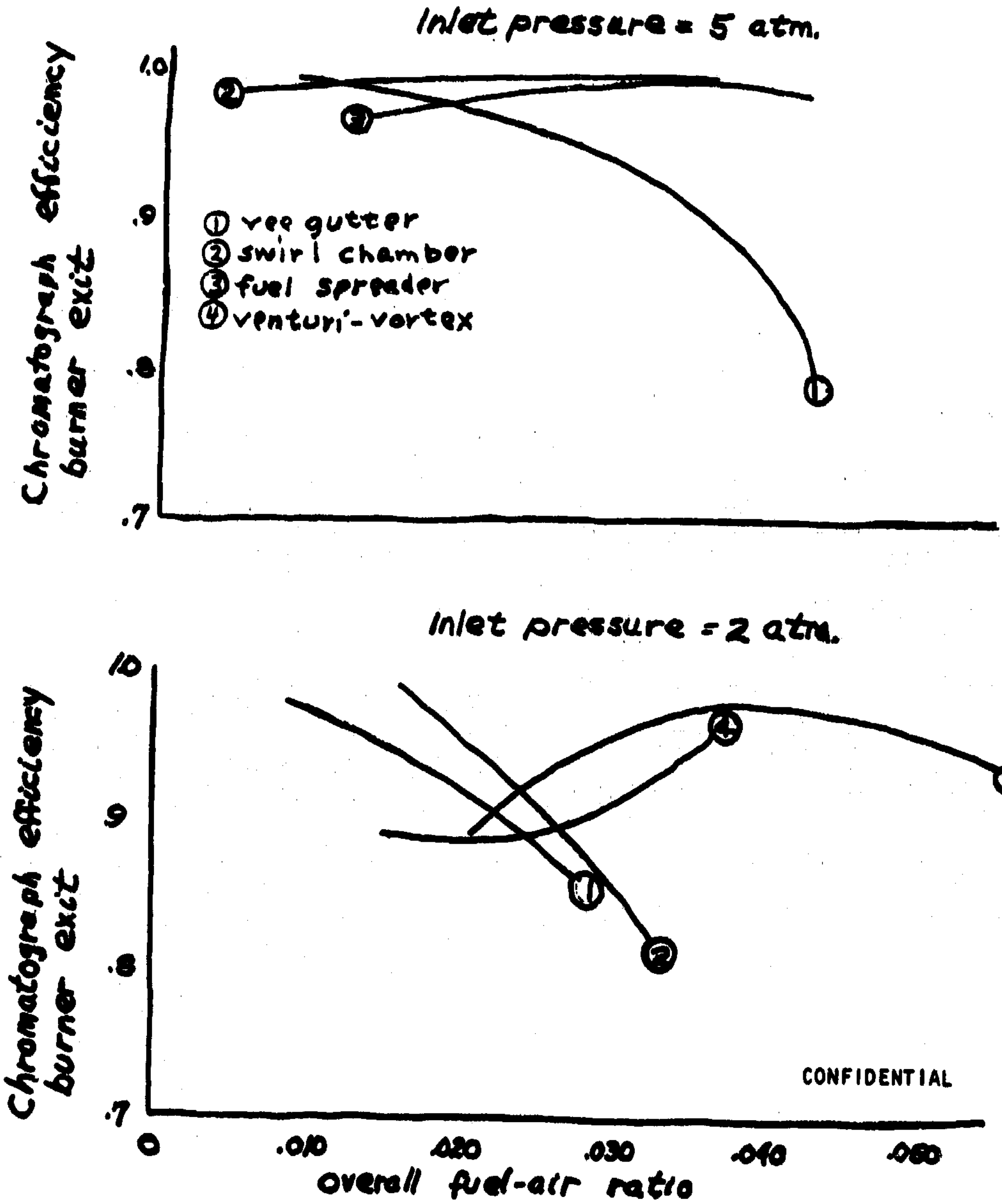

Figure 53. Chromatograph efficiency versus fuel-air ratio at 2 and 5 atmospheres.

Burner Efficiency (cont.)

(C) rapidly above a FAO of 0.017, which coincides with the design fuel-air ratio.

(C) This problem is unique to the Vee gutter module. A postulation to increase the design fuel-air ratio by staging the fuel will be evaluated in Phase II sector testing. Fuel will be injected into the bypass dilution air into a secondary recirculation zone located downstream from the primary and strongest recirculation zone. The recirculation zones were defined on the sixty degree diffuser sector rig flowing water. The venturi-vortex module has a wide angle fuel spray cone. This resulted in combustion on the rig sector walls which distorts the performance evaluation. Improved mixing occurred as fuel-air ratio increased. This is best demonstrated with Figure 53 which shows increasing efficiency with increasing fuel-air ratio over the range tested.

(C) The swirl chamber and fuel-air spreader modules have higher design fuel-air ratios.

(C) Verification of the level of importance of the design fuel-air ratio is shown in Figure 54. Figure 54 also shows the isotherm and zone efficiency profiles at the burner sector mean radial depth at two overall fuel-air ratios.

(C) At the operating condition below the design fuel-air ratio of 0.017 the reaction zone is attached to the Vee gutter, resulting in adequate completion of the reaction at an L/H of 1.75. Increasing the fuel-air ratio above 0.017 results in a blow-off of the reaction zone downstream with insufficient time to complete the reaction.

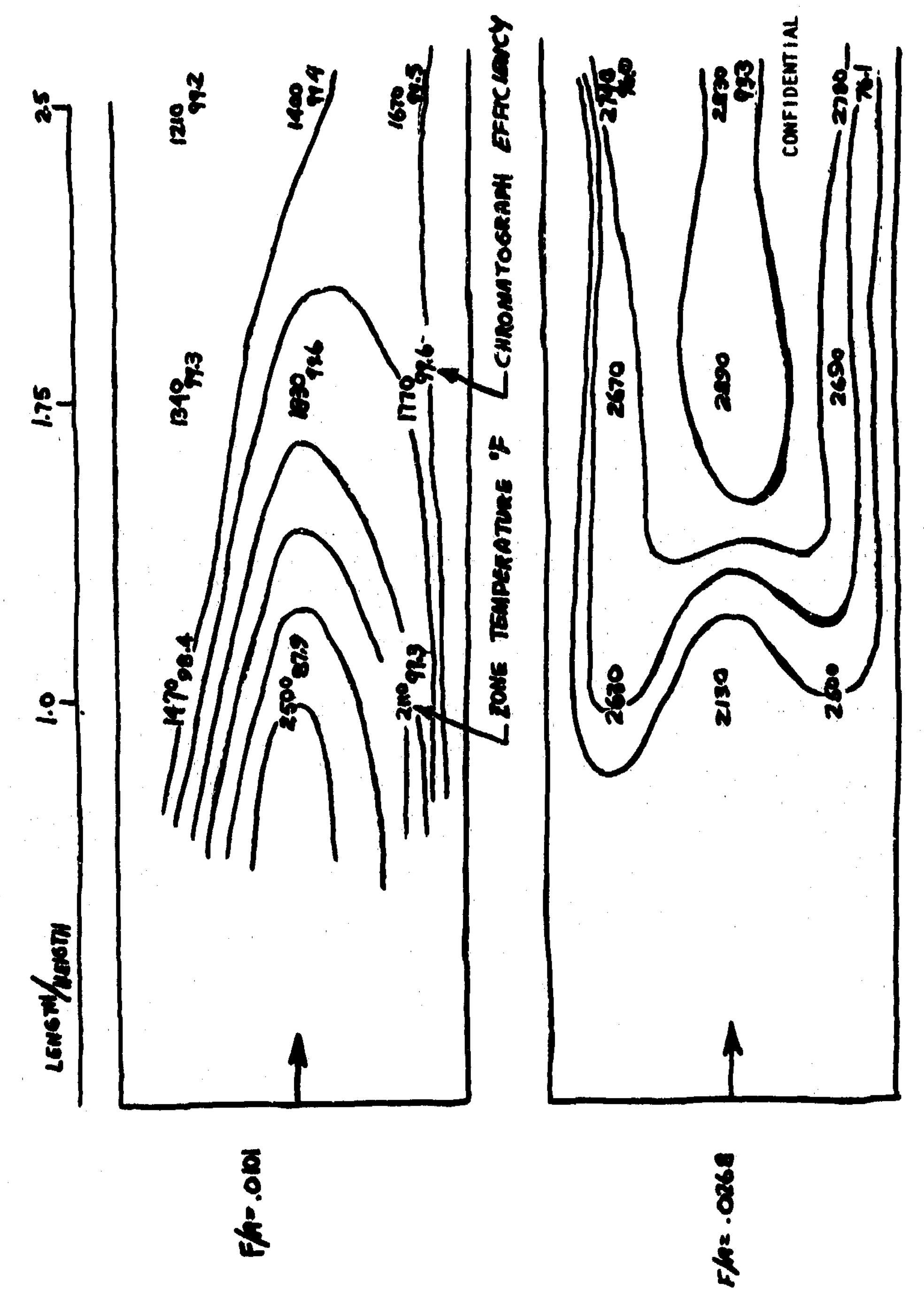

Figure 54. Isotherm and efficiency profiles at the burner sector mean depth for the vee gutter module.

Burner Efficiency (cont.)

(C) The comparison of overall combustion and the effectiveness of dilution mixing air is shown with Figure 55. The various modules have different air mass flow rates which result in different heat loadings. The usual $\frac{T_{max} - T_{avg}}{\text{Temperature rise}}$ parameter has been divided by heat load instead of temperature rise in an attempt to normalize the modules for comparative purposes.

Blowouts

(C) The fuel-air ratio at lean blowout of the various modules is approximately one-third the design fuel-air ratio. This ratio may change during sector testing, but the results indicate that high temperature rise modules will have correspondingly high blowouts.

(C) The blowout points are shown on Figure 56.

Smoke

(C) Exhaust gas smoke samples were taken at each operating condition. There was no trace of smoke generation from any of the modules tested. Static tube sampling probes were used with spot verification samples taken with an isokinetic probe.

2. Contaminated Fuel

(C) Three types of fuel inlet devices were investigated for flowing contaminated fuel to the MIL E 5007B specification. Three units were made from 310 stainless and one unit was made from 347 stainless. Of these devices, three orifices were constructed with thickness equal to two times the diameter. The other orifice had the thickness equal to the diameter. Orifice sizes of

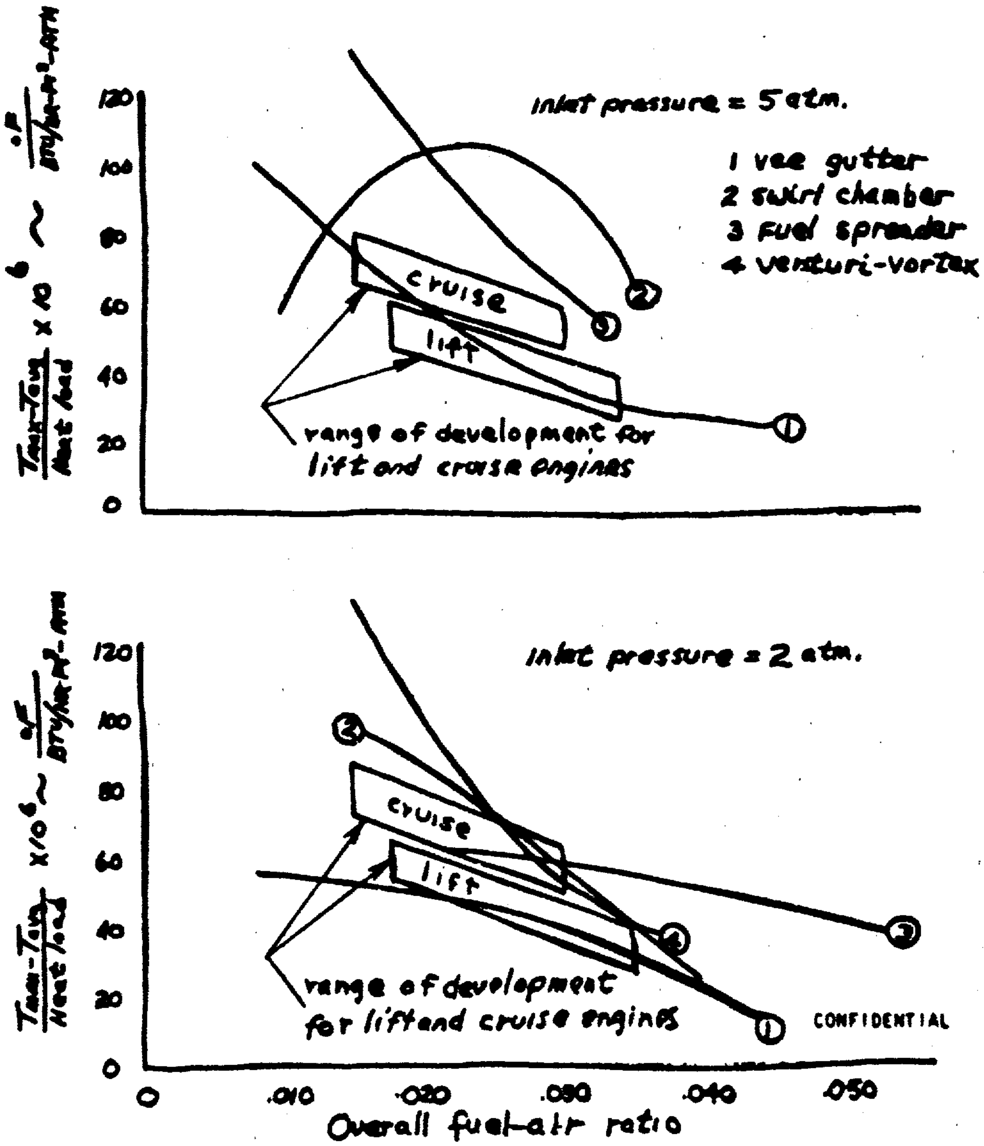

Figure 55. Pattern factor versus overall fuel-air ratio at 2 and 5 atmospheres.

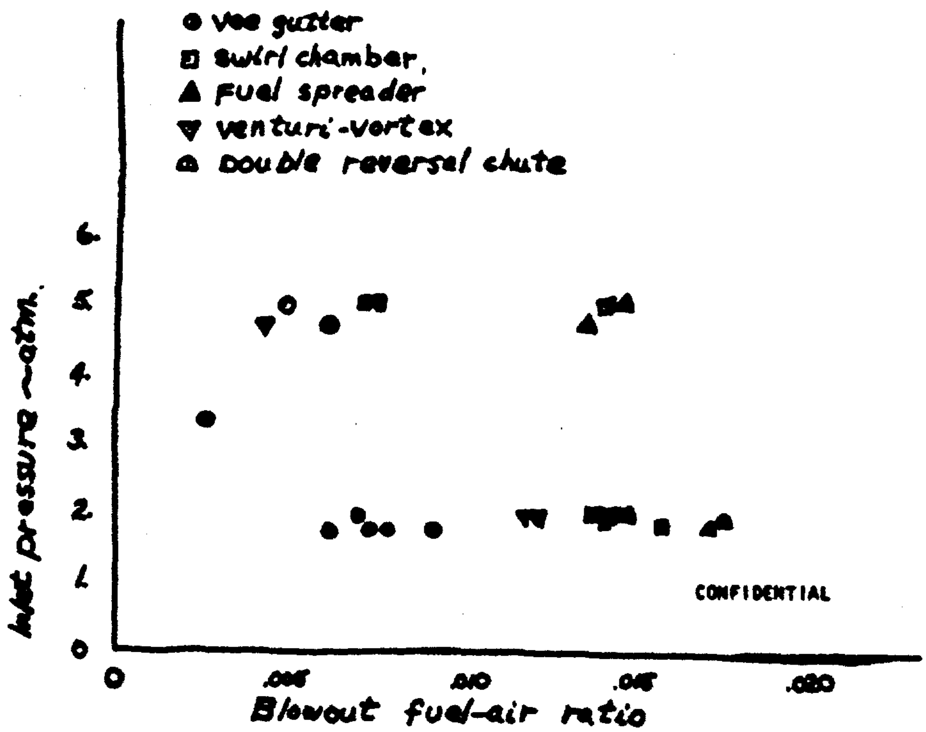

Figure 56. Inlet pressure versus fuel-air ratio at lean blowout.

Contaminated Fuel (cont.)

(C) .027 - .032 were flowed. Shape of the orifice showed indications of clogging. The material had indications of erosion and, therefore, the necessity of using wear resistant material was experienced. Figure 57 shows flow comparisons before and after contaminated fuel testing.

3. Flow Visualization Rigs

(C) In this section is presented diffuser performance data - inlet and outlet velocity profiles - measured for the "A" and "B" diffuser rig models. This data is compared with predicted performance data. Test data obtained correlated closely to the theoretical predicted performance characteristics. The flow visualization photographs of "A" diffuser-combustor are shown in Figure 58. Type "A" diffuser is the surge passage, straight dump annular diffuser. Type "B" diffuser is the two passage annular dump with a circumferential splitter. The diffuser inlet geometry at the trailing edge of the turning vanes remained similar for both types of diffusers tested. Table IX is a summary of significant design and test data for the "A" and "B" diffusers.

Test Configuration

(C) A cross sectional view of the diffuser test rig for testing both diffusers is shown in Figure 59. The geometry of the test rig differs slightly. The inlet of the "A" diffuser has a smooth, flat velocity profile. The "B" type diffuser inlet has integrated turning vanes to generate an inlet velocity profile.

(C) The diffuser inlet instrumentation was located in a plane of the throat one quarter inch downstream of the exit vane trailing edge. Pressures were observed on water manometers. The diffuser discharge instrumentation was mounted similar to the inlet configuration.

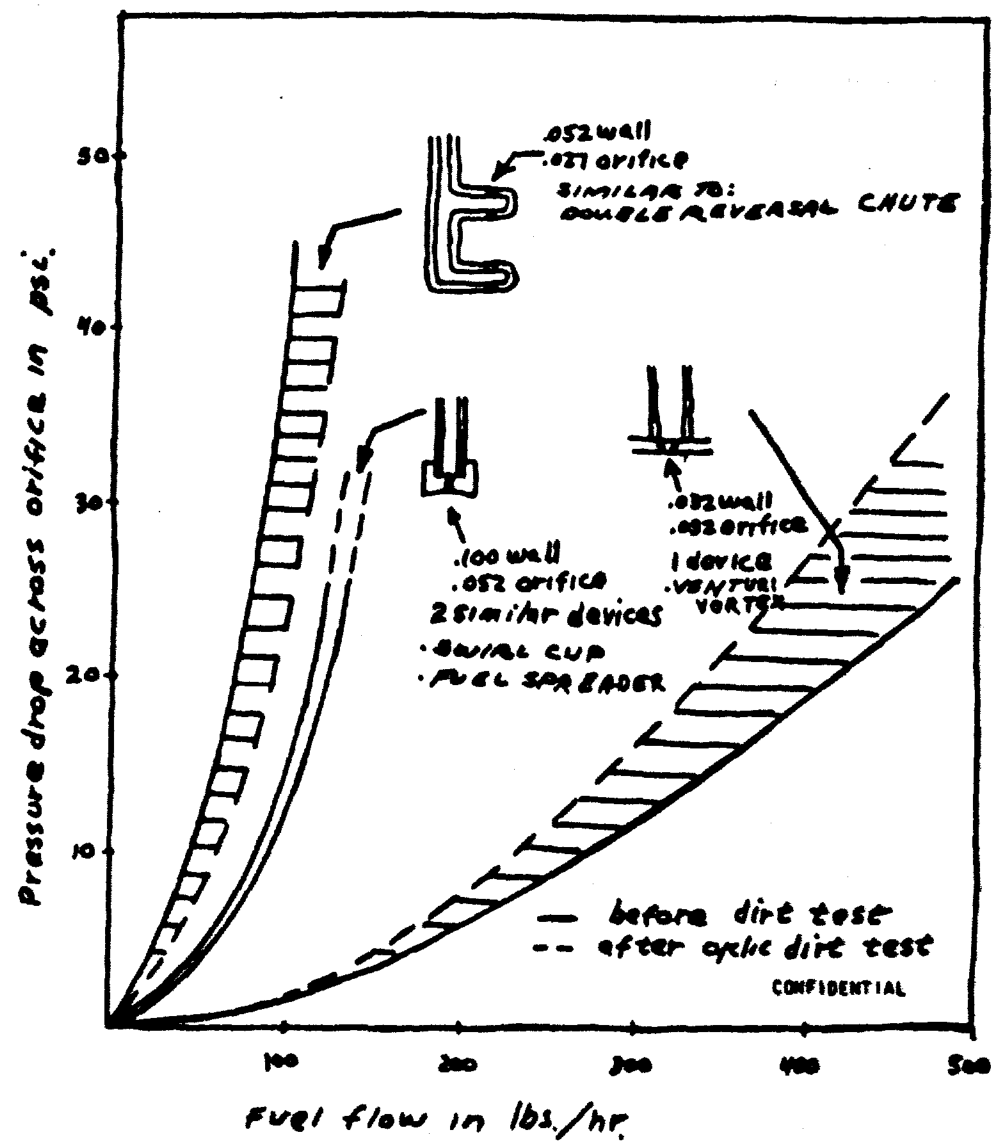

Figure 57. Flow before and after contaminated fuel testing.

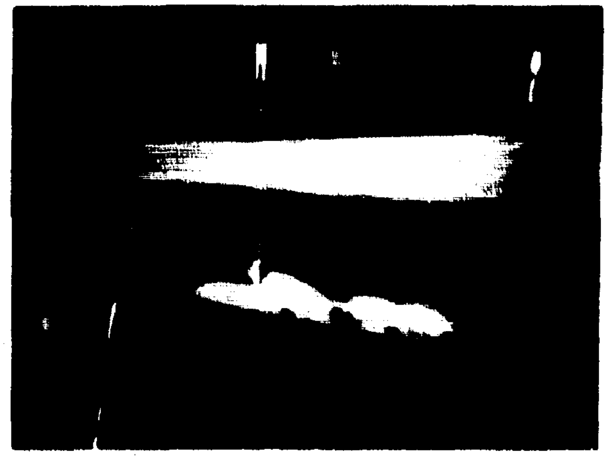

Single path 7 1 2 deg diffuser

Single path 7 1/2 deg diffuser dump area

Figure 58. **Flow tracers showing flow through "A" diffuser and into premix area.**

(C) TABLE IX

"A" - Diffuser Testing

Parameters	Performance Predicted	Performance Test
Diffuser inlet pressure (static to total) Ps_1/Pt_1	0.9410	0.9576
Diffuser inlet Mach number Mn_1	0.296	0.305
Diffuser discharge pressure ratio (static to total) Ps_2/Pt_2	0.9816	0.9806
Diffuser discharge Mach number Mn_2	0.163	0.167
Diffuser pressure recovery Cp	59.0%	63.5%
Diffuser losses (inlet-discharge) Pt/Pt_1	0.6%	0.34%
Pressure drop combustor and module Pt^*/Pt_2	3.5%	3.06%

"B" - Diffuser Testing

	Upper Predicted	Upper Test	Lower Predicted	Lower Test
Diffuser inlet pressure (static to total) Ps_1/Pt_1	.9285	.9180	.9339	.9274
Diffuser inlet Mach number Mn_1	.328	.365	.315	.330
Diffuser discharge pressure ratio (static to total) Ps_2/Pt_2	.9719	.9684	.9721	.9758
Diffuser discharge Mach number Mn_2	.208	.234	.202	.187
Diffuser pressure recovery Cp	43.6%	51.0%	43.5%	51.6%
Diffuser losses (inlet-discharge) Pt/Pt_1	1.25%	1.22%	1.0%	1.18
Pressure drop combustor and module Pt^*/Pt_2 Total	2.64%	4.12%*	2.4%	-

* Both passages

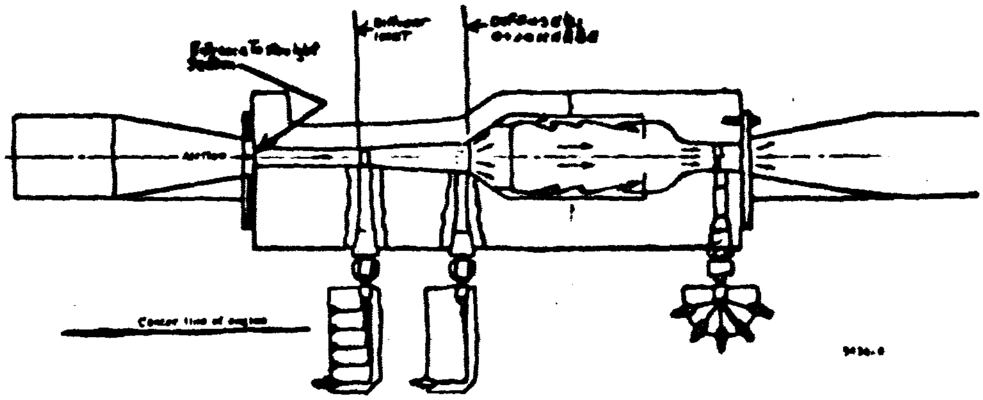

Test rig flow path for "A" diffuser

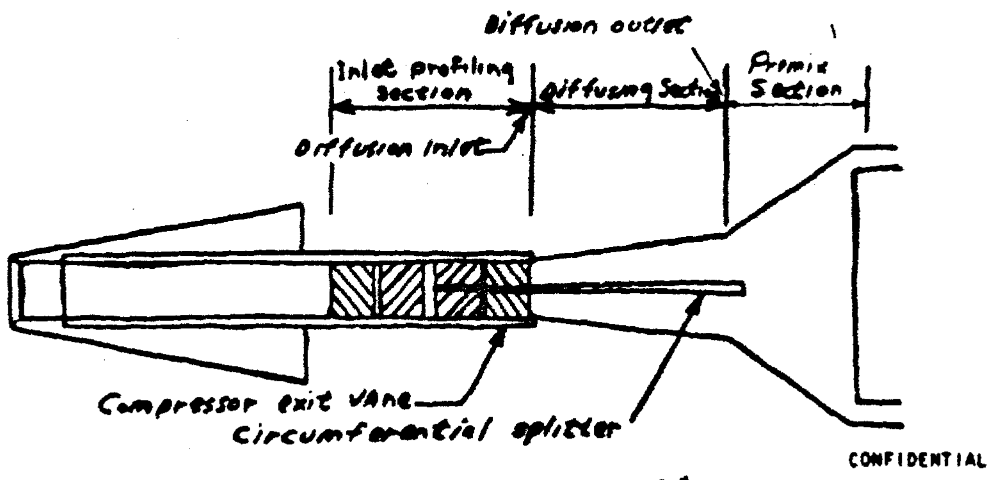

Test rig flow path for "B" diffuser

Figure 59. Test rig flow paths.

Results and Discussion

(C) The purpose of this section is to present a summary of results of an experimental investigation in which parametric studies were performed using rig models of the "A" and "B" type diffusers.

(C) Diffuser pressure recovery (C_p) at the inlet Mach numbers from 0.1 to 0.35 are presented for "A" and "B" diffusers. Typical diffuser velocity profiles are presented for both diffusers at several inlet conditions. The Mach number between the diffuser inlet and exit stations follow closely the predicted pressure recovery and diffuser losses.

Diffuser Efficiency (pressure recovery) "A" Diffuser

(C) Tests on this configuration revealed a slight diffuser efficiency (pressure recovery) increase with an increasing Mach number. The performance of this diffuser was encouraging. Calculations using the test data revealed an average diffuser pressure recovery of C_p= 63.5% which is essentially constant for selected Mach numbers (0.1 to 0.35). This is an excellent pressure recovery for this type of diffuser and is three to four and one half percent higher than the predicted pressure recovery for the original design (see Table IX).

Velocity Profile "A" Diffuser

(C) The inlet velocity was essentially uniform over the annulus height at all inlet conditions investigated. There was no flow separation indicated by the near normal turbulent velocity profiles at the diffuser exit plane for any of the inlet conditions tested. The exit velocity profiles increased as the divergence angle was increased.

(C) The total system losses and diffuser inlet-exit pressure drop are shown in Figure 60.

(C) A comparison of velocity profiles at the diffuser inlet and exit for inlet Mach numbers 0.18 to 0.30 are shown in Figures 61 and 62.

Results and Discussion (cont.)

"B" Type Diffuser

(C) The objective of the "B" diffuser testing was to determine the effect of a circumferential splitter on diffuser performance. The splitter was located on the centerbody of an annular sector of a subsonic diffuser.

Diffuser Pressure Recovery "B" Diffuser

(C) Different inlet Mach number conditions produced slight changes in the pressure recovery characteristics in both the upper and lower passages. The upper passage showed a pressure recovery of C_p = 51.0% versus C_p = 43.6% predicted recovery. The lower passage pressure recovery was C_p = 51.6% as opposed to a predicted C_p = 43.5%. This phenomena of change in the total pressure levels is explained in the velocity profile discussion.

(C) Comparisons of predicted and actual performance data for the "B" diffuser inlet and exit are shown in Table IX . The test data exhibits very close agreement to predicted performance points.

Velocity Profile - "B" Diffuser

(C) The velocity profiles for the diffuser inlet and exit are shown in Figures 63, 64, 65, and 66. The velocity profile did not exhibit general amplification characteristics as diffusion was increased.

(C) It is felt that the Vee gutter module acted as a flow restriction and had a tendency to prevent profile amplification. This lack of velocity profile amplification results in a thinner boundary layer buildup and, consequently, an improvement in pressure recovery (see Table IX).

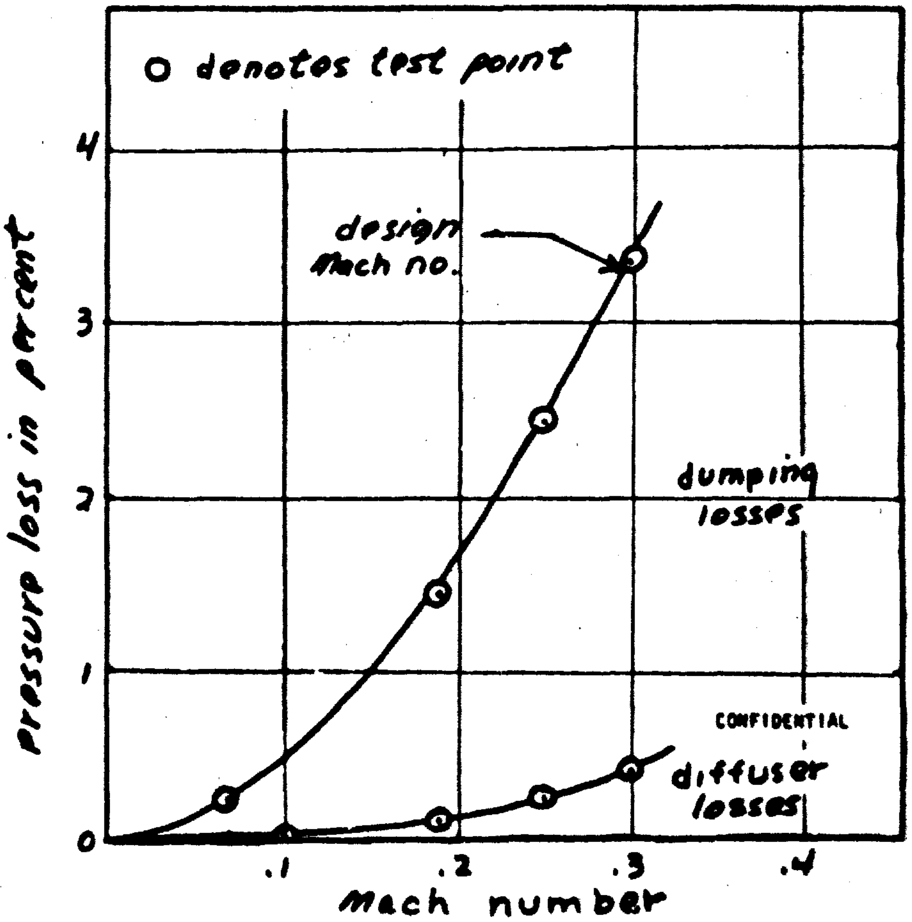

Figure 60. "A" diffuser pressure losses and dump losses versus Mach number.

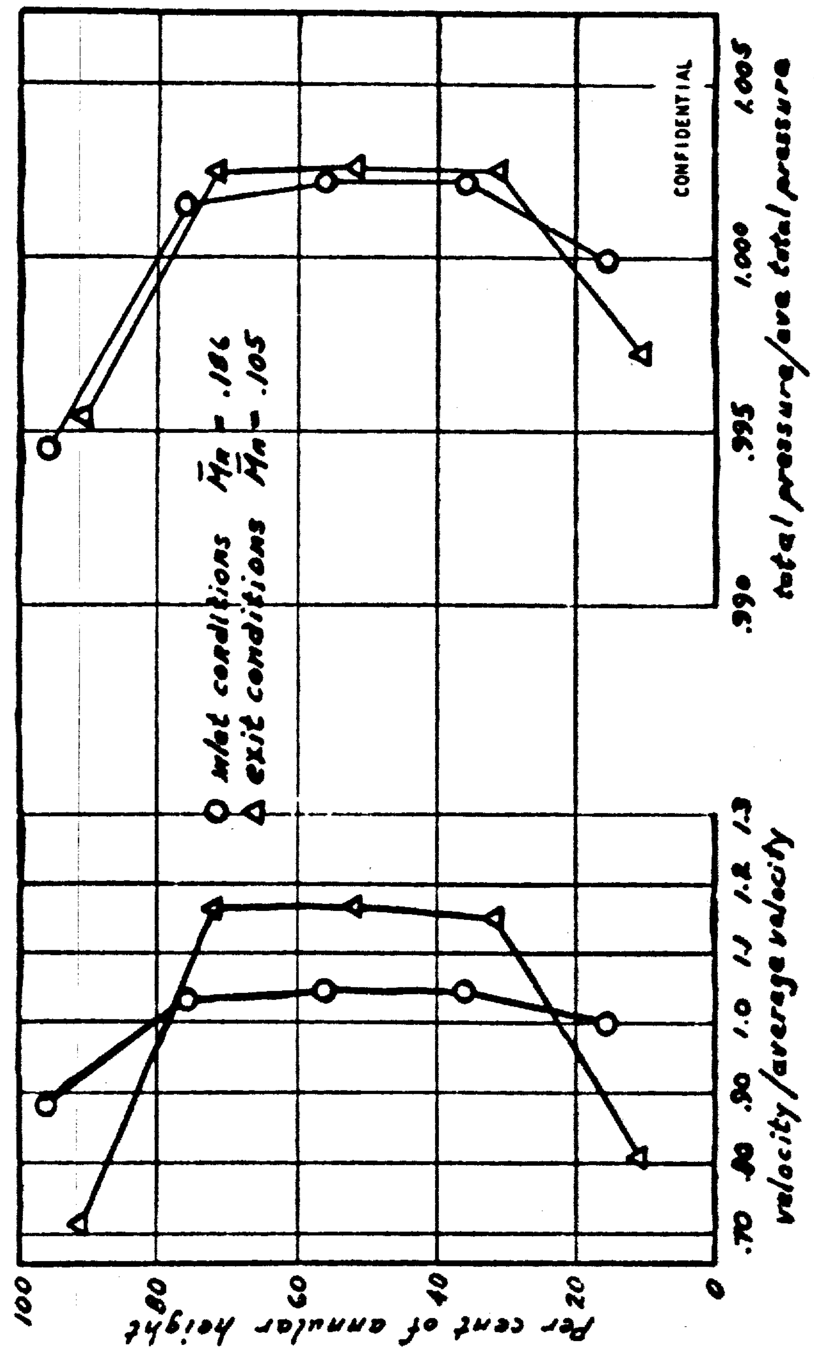

Figure 61. Velocity and pressure profiles from "A" diffuser.

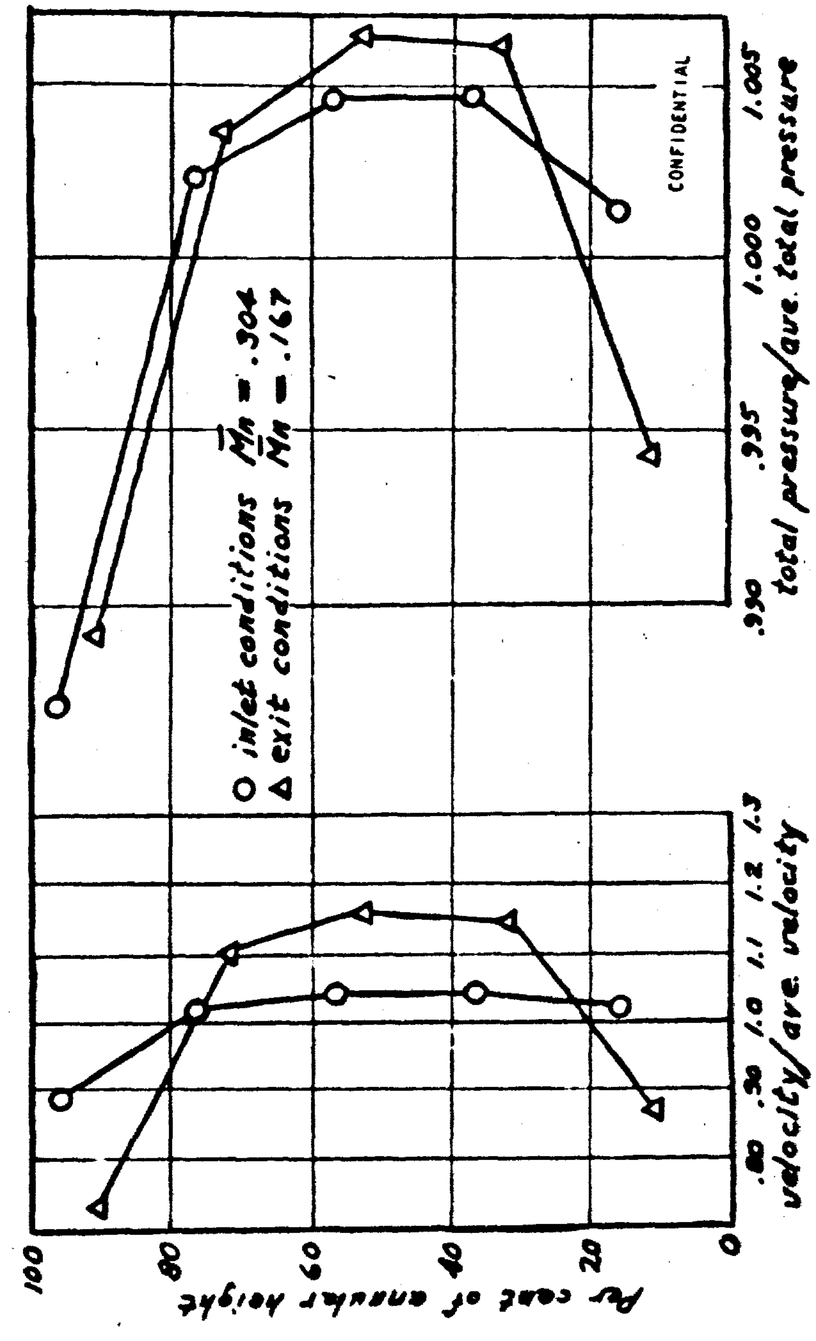

Figure 62. Velocity and pressure profiles from "A" diffuser.

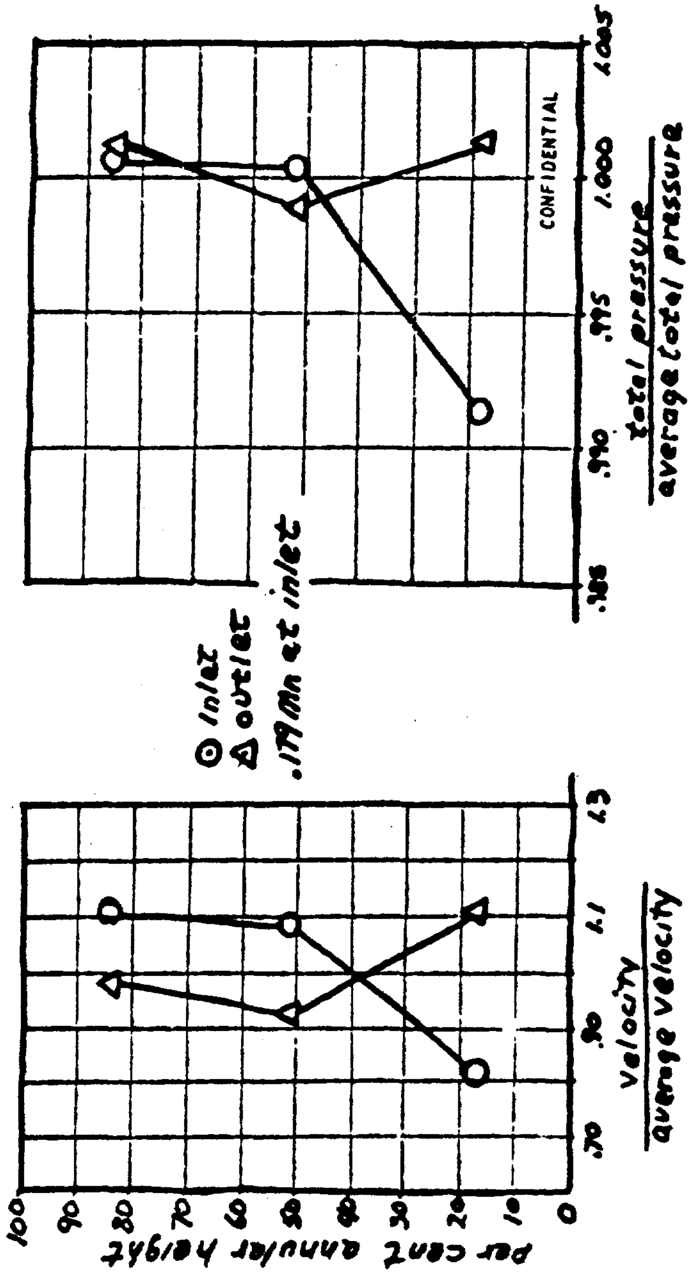

Figure 63. "B" diffuser upper passage profiles.

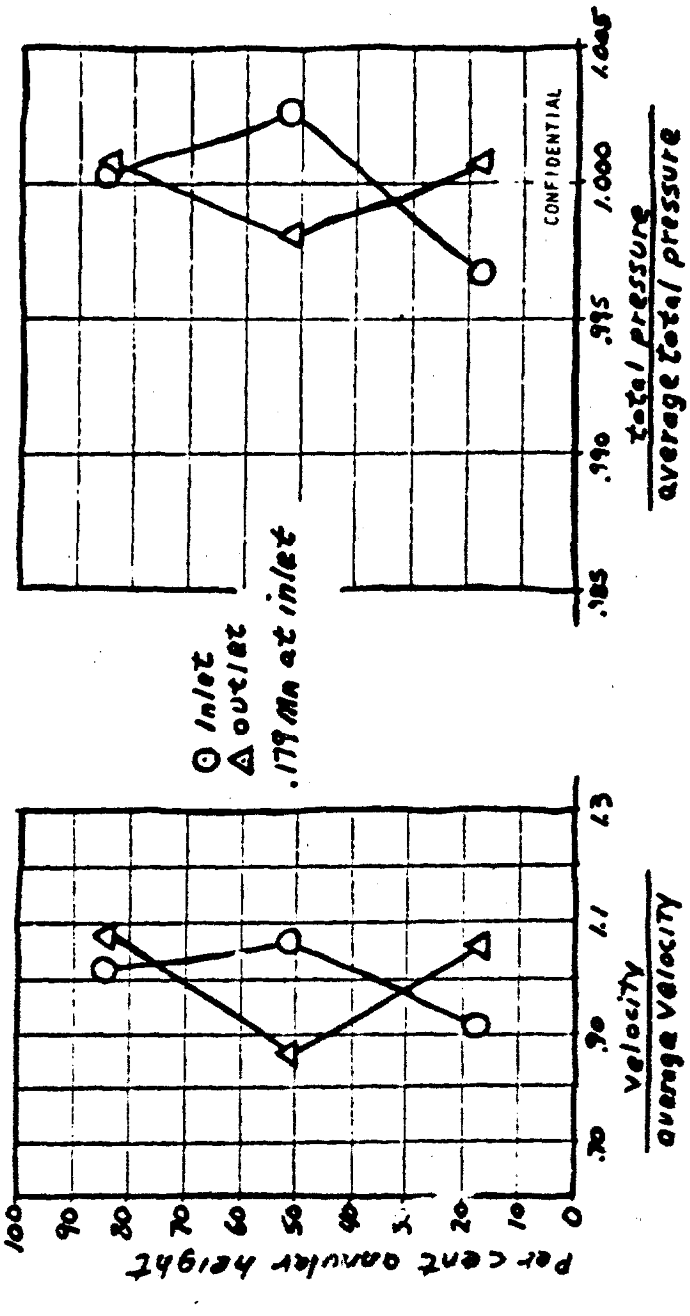

Figure 64. "B" diffuser lower passage profiles.

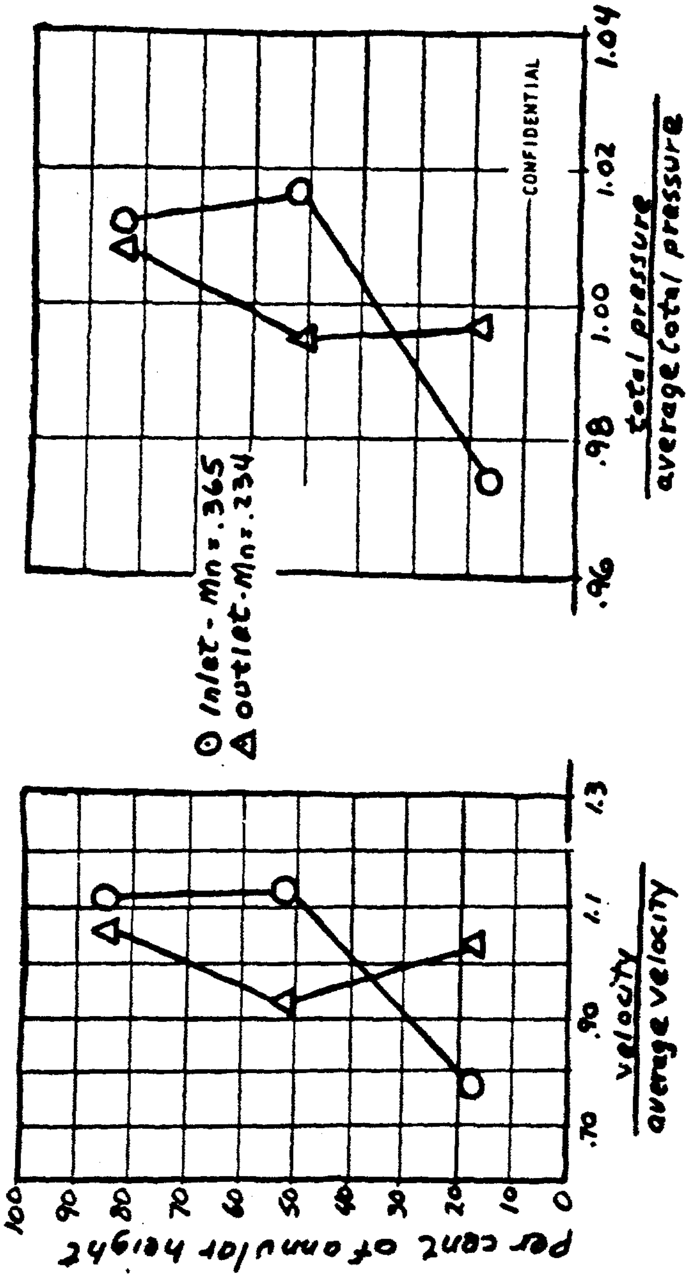

Figure 65. "B" diffuser upper passage profiles.

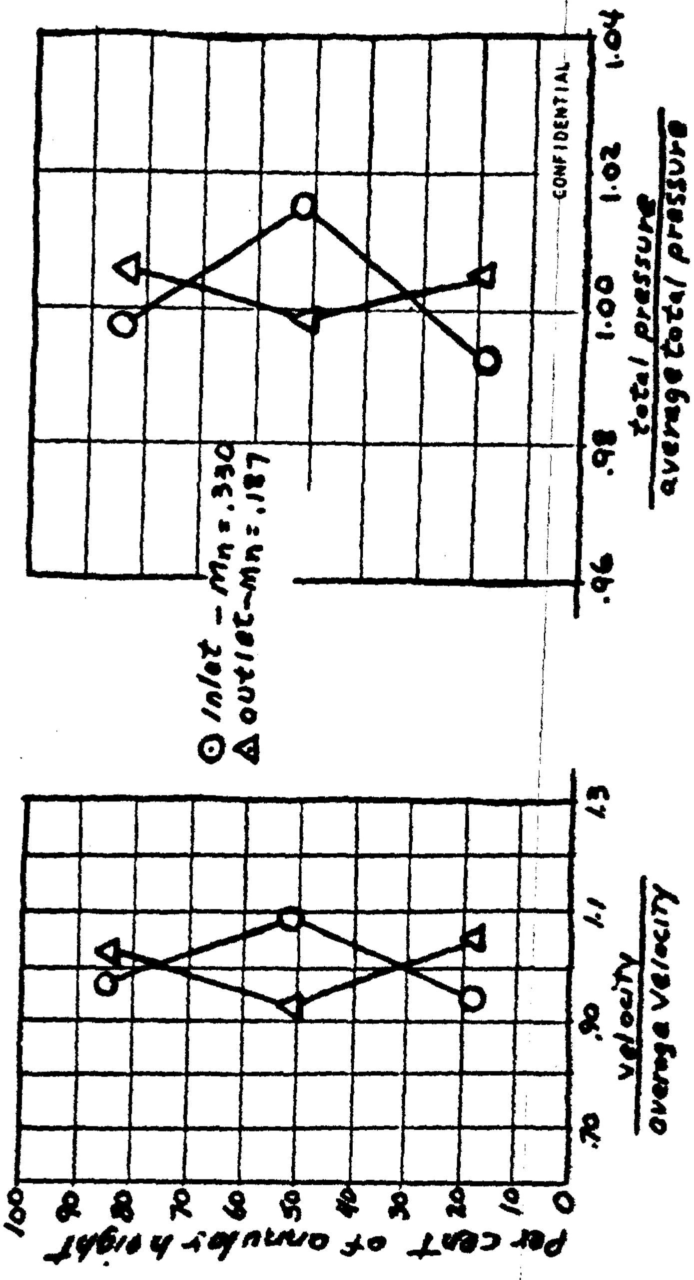

Figure 86. "B" diffuser lower passage profiles.

(C) There was no flow separation indicated by the near flat, turbulent velocity profiles at the diffuser exit plane for any of the inlet conditions tested.

(C) The performance of this diffuser was good. This gives encouragement to use of this type of diffuser for scaling purposes.

(C) The total pressure losses of the system and diffuser inlet-exit pressure drop versus Mach number are shown in Figure 67

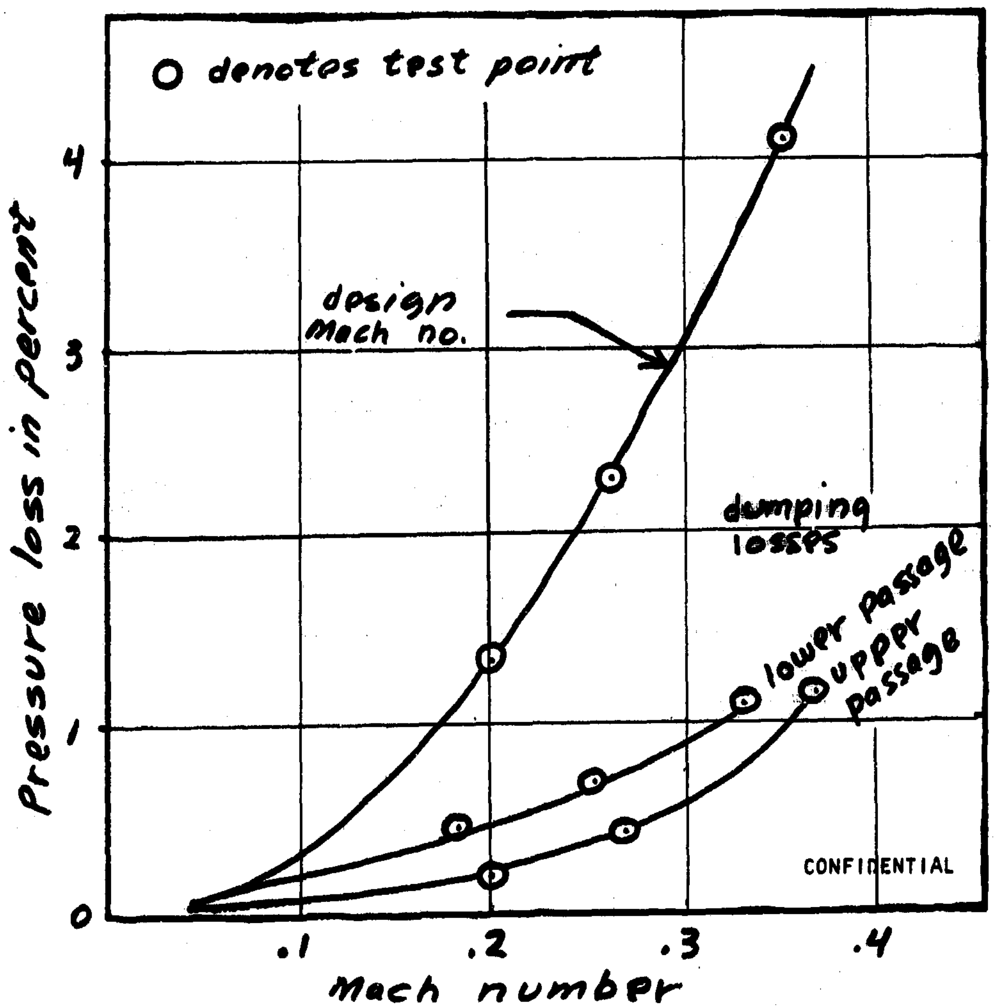

Figure 67. "B" diffuser pressure losses and dump losses versus Mach number.

VIII PHASE II PROGRAM

(C) Phase II will be the continued evaluation of short integrated diffusers and pre-mix modules. The scope of these evaluations will be increased by combining both the diffuser and premix systems. In addition the combined diffuser and premix will be evaluated with a combustion volume equal to or less than that required for pressure atomization. The combustor volume, therefore, will remain flexible during this testing. The cooling of the combustor walls will be explored and defined for the performance testing of Phase III.

(C) The major effort of Phase II will be accomplished using a 60° sector of the flow path of an annular combustor system. Various configurations of diffusers, premix injectors, and combustors will also be used to indicate the system variability with optimization of components, while operating at pressures up to 20 atmospheres and inlet temperatures in excess of 1000°F. The injector computer program initiated in Phase I will be refined and a diffuser computer program initiated.

IX REFERENCES

1. Carlson, J. J., and Johnston, J. P., Effects of Wall Shape on Flow Regimes and Performance in Straight, Two-Dimensional Diffusers (U), Stanford University, PD-11, June 1965

2. Waitman, B. A., Reneau, L. R., and Kline, S. J., "Effects of Inlet Conditions on Performance of Two-Dimensional Diffusers" (U) Journal of Basic Engineering, Transactions ASME, Series D, Vol. 83, 1961

3. Kline, S. J., Abbott, D. E., and Fox, R. W., "Optimum Design of Straight-Walled Diffusers" (U) Journal of Basic Engineering, Transactions ASME, Series D, Vol. 81, 1959

4. Sovran, G., and Klomp, E. D., Experimentally Determined Optimum Geometries for Rectilinear Diffusers with Rectangular, Conical, or Annular Cross-Section (U), General Motors Research Publication, GMR-511, November, 1965

5. Reneau, L. R., Johnston, J. P., and Kline, S. J., Performance and Design of Straight Two-Dimensional Diffusers (U), Stanford University Press, PD-8, September, 1964

6. Henderson, F. D., Effect of Profile and Length on Efficiency of Pump Diffusers (U), Rocket Propulsion Establishment, Technical Note No. 181, September, 1959

7. Longwell, J. P., "Combustion of Liquid Fuels" (U), High Speed Aerodynamics and Jet Propulsion, Vol. II, Combustion Processes, Princeton University Press, 1956

8. Roschke, E. J., Flow Visualization Studies of a Confined, Jet-Driven Water Vortex (U), Jet Propulsion Laboratory, TR No. 32-1004, September 1966

9. Flow of Fluids Through Valves, Fittings, and Pipes (U), Engineering Department, Crane Company, Technical Paper No. 410, 1957

X BIBLIOGRAPHY

Carlson, J. J. and Johnston, J. P., Effects of Wall Shape on Flow Regimes and Performance in Straight, Two-Dimensional Diffusers (U), Stanford University, PD-11, June 1965

Clark, B. J., Breakup of a Liquid Jet in a Transverse Flow of Gas (U), Lewis Research Center, NASA, TN D-2424, August, 1964

Cocanower, A. B., Kline, S. J., and Johnston, J. P., A Unified Method for Predicting the Performance of Subsonic Diffusers of Several Geometries (U), Stanford University, PD-10, May 1965

Fernholz, Von H., "The Theoretical Boundary Layer Investigation for Optimum Design of Sub-Sonic Diffusers" (U) Ingenieur Archiv XXXV Band 1966

Kline, S. J., Abbott, D. E., and Fox, R. W., "Optimum Design of Straight-Walled Diffusers" (U), Journal of Basic Engineering, Transactions ASME, Series D, Vol. 81, 1959

Longwell, J. P., and Weiss, M. A., "Mixing and Distribution of Liquids in High Velocity Air Streams" (U), Industrial and Engineering Chemistry Journal, March 1953

Longwell, J. P., "Combustion of Liquid Fuels" (U), High Speed Aerodynamics and Jet Propulsion, Vol. II, Combustion Processes, Princeton University Press, 1956

Lyshevskiy, A. S., The Coefficient of Free Turbulence in a Jet of Atomized Liquid Fuel (U), NASA TT F-351, April 1965

Mugele, R. A., and Evans, H. D., "Droplet Size Distribution in Sprays" (U), Industrial and Engineering Chemistry Journal, June 1951

Nicholls, J. A., Dabora, E. K., and Raglund, K. W., A Study of Two Phase Detonation as It Relates to Rocket Motor Combustion Instability (U), NASA CR-272, August, 1965

Priem, R. J. and Heidmann, M. F., "Vaporization of Propellants in Rocket Engines" (U), American Rocket Society Journal, November 1959

Putnam, A. A. et al, Injection and Combustion of Liquid Fuels (U), Battelle Memorial Institute, WADC TR56-344, March 1957

Popov, Mintcho, Model Experiments on Atomization of Liquids (U), NASA, TT F-65, July 1961

Roschke, E. J., Experimental Investigation of a Confined, Jet-Driven Water Vortex (U), Jet Propulsion Laboratory, TR No. 32-982, October 1966

Roschke, E. J., Flow Visualization Studies of a Confined, Jet-Driven Water Vortex (U), Jet Propulsion Laboratory, TR No. 32-1004, September 1966

Schuyler, F. L., Combustion Instability: Liquid Stream and Droplet Behavior (U), WADC TR 59-720, September 1960

Sitkei, Gyorgy, Contribution to the Theory of Jet Atomization (U), NASA TT F-129, October 1963

Waitman, B. A., Reneau, L. R., and Kline, S. J., "Effects of Inlet Conditions on Performance of Two-Dimensional Diffusers" (U), Journal of Basic Engineering, Transactions ASME, Series D, Vol. 83, 1961

CONFIDENTIAL

Security Classification

DOCUMENT CONTROL DATA - R&D

(Security classification of title, body of abstract and indexing annotation must be entered when the overall report is classified)

1. ORIGINATING ACTIVITY (Corporate author) Allison Division of General Motors, Indianapolis, Indiana 46206	2a. REPORT SECURITY CLASSIFICATION Confidential contains restricted data
	2b. GROUP

3. REPORT TITLE EXPLORATORY DEVELOPMENT OF REDUCED LENGTH TURBO-PROPULSION COMBUSTION SYSTEMS. PART I—PRELIMINARY COMPONENT DESIGN AND DEVELOPMENT

4. DESCRIPTIVE NOTES (Type of report and inclusive dates)
Phase I final report for the period 1 July 1967 through 31 December 1967

5. AUTHOR(S) (Last name, first name, initial)
Simon, Jack J. | Wyrobek, J. T.
Stettler, Richard J.
MacNaughton, Donald A.

6. REPORT DATE	7a. TOTAL NO. OF PAGES	7b. NO. OF REFS
August 1968	117	9

8a. CONTRACT OR GRANT NO. F33615-67-C-1939	9a. ORIGINATOR'S REPORT NUMBER(S) EDR 5610
b. PROJECT NO. 3066	
c. Task No. 306603	9b. OTHER REPORT NO(S) (Any other numbers that may be assigned this report) AFAPL-TR-68-8
d.	

10. AVAILABILITY/LIMITATION NOTICES

11. SUPPLEMENTARY NOTES Design, test, and results of venturi-vortex fuel module concept to be restricted to government agencies	12. SPONSORING MILITARY ACTIVITY Air Force Aero Propulsion Laboratory, Air Force Systems Command, Wright-Patterson Air Force Base, Ohio 45433

13. ABSTRACT

Advanced design turbo-propulsion engines for future aircraft require a compact, high performance combustion system for high thrust-to-weight ratios and an increased level of reliability. To attain this goal, two concepts based on maximum combustor dome airflow are being developed. The first is an integration of the diffuser and combustor to achieve minimum length and maximum efficiency with smoke free operation. The second is to achieve improved fuel injection using a high density premix fuel injection technique to obtain acceptable exit temperature patterns in a high temperature rise combustor. The fuel injection technique is the development of single modules for premixing of low pressure fuel and high density air ahead of the combustor dome. These modules are capable of accepting contaminated fuels and can be combined to permit testing as sectors of a full annular combustor. (U)

Initial testing of the various fuel injection premix modules and different designs of the integrated diffuser-combustor under Phase I of this program has verified the soundness of the concepts being developed. Based upon these results, the most promising premix modules and the best diffuser-combustor design will be combined as sectors of a full annular combustor for further evaluation. (U)

(Distribution of this abstract is unlimited.)

DD FORM 1 JAN 64 1473

CONFIDENTIAL

Security Classification

14 KEY WORDS	LINK A ROLE	LINK A WT	LINK B ROLE	LINK B WT	LINK C ROLE	LINK C WT
Annular Combustor						
Premix fuel modules						
Integrated diffuser-combustor						
Combustor high dome flow						
Fuel injection techniques						
Fuel-air mixing						
High temperature rise						
Exit temperature profile						
Contaminated fuel						
Smoke free operation						